Insights into the role of an Arabidopsis nuclear matrix binding protein AHL22 in chromatin regulation and hypocotyl growth

Dissertation

zur Erlangung des

Doktorgrades der Naturwissenschaften (Dr. rer. nat.)

der

Naturwissenschaftlichen Fakultät III

-Biowissenschaften-

der Martin-Luther-Universität Halle-Wittenberg

vorgelegt von

Herrn Linhao Xu

geboren am 12.06.1992 in Jianyang City, China

Gutachter:

Jun. -Prof. Dr. Hua Jiang

Prof. Dr. Claudia Köhler

Verteidigt am

09/01/2023

Contents

1 Introduction

1.1 Nuclear matrix

The eukaryotic cell is compartmentalized into a certain boundary structure which contains several organelles and a well-defined nucleus that houses the genetic material. Nuclear organization plays an important role in many cellular processes (Van Bortle and Corces 2012). Increasing evidence suggests that chromatin is structured at several hierarchical levels rather than random packaging to ensure appropriate gene expression (Gibcus and Dekker 2013). DNA is tightly packaged into a nucleus. The human DNA with an approximate length of 3 m or the Arabidopsis genome with over 33,000 genes in 135 Mb (Arabidopsis Genome 2000) is highly compacted to fit into a relatively small nucleus. This compaction does not silence gene expression. However, DNA is accessed in a tightly controlled and dynamic manner for a proper gene expression (Narwade et al. 2019). This controlling "hand" behind, has been called as nuclear matrix.

1.1.1 Discovery of nuclear matrix

In 1974, Berezney and Coffey firstly described the supporting structure for orderly compaction of DNA by biochemically isolating a nuclear fraction showing the appearance of such a non-chromatin structure, and termed it the nuclear matrix (Berezney and Coffey 1974). This brought the name and also the functional concept to describe the skeletal structure inside a nucleus. After that, using electron microscopy, multiple studies followed the concept to show the appearance of nuclear matrix in mammals and plants. In CaSki cells and Arabidopsis cells, a network of fibers/filaments was observed and well distributed throughout a nucleus, connecting nuclear lamina and nucleoli (Figure 1.1) (Nickerson 1998; Calikowski, Meulia, and Meier 2003). However, the nature of these fibers/filaments is still unclear, which makes it a debate. For the most concerns, the nuclear matrix may contain other artifactual nuclear compartments caused by the preparation of the nuclear matrix (Hancock 2000). The preparation of nuclear matrix involves DNase I digestion and high salt treatment to remove chromatin and soluble proteins (Nickerson 2001). However, factors like heat temperature (37-42°C), salt concentration, and crosslinking may cause extra precipitation of proteins in the nuclear matrix (Berezney and Coffey 1977; Kaufmann and Shaper 1984; Martelli et al. 1991). In a simplified view, the nuclear matrix is resistant to nucleolytic enzymes, high ionic strength buffers and nonionic detergents (Wasag and Lenartowski 2016).
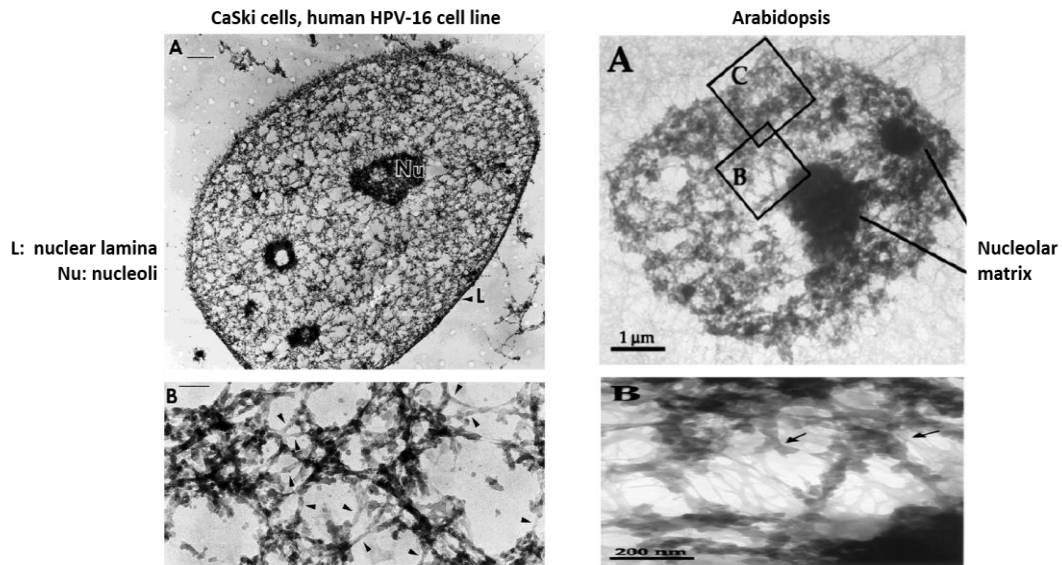
Figure 1.1. Electron microscope analysis of the nuclear matrix of CaSki cells (left) and *Arabidopsis thaliana* (right). Modified from (Nickerson 1998; Calikowski, Meulia, and Meier 2003).

The nuclear matrix is a dynamic nuclear compartment. In the space of a nucleus, nuclear matrix regions are a part of chromosome territory, and the remaining space is called the interchromatin domain (Cremer et al. 2000). During the nuclear matrix preparation, attached chromatin and proteins are mostly from the interchromatin domain. Transcription and replication factories were found in chromosome territory and function on the nuclear matrix platform (Hozak et al. 1993; Berezney et al. 1995; Iborra et al. 1996). On the platform, many compartments were studied to illustrate the function of the nuclear matrix, such as matrix attachment regions (MARs) and nuclear matrix-associated proteins (Figure 1.2).
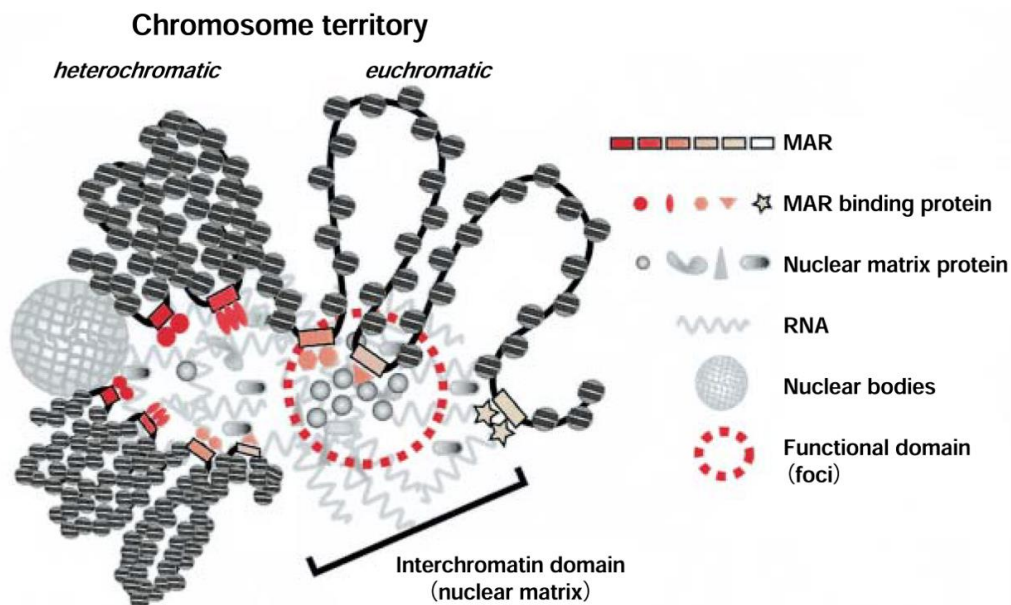
Figure 1.2. Schematic representation of nuclear compartments (Tsutsui, Sano, and Tsutsui 2005).

1.1.2 Matrix attachment regions (MARs)

Matrix attachment regions (MARs), also known as scaffold attachment regions (SARs), are defined as DNA elements that specifically bind to the nuclear matrix and as DNA fragments copurified with the nuclear matrix during the preparation of the nuclear matrix (Michalowski et al. 1999) (Figure 1.2). MARs are short DNA sequences present in all higher eukaryotes, including mammals and plants (Bode et al. 1996; Allen, Spiker, and Thompson 2000). These DNA sequences are notable for their AT richness and likely narrowing the minor groove (Gasser et al. 1989; Bode et al. 1995). MARs play critical roles in defining structural units of chromatin by binding to the nuclear matrix and organizing the chromatin into distinct loop domains (Heng et al. 2004; Girod et al. 2007; Chavali, Funa, and Chavali 2011). They can also influence transcription in both positive and negative ways (Allen, Spiker, and Thompson 2000). To date, many studies have shown the function of MARs in gene expression.

For example, in the human genome, MARs identified from chromosomes 14 and 18 are preferably located in silenced genes and near transcription start sites (TSSs) associated with RNA polymerase II binding regions by NaCl extraction and LIS extraction, respectively (Linnemann, Platts, and Krawetz 2009; Keaton et al. 2011). In contrast, genes from chromosome 19 that have a close association with the nuclear matrix are transcribed actively (Croft et al. 1999). A genome-wide analysis of MARs binding patterns from 14 different human MARs binding proteins reveals that MARs are around TSS of many genes and act as hotspots for the integration of retroviruses. It highlights the importance of these elements for the transcriptional regulation of genes (Narwade et al. 2019).

The large region first characterized in plants is 280 kb of the maize (*Zea mays*) genome, where MARs mark the boundaries of domains conserved between maize and sorghum (Avramova et al. 1995). In Arabidopsis, genome-wide in silico mapping of MARs suggests that Arabidopsis intragenic MARs preferentially locate near the 5'-half of a gene, mostly within introns 1 and 2, and negatively correlate with transcription level (Rudd et al. 2004). Further analysis of intragenic MARs on spatiotemporal regulation of transcription reveals that intragenic S/MAR marked genes are less expressed and show a profound specificity for tissues, organs, and developmental phases. This characteristic is even more pronounced for transcription factor genes (Tetko et al. 2006). Besides the expression data from the online database, In vivo mapping of Arabidopsis MARs at chromosome 4 shows that Arabidopsis MARs define structural domains with a preference for locating in transcription start sites, leading to an increased expression of genes targeted by MARs rather than the less expressed level from in silico analysis (Pascuzzi et al. 2014). Similar to MARs on spatiotemporal regulation, MARs from chromosome 4 are particularly pronounced in the case of transcription factors. Moreover, MARs at chromosome 4 are preferentially enriched in poly (dA: dT) tracts, resulting in at least one nucleosome depletion in MARs-enriched regions (Pascuzzi et al. 2014).

1.1.3 Nuclear matrix-associated proteins

Berezney and Coffey identified three lamina proteins as nuclear matrix proteins from rat liver in their initial research (Berezney and Coffey 1974, 1977). However, the kingdom for the nuclear matrix-associated proteins is much more complicated. Different preparation procedures can result in different compositions of nuclear matrixes (Tsutsui, Sano, and Tsutsui 2005). Followed the study, scientists have identified more proteins as nuclear matrix-associated proteins, including nuclear matrix proteins and MAR binding proteins.

Nuclear matrix proteins have been well studied by nuclear matrix proteomic analysis. A nuclear matrix protein database (NMPdb) was established and found around 400 nuclear matrix proteins from 3000 scientific articles in PubMed (Mika and Rost 2005). Experimental analysis shows that lamins (Hozak et al. 1995), actin (Amankwah and De Boni 1994), proteins of nuclear ribonucleoproteins (RNP) particles (He, Martin, and Penman 1991; Mattern et al. 1996; Mattern et al. 1997), matrins (Nakayasu and Berezney 1991; Zeitz et al. 2009), DNA topoisomerase II (Berrios, Osheroff, and Fisher 1985; Feister et al. 2000), and some other proteins (Albrethsen, Knol, and Jimenez 2009) are components of nuclear matrix proteins in animals. In *Arabidopsis*, proteins identified from proteomic analysis of the nuclear matrix show a high correlation of proteins associated with the nucleolus, including IMP4, Nop56, fibrillarins, nucleolin, homologs of eEF-1, HSP/HSC70, DnaJ, ribosomal components and a putative histone deacetylase (Calikowski, Meulia, and Meier 2003).

MAR binding proteins can recruit MAR-included DNA elements to the nuclear matrix (Tsutsui, Sano, and Tsutsui 2005). These proteins usually contain AT-hook motifs, which can specifically bind to the AT-rich DNA sequence (Razin et al. 2014). They can also interact with other proteins and RNA to form larger complexes, serving as functional domains involved in multiple cellular processes such as gene transcription and expression, packaging of the chromosome, cell development, and cell apoptosis (Tsutsui, Sano, and Tsutsui 2005; Wang et al. 2010). MAR binding proteins can be detected from nuclear matrix proteomic data, together they are called as nuclear matrix associated proteins. In animals, several MAR binding proteins have been identified (Wang et al. 2010). AT-hook motif-containing special AT-rich sequence-binding protein 1 (SATB1) and scaffold attachment factor A (SAF-A)/HNRNPU are the most studied. SATB1 is mainly expressed in the thymus and plays an important role in transcriptional regulation, chromatin organization, and histone modification (Dickinson et al. 1992; Yasui et al. 2002; Cai, Han, and Kohwi-Shigematsu 2003; Kumar et al. 2007; Han et al. 2008; Kohwi-Shigematsu et al. 2012). SAFA recruits MARs to different regions of the matrix compartment with multiple binding partners (Martens et al. 2002; Helbig and Fackelmayer 2003). Additionally, SAFA interacts with chromatin-associated RNAs and non-coding RNAs to regulate 3D chromatin architecture (Hacisuleyman et al. 2014; Fan et al. 2018). Another nuclear matrix-associated protein SAFB, sharing similar domains as SAFA,

cooperates with non-coding RNAs to stabilize heterochromatin architecture through phase separation (Huo et al. 2020). In plants, tomato MAR binding filament-like protein 1 (MFP1), a MAR DNA binding protein, is associated with speckle-like structures at the nuclear periphery through the conserved N-terminal domain (Meier et al. 1996; Gindullis, Peffer, and Meier 1999). Wheat AT hook-containing MAR binding protein1 (AHM1) binds to MARs through C-terminal AT-hook and functions between the intranuclear framework and MARs (Morisawa et al. 2000). Arabidopsis AT-hook motif nuclear-localized proteins (AHLs) also preferably bind to MARs (Fujimoto et al. 2004; Lim et al. 2007; Xu et al. 2013). However, the molecular mechanisms of MAR binding proteins regulating plant development remain exclusive.

1.2 AT-Hook motif nuclear proteins

The structure of chromatin is dynamic and regulated by different post-translational modifications on histone tails, the replacement of core histones by histone variants, and a wide range of non-histone nuclear proteins (Rosa and Shaw 2013). High mobility group (HMG) proteins are a set of non-histone nuclear proteins. In mammals, HMG proteins are composed of three distinct families, including the HMG-1 box family, HMG-14/-17 family and HMG-I(Y) (a.k.a. HMGA) family (Aravind and Landsman 1998; Bustin 2001). These proteins play important roles in the chromatin structure and act as transcription factor cofactors involved in multiple cellular processes. Among these families, HMGA proteins were shown to bind to the minor groove of short stretches of AT-rich DNA via a highly conserved motif called an AT-hook motif (Aravind and Landsman 1998). This core AT-hook motif is conserved in proteins found in mammals to plants and is not unique to HMGA proteins. Such non-HGMA proteins include transcription factors and chromatin remodeling proteins (Cairns et al. 1999; Singh, D'Silva, and Holak 2006; Su et al. 2006).

1.2.1 AT-hook Motif Nuclear Localized proteins (AHLs) in plants

During land plant evolution, AHLs are set of non-HGMA proteins and conserved in all sequenced land plants, ranging from the early-diverging *Physcomitrella patens* and *Selaginella* to a variety of monocot and dicot flowering plants, such as *Arabidopsis thaliana*, *Sorghum bicolor*, *Zea mays*, and *Populus* trichocarpa (Gallavotti et al. 2011; Zhao et al. 2014). Members of AHL proteins contain two conserved structural units, the AT-hook motif that enables binding to AT-rich DNA and a Plant and Prokaryotic Conserved (PPC) domain, also referred to as Domain of Unknown Function #296 (DUF296) (Zhao et al. 2013; Zhao et al. 2014). Based on the number and composition of these two structural units, AHL proteins are classified into three types (type I/type II/type III). After the separation of *Physcomitrella patens* from the vascular plant lineage, they are further grouped into two different clades: Clade A (type I) and Clade B (type II and type III). AHL proteins from different land plants share conserved functions in plant development (Zhao et al. 2014).

The *Arabidopsis thaliana* genome encodes 29 AHL proteins with the two conserved functional units. They are classified into two clades. Clade A AHLs are intronless with only one AT-hook motif and a single PPC/DUF296 domain, including AHL15 to AHL29. Clade B AHLs are intron-containing AHLs with either one or two AT-hook motif(s) and a single PPC/DUF296 domain, including AHL1 to AHL14 (Figure 1.3) (Zhao et al. 2013).
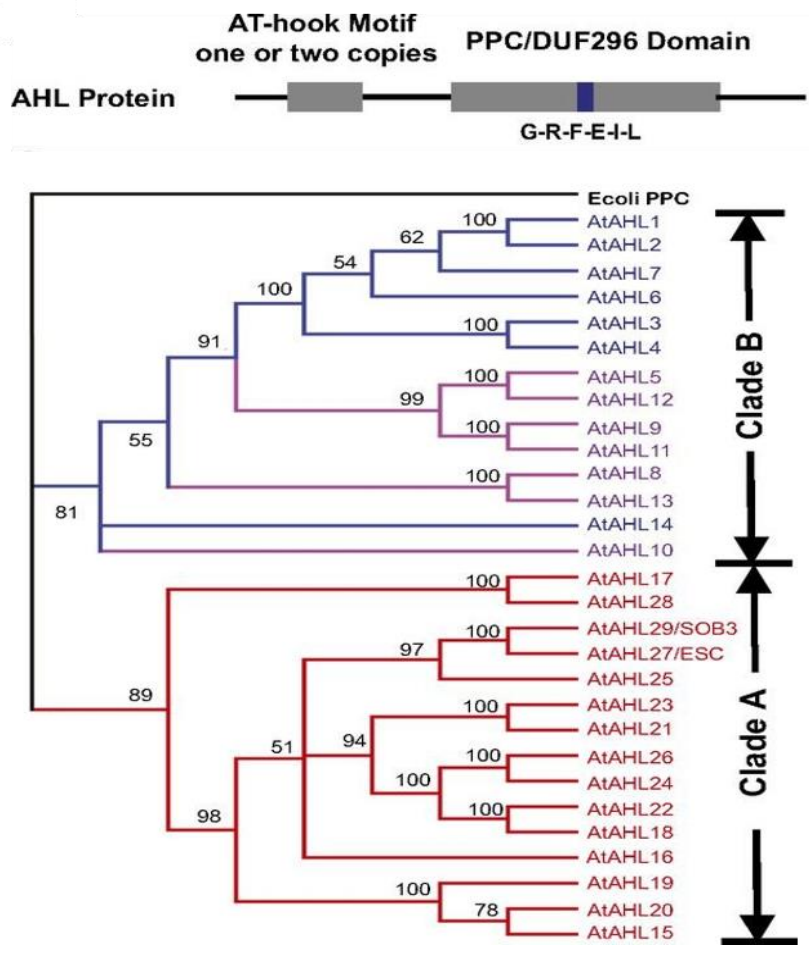
Figure 1.3. The AHL gene family in *Arabidopsis thaliana*.
Structures of the AHL proteins. A conserved six-amino-acid region in the PPC/DUF296 domain is highlighted by the blue box (top panel). Phylogeny of the AHL gene family using Bayesian analysis (bottom panel). Modified from (Zhao et al. 2013).

The AT-hook motif is important for DNA-protein interaction. The mutation of the core RGRP sequence to RGAA within the AT-hook motif of AHL22 abolishes the binding of AHL22 to the promoter region of *FLOWERING LOCUS T* (*FT*) (Yun et al. 2012). Another mutation *sob3-6* (mutation of AHL29), was first screened by an ethyl methanesulfonate (EMS) mutagenesis for suppressors of the short-hypocotyl phenotype caused by overexpression of SOB3 in the *phyB-4* background. The *sob3-6* allele contains an arginine to histidine (R77 to H) mutation in the central amino acid of the AT-hook motif, causing an extremely longer hypocotyl phenotype (Street et al. 2008). A similar phenotype was observed in the SOB3 paralog ESC when the

substitution of arginine disrupted the AT-hook motif to histidine (R91 to H) (Zhao et al. 2013).

The PPC domain is crucial for protein-protein interaction. AHL proteins interact with other non-AHL DNA binding proteins, including core histones and transcription factor TCP4. In the PPC domain, a conserved six-amino-acid region, Gly-Arg-Phe-Glu-Ile-Leu (G-R-F-E-I-L) (Figure 1.3), is required to interact between SOB3 or ESC and TCP4. However, the deletion of this six-amino-acid region does not disrupt the interaction between AHL proteins (Zhao et al. 2013).

1.2.2 Function of Arabidopsis AHLs

Arabidopsis AHLs are involved in multiple aspects of plant development. Until now, 13 AHL members have been characterized, including AHL1, AHL3, AHL4, AHL10, AHL15, AHL16 (TRANSPOSABLEELEMENT SILENCING VIA AT-HOOK/TEK), AHL18, AHL19, AHL20, AHL22, AHL25, AHL27 (ESCAROLA/ESC) and AHL29 (SUPPRESSOR OF PHYTOCHROME B4-#3/SOB3) (Table 1.1). AHLs are highly functionally redundant. Therefore, the function of most AHLs are analyzed from the overexpression of individual *AHL* genes.

Nine AHL members from clade A were characterized (Table 1.1). In the flowering time and flower development, overexpression of AHL20 or AHL22 delays the flowering time by repressing the expression of *FLOWERING LOCUS T* (FT) (Xiao et al. 2009; Yun et al. 2012; Tayengwa et al. 2020). The reduction of *FT* is modulated by the reduced level of H3 acetylation and elevated H3K9me2 level in the *FT* chromatin via the interaction between AHL22 and histone deacetylases (HDA6, HDA9, HDA19) (Yun et al. 2012). Besides, AHL22 acts as floral repressors in the vernalization pathway to promote flowering (Xi et al. 2020). By contrast, in *Arabidopsis Landsberg erecta*, knockdown of *AHL16/TEK* leads to late flowering by activating the TE-like repeat-containing floral repressor genes *FLOWERING LOCUS C* (*FLC*), *FWA*, *MADS AFFECTING FLOWERING 4* (*MAF4*) and *MAF5*, through increased histone H3 acetylation, reduced H3K9me2 and DNA hypomethylation. Like AHL22, TEK can also interact with retinoblastoma-associated proteins (FVE and MSI5) that mediate histone deacetylation (Xu, Gan, and Ito 2013; Xu et al. 2013). In regulating hypocotyl elongation, AHLs function redundantly to repress hypocotyl growth. Loss-of-function analysis with multiple-AHL-null mutants shows a slightly increased hypocotyl growth under light and shorter than the phenotype of a dominant-negative *sob3-6* mutant (Street et al. 2008; Zhao et al. 2013). The molecular mechanism behind this repression is that AHLs suppress the expression of *YUCCA8* (*YUC8*) and members of the *SMALL AUXIN UP-REGULATED RNA19* (*SAUR19*) subfamily through the auxin signaling pathway (Favero et al. 2016). The expression of the *SAUR19* subfamily can also be affected by brassinosteroid signaling, indicating an interaction between signaling pathways in AHL-dependent hypocotyl regulation (Favero, Le, and Neff 2017). Additionally, SOB3 and ESC associate with ATP-dependent chromatin

remodeling to regulate the expression of an auxin biosynthesis gene *YUC9* to inhibit hypocotyl elongation (Lee and Seo 2017).

Table 1.1. Summary of AHLs known functions in *Arabidopsis thaliana*.

Gene ID	Function	Reference
AHL1	MAR binding protein	(Fujimoto et al. 2004)
AHL3	Vascular Tissue Patterning	(Zhou et al. 2013)
AHL4	Vascular Tissue Patterning	(Zhou et al. 2013)
AHL10	Reproductive isolation	(Jiang et al. 2017),
	Stress growth regulation	(Wong et al. 2019)
AHL29/SOB3	Hypocotyl elongation	(Street et al. 2008; Zhao et al. 2013;
	Petiole growth	Favero et al. 2016; Favero, Le, and Neff 2017; Lee and Seo 2017), (Favero et al. 2020)
AHL27/ESC	Hypocotyl elongation	(Street et al. 2008; Zhao et al. 2013;
	Leaf senescence	Lee and Seo 2017), (Lim et al. 2007)
AHL25	homeostasis of GAs	(Matsushita et al. 2007)
AHL22	Flowering time	(Xiao et al. 2009; Yun et al. 2012),
	Hypocotyl elongation	(Xi et al. 2020)
AHL18	Root system architecture	(Sirl et al. 2020)
AHL16/TEK	Flowering time	(Xu, Gan, and Ito 2013; Xu et al. 2013),
	TE silencing	(Jia et al. 2014; Lou et al. 2014; Xiong
	nexine formation	et al. 2020)
AHL19	Plant defense	(Yadeta et al. 2011)
AHL20	Flowering time	(Tayengwa et al. 2020),
	Plant immunity	(Lu, Zou, and Feng 2010)
AHL15	Plant longevity	(Karami et al. 2020),
	Somatic embryogenesis	(Karami et al. 2021),
	Genome duplication	(Rahimi et al. 2022)
	Secondary xylem formation	

In addition, AHLs are involved in other developmental processes. SOB3 and other AHLs restrict petiole growth by antagonizing PIF4-mediated transcriptional activation related to growth and plant hormone pathways, such as cell growth, cell wall metabolism, auxin signaling, BR signaling, and ethylene signaling (Favero et al. 2020). Overexpression of *ESC* negatively regulates leaf senescence by modifying the chromatin architecture (Lim et al. 2007). The expression pattern of *AHL18* provides a function in the modulation of root system architecture through regulation of root apical meristem activity and lateral root development (Sirl et al. 2020). AHLs play a dual role in plant defense. Overexpression of *AHL19* enhances the resistance to the vascular wilt species *Verticillium dahliae* and positively regulates plant defense (Yadeta et al. 2011). However, overexpression of *AHL20* enhances the susceptibility to virulent *Pseudomonas syringae* bacteria and negatively regulates plant defenses (Lu, Zou, and Feng 2010). AHL25/AGF1 (AT-hook protein of GA feedback regulation 1)

plays a role in maintaining the negative feedback of GA 3-oxidase in gibberellin signaling (Matsushita et al. 2007). Instead of flowering time and repeat-containing genes silencing in *Arabidopsis Landsberg erecta* ecotype, TEK is essential for nexine formation in the development of pollen wall in Col-0 by regulating the expression of Arabinogalactan proteins (AGPs) positively and CALLOSE SYNTHASE5 (CalS5) negatively (Jia et al. 2014; Lou et al. 2014; Xiong et al. 2020).

Recent studies showed that AHL15 suppresses axillary meristems (AMs) maturation and promotes the plant's lifespan by acting downstream of flowering genes (*SOC1*, *FUL*) and upstream of the plant gibberellic acid pathway (Karami et al. 2020). Overexpression of *AHL15* induces somatic embryogenesis (SE) and polyploidization by acting as downstream targets of BABY BOOM (BBM) and heterochromatin decondensation (Karami et al. 2021). Moreover, AHL15 is required for secondary xylem formation via promoting cytokinin levels in controlling vascular cambium activity (Rahimi et al. 2022).

Clade B has four characterized AHL members (Table 1.1). AHL1 was first screened by random GFP:: cDNA fusions and functions as MAR binding protein in interphase nuclei, covering the chromosomes during mitosis (Fujimoto et al. 2004). AHL4 interacts with AHL3 to facilitate intercellular trafficking and co-regulate vascular tissue boundaries in *Arabidopsis thaliana* roots (Zhou et al. 2013). AHL10 is involved in post-zygotic reproductive isolation by interacting with ADMETOS (ADM) and SET domain-containing SU(VAR)3–9 homolog SUVH9, leading to the accumulation of H3K9me2 at TEs (Jiang et al. 2017). Moreover, phosphorylation of AHL10 S314 affected by Highly ABA-Induced 1 (HAI1) is required for plant stress growth regulation (Wong et al. 2019).

1.2.3 Auxin and hypocotyl elongation

Molecular genetic studies reveal that Arabidopsis AHLs are involved in multiple plant hormone signaling pathways. Of which, auxin signaling plays an important role in hypocotyl elongation. Auxin is a key regulator of plant development which influences cell division, cell elongation, programmed cell death, etc. (Paponov et al. 2008). Arabidopsis hypocotyl elongation is predominantly controlled by cell elongation rather than cell division (Gendreau et al. 1997). Cell elongation is strictly controlled in hypocotyl through precise transcriptional regulation of genes associated with cell elongation, and auxin is involved in this transcriptional regulation.

The biosynthesis of auxin is well established by a Trp-dependent pathway: the TAA/YUC (TRYPTOPHAN AMINOTRANSFERASE OF ARABIDOPSIS/YUCCA) pathway (Zhao 2018; Casanova-Saez and Voss 2019). This pathway consists of two steps. First, Trp is metabolized into indole-3-pyruvate (IPyA) by aminotransferases from the TAA family. Second, IPyA undergoes oxidative decarboxylation catalyzed by the YUC family of flavin-containing monooxygenases to produce Indole-3-acetic acid (IAA) (Zhao et al.

2001; Zheng et al. 2013; Zhao 2018). Arabidopsis AHLs repress auxin biosynthesis genes *YUC8* and *YUC9* to negatively regulate auxin biosynthesis and inhibit hypocotyl elongation (Favero et al. 2016; Lee and Seo 2017). The concentration of auxin is crucial for plant growth. Low concentrations of exogenous auxin usually promote growth, whereas high concentrations inhibit growth (Lincoln, Britton, and Estelle 1990; Collett, Harberd, and Leyser 2000).

The maintenance of auxin begins with TRANSPORT INHIBITOR RESPONSE 1/AUXIN SIGNALING F-BOX (TIR1/AFB) binding to auxin directly. TIR1 and auxin can interact with another auxin receptor AUX/IAA repressor proteins (Dharmasiri, Dharmasiri, and Estelle 2005; Kepinski and Leyser 2005). AUX/IAA proteins are ubiquitinated by a ubiquitin-protein ligase E3 called SCF$^{TIR1/AFB}$, leading to protein degradation by the 26S proteasome (Gray et al. 2001; Maraschin Fdos, Memelink, and Offringa 2009). This degradation releases auxin response factors (ARFs) to activate the transcription of auxin-response genes.

SMALL AUXIN UP RNA (*SAUR*) genes are a set of auxin-response genes that are the direct targets of ARFs induced by auxin. In Arabidopsis, there are 81 *SAURs* with two pseudogenes (Hagen and Guilfoyle 2002). Among these genes, the SAUR19 subfamily, including SAUR19 to SAUR24, promotes hypocotyl elongation by cell expansion (Spartz et al. 2012; Spartz et al. 2014). The acid growth mechanism proposes mechanistic insight into SAUR-mediated cell expansion. SAURs promote apoplast acidification by interacting with type 2C protein phosphatases (PP2Cs) and reducing their ability to dephosphorylate and deactivate H$^+$-ATPases in the plasma membrane. These H$^+$-ATPases are crucial for cell expansion through pumping protons from the cytoplasm into the apoplast. The blocking of protons from the cytoplasm into the apoplast results in a decreased level of pH in the apoplastic, leading to cell expansion (Rayle and Cleland 1970; Rayle and Cleland 1980, 1992; Spartz et al. 2014). Recently, a study showed that SAUR15 interacts with BRASSINOSTEROID-INSENSITIVE 1 (BRI1), promoting direct activation of plasma membrane H$^+$-ATPase (PM H$^+$-ATPase) via phosphorylation, resulting in cell expansion (Li et al. 2022). Arabidopsis AHLs repress hypocotyl elongation by direct binding to *SAUR19* subfamily genes and negatively regulating their expression through both auxin and BR signaling pathways (Moreno-Romero et al. 2016; Favero, Le, and Neff 2017; Lee and Seo 2017).

1.3 Histone modifications

In eukaryotes, chromatin is a highly condensed structure composed of DNA and histones and involved in many nuclear activities, such as replication, transcription, and DNA repair (Luger, Mader, et al. 1997; Marmorstein 2001). The basic unit of chromatin is the nucleosome which consists of 147 base pairs of DNA wrapped around a histone octamer (Cutter and Hayes 2015). The histone octamer is composed of two sets of core histone proteins (H2A, H2B, H3 and H4) (Luger, Rechsteiner, et al. 1997). Nucleosomes are linked by linker DNA and histone H1, further condensing into

a higher-order chromosome structure (Oudet, Gross-Bellard, and Chambon 1975; Luger and Hansen 2005). By packaging nucleosomes, chromatin exits in at least two distinct functional forms: a condensed form called heterochromatin and a looser form called euchromatin. The amino-terminal tails of the core histones undergo various post-translational modifications, such as methylation, acetylation, ubiquitination, phosphorylation, sumoylation and ADP-ribosylation, which play a cruicial role in chromatin structure and function (Jenuwein and Allis 2001) (Figure 1.4). These modifications are deposited, removed,   and interpreted by their writers, erasers, and readers, respectively (Xiao, Lee, and Wagner 2016). Among these modifications, histone methylation and acetylation are the most-studied histone marks in both metazoans and plants.

Active marks

Histone acetylations, H3K4me3, H3K36me2/3

Repressive marks

H3K9me2, H3K27me3
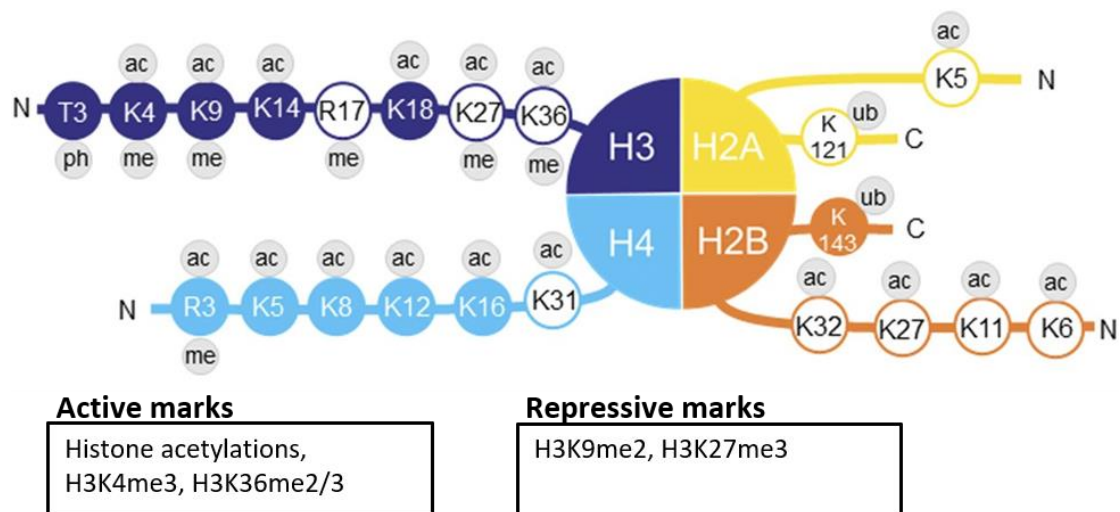
Figure 1.4. Modifications at the tails of core histones (H2A, H2B, H3, H4) with active or repressive marks, including methylation (me), acetylation (ac), ubiquitination (ub), and phosphorylation (ph). Modified from (Ueda and Seki 2020).

1.3.1 Histone methylation

Histone methylation plays a fundamental role in plant development by influencing gene expression and chromatin landscape. On histone tails, methylation was found on lysine (K) and arginine (R) to different extents. Lysine can be mono-, di- or trimethylated, whereas arginine can be only mono- and dimethylated (Kouzarides 2007; Xiao, Lee, and Wagner 2016). The methylation at histones lysines are well studied and can be classified into both transcriptional activation marks (H3K4 and H3K36) and repression marks (H3K9 and H3K27) (Liu et al. 2010; Bannister and Kouzarides 2011) (Figure 1.4). I will further focus on the regulation of histone lysine methylation.

Histone methylation writers

The enzymes responsible for histone lysine methylation are histone lysine methyltransferases (HKMTs) which are a large family of SET Domain Group (SDG) proteins conserved in both animals and plants (Ng et al. 2007).

H3K4 methylation has three types of methylation, H3K4me1, H3K4me2, and H3K4me3. They are mostly distributed in genic regions. H3K4me2/3 are enriched at the promoters and 5' end of coding genes, whereas H3K4me1 is located at the gene body (Li et al. 2008; Zhang et al. 2009). In general, H3K4me3 is highly correlated with active gene expression, while H3K4me1/2 is enriched in both active and inactive genes (Li et al. 2008; Zhang et al. 2009). Several SDGs write H3K4me in Arabidopsis. ARABIDOPSIS TRITHORAX1 (ATX1) deposits H3K4me3 while ATX2 writes H3K4me2 in the genome (Saleh et al. 2008). SDG2, SDG25, SDG26, and SDG4 can add multiple methyl groups to H3K4 or are required for other lysine methylation, like H3K36me (Cartagena et al. 2008; Tamada et al. 2009; Berr et al. 2010; Berr et al. 2015).

H3K36 methylation has three types methylation H3K36me1, H3K36me2, and H3K36me3 in Arabidopsis. For H3K36me2/3, the major H3K36me is added by SDG8 (Dong, Ma, and Li 2008; Xu et al. 2008). ASH1-related protein 3 (ASHR3) is reported to be a writer of H3K36me1 (Kumpf et al. 2014). H3K36me2/3 are associated with active gene expression and transcription elongation. The distribution of H3K36me2 and H3K36me3 is in actively transcribed genes with a preference for 3' end and 5' end of genes, respectively (Sequeira-Mendes et al. 2014).

H3K9 methylation occurs in both animals and plants as H3K9me1, H3K9me2, and H3K9me3. Compared to mammalian H3K9me3, which is the most abundant K9 methylation in constitutive heterochromatin (Peters et al. 2003; Rice et al. 2003), a little H3K9me3 can be detected in euchromatic regions in plants (Johnson et al. 2004). In Arabidopsis, most H3K9 methylation is H3K9me1/2 which has a conserved function as a silenced mark in heterochromatic regions (Jackson et al. 2004; Fuchs et al. 2006). Consistent with its function, H3K9me2 is enriched in transposons and repeated sequences (Lippman et al. 2004; Bernatavichute et al. 2008). KRYPTONITE (KYP), also known as SU(VAR)3-9-HOMOLOG 4 (SUVH4), was first identified as H3K9me2 methyltransferase. SUVH5 and SUVH6, two close homologs of SUVH4, play minor roles in establishing H3K9me2 (Jackson et al. 2002; Stroud et al. 2014; Li, Harris, et al. 2018). SU(VAR)3-9-RELATED protein 5 (SUVR5) can deposit H3K9me2 in a DNA methylation–independent manner (Caro et al. 2012). SUVR4 has a methyltransferase preference for H3K9me1, which convert it into H3K9me2 (ubiquitin) and H3K9me3 (without ubiquitin) *in vitro* (Thorstensen et al. 2006).

H3K27 methylation is another repressive histone mark in animals and higher plants. Like the other lysine methylations, H3K27 can also be methylated to H3K27me1, H3K27me2, and H3K27me3. In Arabidopsis, H3K27me1 is enriched in pericentromeric heterochromatin, which is essential for genome stability (Jacob et al. 2010; Dong et

al. 2021; Davarinejad et al. 2022). The enzymes writing H3K27me1 are ARABIDOPSIS TRITHORAXRELATED PROTEIN 5 (ATXR5) and ATXR6 (Jacob et al. 2009). Unlike H3K27me1, H3K27me3 localizes to the genic regions with a preference for the 5' end of genes and plays a role in transcription repression, which is involved in multiple cellular processes (Turck et al. 2007; Zhang et al. 2007; Mozgova, Kohler, and Hennig 2015; Xiao and Wagner 2015). The deposition of H3K27me3 is controlled by the evolutionarily conserved Polycomb Repressive Complex 2 (PRC2), consisting of three catalytic subunits: CURLY LEAF (CLF), SWINGER (SWN), and MEDEA (MEA) (Goodrich et al. 1997; Grossniklaus et al. 1998; Pien and Grossniklaus 2007; Margueron and Reinberg 2011). Although PRC2 may also contribute to the deposition of H3K27me2 in euchromatin, the primary writer of H3K27me2 remains unidentified (Lindroth et al. 2004).

Histone methylation erasers

Most covalent histone modifications are reversible. To stabilize the chromatin environment, histone methylation is dynamically controlled by the writers (histone methyltransferases) and the erasers (histone demethylases). In Arabidopsis, the erasers include two types of demethylases. Lysine-specific demethylase1 (LSD1) has four members: FLOWERING LOCUS D (FLD) and LSD1-LIKE 1/2/3 (LDL1/2/3) (Shi et al. 2004). Another type is a group of 21 Jumonji C (JmjC) domain-containing proteins, including five subfamilies (KDM5/JARID1 group, KDM4/JHDM3 group, KDM3/JHDM2 group, JMJD6 group, and JmjC domain-only group) (Tsukada et al. 2006).

H3K4 demethylation is catalyzed by multiple demethylases. FLD and LDL1/2 are responsible for removing H3K4me1/2 to repress *FLC* gene expression in flowering time control (He, Michaels, and Amasino 2003; Jiang et al. 2007; Liu et al. 2007). Apart from LSD1 proteins, JMJ14/15 can remove all types of H3K4 methylation. JMJ18 removes H3K4me2/3 regarding flowering time and gametophyte development (Lu et al. 2010; Yang, Han, et al. 2012; Yang, Mo, et al. 2012). H3K36 demethylation is still unclear in Arabidopsis. In animals, H3K36me1/2 are removed by KDM2/JHDM1 proteins which are not found in Arabidopsis (Lu et al. 2008). Studies showed that JMJ30, a protein related to the circadian period and flowering time, can reduce the level of H3K36me2. However, the activity of JMJ30 in removing H3K36me is still under debate (Lu, Knowles, et al. 2011; Gan et al. 2014; Yan et al. 2014).

H3K27 demethylation is mainly catalyzed by KDM4/JHDM3 group proteins. Early Flowering 6 (ELF6/JMJ11) and its close homolog Relative of Early Flowering 6 (REF6/JMJ12) are two major erasers responsible for H3K27me2/3 demethylation and play contrary roles in the regulation of flowering time (Noh et al. 2004). REF6 promotes flowering time by repressing *FLC* expression, while ELF6 represses flowering time in a photoperiod-dependent pathway (Noh et al. 2004; Lu, Cui, et al. 2011; Mozgova, Kohler, and Hennig 2015). The divergent roles result from their target's preference. Moreover, the demethylation activity of REF6 is essential for

thermomorphogenesis in Arabidopsis. The other JMJ protein from the same family, JMJ13, also acts as H3K27me3 demethylase in repressing flowering time (Yan et al. 2018). Thus, the three proteins display pleiotropic, redundant functions in plant development. Besides the KNM4/JHDM3 family proteins, JMJ30 and JMJ32 demethylate H3K27me3 levels at the *FLC* locus in response to higher temperature stimuli (Gan et al. 2014).

H3K9 demethylation is removed by KDM3/JHDM2 group proteins, including Increase in Bonsai Methylation 1 (IBM1/JMJ25), JMJ27, JMJ28, JMJ29, and JMJ24. Among the family, IBM1 is essential for the demethylation of H3K9me1/2 to prevent the accumulation of H3K9me1/2 and CHG DNA methylation on active genes (Saze et al. 2008; Miura et al. 2009). Consistent with its function, the phenotype of *ibm1* can be suppressed by mutants of *KYP* and *DMTases CHROMOMETHYLASE 3* (*CMT3*) (Saze et al. 2008). JMJ27 displays H3K9me1/2 demethylase activity and modulates defense against pathogens and flowering time regulation (Dutta et al. 2017). JMJ28 interacts with the FBH transcription factors to remove H3K9me2 from the *CO* locus (Hung et al. 2021). Moreover, the H3K27 demethylases REF6 and ELF6 are capable of removing H3K9me3 in brassinosteroid signaling (Yu et al. 2008).

Histone methylation readers

The histone methyltransferase and demethylases maintain the dynamics of histone methylation. These epigenetic marks usually recruit some proteins (readers) for the proper downstream function. Unlike the writers and erasers with a specific family of proteins, the readers vary in different types of proteins based on the containing domains. In plants, domains that recognize histone lysine methylation include Chromodomain, Tudor domain, Malignant Brain Tumor (MBT), PWWP (Pro-Trp-Trp-Pro), Agenet, the Plant Homeodomain finger (PHD), Bromo-Adjacent Homology (BAH), and WD40 (Taverna et al. 2007; Yun et al. 2011). H3K4 methylation readers mostly are PHD finger domain-containing proteins. Arabidopsis ORC1, the large subunit of the origin recognition complex function in initializing DNA replication, can bind to H3K4me3 through the PHD finger domain and active gene expression (de la Paz Sanchez and Gutierrez 2009). WDR5a, a homolog of human COMPASS-like complexes, binds H3K4 methylated peptides to establish the winter-annual growth habit (Jiang, Gu, and He 2009). Alphin1-like proteins (ALs) bind H3K4me3 and influence seed maturation genes (Molitor et al. 2014). AtING1 and AtING2 can also bind H3K4me2/3 *in vitro* (Lee et al. 2009). Two other PHD domain-containing proteins, SHORT LIFE (SHL) and EARLY BOLTING IN SHORT DAYS (EBS) recognize H3K4me2/3 and function in the repression of flowering genes (Lopez-Gonzalez et al. 2014).

H3K36 methylation readers are chromo domain-containing proteins. In Arabidopsis, MORF4-related gene 1 (MRG1) and MRG2 bind to H3K36me3 and interact with H4-specific acetyltransferases (HAM1 and HAM2) to function redundantly in the activation of flowering time genes (Bu et al. 2014; Xu et al. 2014). Moreover, MRG1/2

can bind to H3K4me3 *in vitro* (Bu et al. 2014). A recent study shows that MRG2 interacts with NAP1-RELATED PROTEIN 1 (NRP1) and NRP2, members of the NUCLEOSOME ASSEMBLY PROTEIN 1 (NAP1) family, and may be involved in transcriptional activation of gene genome-widely (An et al. 2020).

H3K27 methylation readers include LIKE HETEROCHROMOTIN PROTEIN 1 (LHP1), EBS, and SHL. LHP1 is the only homolog of animal HETEROCHROMOTIN PROTEIN 1 (HP1). Unlike HP1 binding to H3K9me3 methylation in animals, plant PRC1 component LHP1 recognizes H3K27me3 through its chromodomain instead (Turck et al. 2007; Zhang et al. 2007). This binding is required for PRC2-mediated silencing (Mylne et al. 2006). As mentioned for H3K4 methylation readers, EBS and SHL can also bind to H3K27me3 via the BAH domain (Li, Fu, et al. 2018; Qian et al. 2018; Yang et al. 2018). The BAH domain forms a complex with PRC1 component EMBRYONIC FLOWER 1 (EMF1) and mediates genome-wide transcriptional repression, fulfilling a conserved PRC1-like function in higher plants (Li, Fu, et al. 2018). In addition, the BAH-H3K27me3 and PHD-H3K4me3 modules provide insights into a bivalent chromatin reader, which functions as a switch in binding both active and repressive histone marks (Qian et al. 2018; Yang et al. 2018).

H3K9 methylation reader is the plant-specific AGENET DOMAIN CONTAINING PROTEIN 1 (ADCP1) which plays an essential role in heterochromatin formation and transposon silencing by modulating H3K9 and DNA methylation levels (Zhang et al. 2018; Harris and Jacobsen 2019; Zhao, Cheng, et al. 2019). The ADCP1 encodes three pairs of Agenet domains, and each domain binds to H3K9 methylation, mainly H3K9me2 (Zhang et al. 2018; Zhao, Cheng, et al. 2019). The mechanism for how ADCP1 promotes silencing is still unclear. Since *adcp1* itself shows a loss of H3K9me2 and non-CG methylation. Scientists raised many possibilities to answer the question. One is that ADCP1 mediates heterochromatin phase separation and promotes the activity of H3K9 methylation writers and DNA methyltransferases (Harris and Jacobsen 2019; Zhao, Cheng, et al. 2019). Thus, ADCP1 functions equivalently to animal HP1 in the readout of the heterochromatic mark H3K9 methylation.

1.3.2 Histone acetylation

Another histone modification highly related to gene expression is histone acetylation which consists of an acetyl group (acetyl-CoA) on the lysine residues of histone N-terminal tails and functions as a hallmark of transcriptional activation. Acetylation occurs on all types of histones (H2A, H2B, H3, H4). Like other histone modifications, histone acetylation is also reversible. The acetyl group is deposited by Histone Acetyltransferases (HATs) and removed by Histone Deacetylases (HDACs), respectively (Bjerling et al. 2002; Pandey et al. 2002; Kouzarides 2007). HATs neutralize the positive charge of the core histones via adding the acetyl group, resulting in a less compact DNA-histone interaction (open chromatin state). This open chromatin state allows RNA polymerase and transcription factors to bind more

efficiently to genes to promote transcription (Eberharter and Becker 2002; Clayton, Hazzalin, and Mahadevan 2006). By contrast, HDACs remove the acetyl group from histone, causing gene repression by blocking the binding of RNA polymerase and transcription factors to genes (Gallinari et al. 2007). Thus, HATs and HDACs determine genome accessibility and are associated with gene activation and repression, respectively.

Histone acetyltransferases

Arabidopsis histone acetyltransferases include 12 HATs and are classified into four types: GNAT (GCN5-related N-terminal acetyltransferases), MYST (MOZ, Ybf2/Sas3, Sas2, and Tip60-related), CBP (p300/CREB-binding protein), and TAF1 (TATA-binding protein-associated factor) (Servet, Conde e Silva, and Zhou 2010; Boycheva, Vassileva, and Iantcheva 2014). These four groups of HATs are symbolized by HAG, HAM, HAC, and HAF, respectively (Pandey et al. 2002). HAG contains General Control Nondepressible 5 (GCN5, also named HAG1), Elongator complex protein 3 (ELP3, also named HAG3), and HAG2; HAM contains HAM1 and HAM2; HAC contains HAC1, HAC2, HAC4, HAC5, and HAC12; HAF contains HAF1 and HAF2 (Servet, Conde e Silva, and Zhou 2010; Boycheva, Vassileva, and Iantcheva 2014). These HATs possess different domains and function differently in various aspects of plant development.

As the most studied HATs in Arabidopsis, GCN5 regulates genome stability and mediates several signaling-induced gene expression pathways. A recent study shows that GCN5 mediates transcriptional de-repression and genomic instability under the absence of H3.1K27me1 by acetylating H3 lysine residues, especially H3.1K27ac and H3.1K36ac (Dong et al. 2021). In signaling pathways, GCN5 forms a complex with (ALTERATION/DEFICIENCY IN ACTIVATION 2a) ADA2a and ADA2b and is required for transcription activation (Mao et al. 2006). In auxin signaling, ADA2b is required for histone acetylation at several auxin-responsive loci (Anzola et al. 2010). The transcription factor bZIP11 recruits the ADA2b-GCN5 complex to auxin-responsive genes such as *GH3.3* and *IAA3*, resulting in an increased H3K27ac level and RNA polymerase II activity (Weiste and Droge-Laser 2014). In light signaling, GCN5 regulates H3K9, H3K27, H4K12, and H3K14 acetylation on the promoter regions of light-inducible genes (Benhamed et al. 2006). Under salt stress, GCN5 is required for H3K9/14ac and transcriptional activation of *MYB54*, *CTL1* (*CHITINASE-LIKE PROTEIN 1*), and *PGX3* (*POLYGALACTURONASE INVOLVED IN EXPANSION3*) (Zheng et al. 2019). In addition, during callus development, GCN5 increases the expression of root meristem genes, *WOX5/14* (*WUSCHEL RELATED HOMEOBOX 5/14*), *SCR* (*SCARECROW*), and *PLT1/2* (*PLETHORA 1/2*) by accumulating histone acetylation (Kim et al. 2018). Moreover, GCN5 is also essential for heat stress response (Hu et al. 2015). The other HATs are similar to GCN5, which is involved in various signaling pathways to regulate plant development.

Histone deacetylases

Arabidopsis histone deacetylases include 18 HDACs and are classified into three sub-families: Reduced Potassium Dependence3/Histone Deacetylase-1 (RPD3/HDA1), NAD-dependent Sirtuin-like HDACs (SIR2), and a plant-specific histone deacetylase 2 (HD2). RPD3 contains Class I (HDA6, HDA7, HDA9, HDA10, HDA17, and HDA19), Class II (HDA5, HDA8, HDA14, HDA15, and HDA18), and Class IV (HDA2). SIR2 contains SRT1 and SRT2. Plant-specific HD2 has four members (HD2A, HD2B, HD2C, and HD2D) (Pandey et al. 2002; Jiang et al. 2020; Kumar, Thakur, and Prasad 2021). As most HDACs lack a DNA binding domain, they require transcription factors and/or other DNA binding factors to bring them to chromatin and regulate different aspects of biological processes (Pandey et al. 2002; Kagale, Links, and Rozwadowski 2010; Liu et al. 2014).

HDA6 was first identified as involved in transgene silencing by regulating DNA methylation and H3K9me2 (Murfett et al. 2001; Probst et al. 2004) (REF). Moreover, HDA6 interacts with CG methyltransferase MET1 to silence transposable elements (TEs) and repeat sequences (Liu et al. 2012). Furthermore, HDA6 interacts with the H3K9 methyltransferases SUVH4/5/6 (SU(VAR)3-9 HOMOLOG 4/5/6) to silence TEs through modulating histone H3K9 methylation and H3 deacetylation (Yu et al. 2017). Besides, HDA6 plays a role in plant development and environmental response. HDA6 can interact with FLOWERING LOCUS D (FLD) and the histone binding protein FVE to repress *FLOWERING LOCUS C* (*FLC*) expression (Yu et al. 2011). Together with a complex of LDL1/LDL2 and HDA6, two core clock genes *CIRCADIAN CLOCK-ASSOCIATED1* (*CCA1*) and *LATE ELONGATED HYPOCOTYL* (*LHY*) repress the expression of *TIMING OF CAB EXPRESSION1* (*TOC1*) in the morning (Hung et al. 2018). In turn, TOC1 can work together with the complex to suppress the expression of *CCA1* and *LHY* in the evening (Hung et al. 2019).

HDA9 is also involved in multiple complexes in response to different biological processes. The HDA9-ELF3 (EARLY FLOWERING 3) complex regulates TOC1 expression by targeting the promoter region of TOC1, causing a decreased level of H3ac (Lee, Mas, and Seo 2019). The HDA9-HY5 (ELONGATED HYPOCOTYL 5) complex mediates light-to-dark autophagy by modulating histone H3K9/K27 acetylation level of autophagy-related genes (*ATGs*) (Yang, Shen, et al. 2020). The HDA9-WRKY53 complex binds to genes associated with leaf development and Nod-Like Receptor (NLR) genes involved in plant immunity (Yang, Chen, et al. 2020). The HDA9-PWR (POWERDRESS)-HOS15 (HIGH EXPRESSION OF OSMOTICALLY RESPONSIVE GENES 15) complex regulates numerous biological processes, including seed germination, thermomorphogenesis, flowering time, and leaf senescence (Chen et al. 2016; Kim et al. 2016; Suzuki et al. 2018; Tasset et al. 2018; Mayer et al. 2019; Park et al. 2019).

HDA19 is involved in plant hormone pathways where the HDA19-TPL/TPR (TOPLESS/TOPLESSRELATED) complex functions as a key regulator. HDA19 is required for TPL to regulate apical embryonic fate (Long et al. 2006). In auxin signaling, the

AUXIN/INDOLE-3-ACETIC ACID (Aux/IAA) repressors interact with the HDA19-TPL complex to repress the activity of AUXIN RESPONSE FACTOR (ARF) transcription factors (Szemenyei, Hannon, and Long 2008; Lavy and Estelle 2016). In the brassinosteroid (BR) signaling, BRI1-EMS-SUPPRESSOR1 (BES1) and BZR1 interact with the HDA19-TPL/TPR complex in a BR-enhanced manner (Oh et al. 2014; Ryu et al. 2014). Furthermore, HDA19 interacts with two WRKY transcription factors, WRKY38 and WRKY62, in basal resistance to the bacterial pathogen (Kim et al. 2008).

HDA15 is the most studied HDAC in Class II from the RPD3 subgroup. Like the HDACs from Class I (HDA6, HDA9, HDA19), HDA15 also forms a complex with other co-factors in different plant developments. In light signaling, the localization of HDA15 is driven by light. Under dark treatment, the signal of HDA15 exports from the nucleolar (Alinsug et al. 2012). HDA15 associates with PHYTOCHROME INTERACTING FACTOR3 (PIF3) to repress chlorophyll biosynthesis and photosynthesis gene expression by decreasing the H3 and H4 acetylation levels (Liu et al. 2013). Like PIF3, the HDA15-PIF1 complex negatively regulates the expression of seed germination genes in the dark by reducing the H3ac level (Gu et al. 2017). In the hypocotyl regulation, HDA15 interacts with ELONGATED HYPOCOTYL5 (HY5) and Nuclear Factor-YC homologs (NF-YCs) to repress hypocotyl elongation by targeting the promoter of a set of cell wall organization and auxin signaling genes, causing H4 hypoacetylation and transcription repression (Tang et al. 2017; Zhao, Peng, et al. 2019). Furthermore, in the ABA signaling, HDA15 interacts with transcription factor MYB96 to promote ABA signaling by repressing a subset of RHO GTPASE OF PLANTS (ROP) genes, leading to H3/H4 hypoacetylation and transcription repression (Lee and Seo 2019).

1.4 Aim of the thesis

As nuclear matrix binding protein, AT-hook motif Nuclear Localized proteins (AHLs) in Arabidopsis play essential roles in many aspects of plant development and growth, including flowering time, hypocotyl elongation, vascular tissue patterning, petiole growth, plant immunity and defense, hormonal response, etc. (Table 1.1). The nuclear matrix acts as a supporting structure of nuclei, essential for the DNA compartment and chromatin organization (Narwade et al. 2019). Moreover, the nuclear matrix participates in several cellular processes, such as DNA replication/repair, transcriptional control, and histone modifications (Wasag and Lenartowski 2016). While many targeted genes involved in different aspects of plant growth and development were already identified, the contribution of nuclear matrix and chromatin modifications to their transcriptional regulation remains undiscovered. In this thesis, I aim to:

i) Identify the interactors of the AHL family and understand the function of the AHL complex.
Previous studies have revealed the interactor network of AHL29/SOB3 and AHL27/ESC

by Y2H library screening. I will employ Tandem affinity purification (TAP) followed by mass spectrometric analysis to identify the interactors of one of the AHLs, AHL22. From the physical interaction among different proteins with the AHL22 protein, I will further investigate the function of the AHL complex through genetics and transcriptome analysis.

ii) Isolate nuclear matrix and investigate its role in transcriptional regulation.
In vivo study of nuclear matrix in Arabidopsis remains poorly understood. In this thesis, I will isolate Arabidopsis nuclear matrix and investigate the genome-wide matrix attachment regions (MARs) and nuclear matrix-associated proteins by whole-genome sequencing analysis and LIQUID CHROMATOGRAPHY MASS SPECTROMETRY (LCMS), respectively. I will further validate whether the MARs are associated with transcriptional control by comparing the genome-wide MARs data with transcriptome data.

iii) Reveal the epigenetic signature of the AHL-mediated transcription.
As overexpression of AHL22 positively regulates H3K9me2 accumulation at specific loci to repress gene expression in flowering time regulation. This correlation is because of the interaction between AHL22 and histone deacetylases (HDACs). I will extend the knowledge to other AHL-mediated plant development, like hypocotyl elongation, and identify which HDAC and epigenetic signatures are required for AHL-mediated transcription.

2 Materials and methods

2.1 Plant materials and growth conditions

The *Arabidopsis thaliana* Columbia (Col-0) ecotype was used as the wild type. The following T-DNA mutants were used: *ahl22-1* (SALK_018866), *ahl18-1* (SAIL_779_H11), and *hda15-1* (SALK_004027) were ordered from Nottingham Arabidopsis Stock Center (NASC). *sob3-6* and *sob3-4 esc-8* double mutants were kindly provided by Dr. Michael M. Neff and described in (Zhao et al. 2013). The *frs7-1 frs12-1* double mutant, and overexpression lines of 35S::FRS7-HA and 35S::FRS12-HA were kindly provided by Dr. Rebecca De Clercq and described in (Ritter et al. 2017). Seeds were surface sterilized in a solution containing 75% (v/v) ethanol with 0.1% (v/v) Triton X-100 for 10 minutes and rinsed with 95% ethanol three times before being sown on ½ MS plates (half-strength Murashige and Skoog medium, 1% sucrose, 1% plant agar). The plates were kept at 4°C in the dark for 5 days to synchronize germination before being moved into the Chamber and grown vertically under LD conditions (16h at 23 °C under 22 $\mu mol \cdot m^{-2} \cdot s^{-1}$ continuous white light, 8h at 23 °C dark with 70% humidity) for 5 days.

2.2 Plasmid construction and generation of transgenic plants

Full-length CDS with or without stop codon of *AHL22* (AT2G45430) or *AHL29* (AT1G76500) or *HDA15* (AT3G18520) or *FRS7* (AT3G06250) or *FRS12* (AT5G18960) were cloned into TSK108 or pDonar201 or pENTR/D vector (Invitrogen) entry vector. The deletion of the six-amino-acid region in AHL22 (Δ AHL22) was created from entry vector pDonr-AHL22 via site-directed mutagenesis using the Fast Mutagenesis Kit V2 (Vazyme, C214-02). For overexpression of AHL22 lines (35S::AHL22), constructs were recombined into a pB7WG2 binary vector using the LR reaction kit (Invitrogen, 11791020). The pB7WG2 destination vectors were transformed into *Agrobacterium* strain *GV3101* and then transformed into Arabidopsis Col-0 plants using the floral dip method (Clough and Bent 1998). Transgenic plants were selected on ½ MS plates containing 30 $\mu g \cdot L^{-1}$ Basta. All primers used in this study are listed in Supplementary Table 1.

2.3 Hypocotyl Measurement

After moving the plates into the growth chamber, plated seeds were checked after 2 days, and only those with synchronized germination were included in phenotypic analysis. 5-day-old seedlings were then scanned, and the hypocotyl lengths were quantified using ImageJ software. Three independent measurements were taken with n=30 in each measurement. Statistical analyses were performed by unpaired

two-tailed Student's t-test.

2.4 TAP-MS

For Tandem Affinity Purification (TAP), AHL22 was Gateway-recombined in the pKCTAP vector fused with the GS tag in the C-terminal. TAP experiments were performed on Arabidopsis cell cultures (PSB-D) with protein G-and streptavidin-binding peptide (GS)-tagged bait. Protein interactors were identified by mass spectrometry using an Orbitrap mass spectrometer, and nonspecific background proteins were filtered out as previously described (Van Leene et al. 2015). Two biological replicates were analyzed.

2.5 Bimolecular fluorescence complementation (BiFC)

The full-length coding sequences of AHL22, AHL29, FRS7, FRS12, HDA15 and the deletion version of AHL22 (Δ AHL22) were cloned into the pSITE-nEYFP-N1 or pSITE-cEYFP-C1 vectors (Kerppola 2006) using the LR reaction kit (Invitrogen, 11791020). Constructs were transiently expressed by *A. tumefaciens*-mediated transformation to 1-month-old *N. benthamiana* plants using an infiltration buffer composed of 10 mM MgCl2, 10 mM MES and 100 mM acetosyringone with OD=0.8, and the addition of a Hcpro-expressing *Agrobacterium strain* to boost protein expression. The YFP signal was observed 2-days after infiltration using a Zeiss confocal laser scanning microscope (LSM780). H3.3-RFP was used as the marker protein of the nuclei.

2.6 Co-immunoprecipitation (Co-IP)

To express tag-fused proteins in *N. benthamiana*, the entry vector TSK108-AHL22 fused with 3FLAG and TSK108-FRS7 or TSK108-FRS12 were recombined into a pB7WG2 and a pH7FWG2 binary vector using the LR reaction kit (Invitrogen, 11791020), respectively. *Agrobacterium* strains containing the constructs were co-infiltrated into *N. benthamiana* plant leaves. After 2–3 days, *N. benthamiana* leaves were collected with corresponding expression constructs as indicated. WT indicated *N. benthamiana* leaves without constructs. Co-IPs were performed as previously described in (Potok et al. 2019). Briefly, tissues were ground in liquid nitrogen and resuspended in 5 ml of IP buffer (50 mM Tris HCl pH 7.5, 150 mM NaCl, 5 mM MgCl$_2$, 0. 1 % NP 40, 0.5 mM DTT, 10 % glycerol, 1 mM PMSF, 1 µg/µL pepstatin, proteinase inhibitor cocktail (Roche, 11836145001)). The mixture was incubated on ice for 20 min and centrifuged at 4000g for 10 min at 4 °C. The supernatant was filtered through a double layer of Miracloth. The flow-through was incubated with 25 µl GFP-Trap Magnetic Agarose (Chromotek, gtma-20) overnight at 4 °C. After incubation, beads were collected and washed five times with IP buffer, 5 min each wash at 4 °C with rotation. Elution was performed by incubating beads in

PBS and 4xSDS buffer at 95 °C for 10 min. Western blotting was performed with an anti-GFP (B-2) antibody (SANTA CRUZ sc-9996, 1:50) and anti-FLAG antibody (F1804, Sigma, 1:1000). Signals were detected by the ChemiDoc (BIO-RAD).

2.7 RNA extraction and qRT-PCR analysis

Total RNA from 5-day-old whole plants was extracted using the MagMAX™ Plant RNA Isolation kit (Thermo Fisher #A33784) according to the manufacturer's instructions. Second-strand cDNA was synthesized using the cDNA Synthesis kit (Thermo Fisher, K1612). qRT-PCR reactions contained Solis BioDyne-5x Hot FIREPol®EvaGreen®qPCR Supermix (ROX, Solis BioDyne, 08-36-00008), and the runs were performed in a QuantStudio 6 Flex Real-Time PCR System (Applied Biosystems). Three biological replicates were performed, using GADPH as the reference gene. The primers used are listed in Supplementary Table 1.

2.8 RNA-seq

Total RNA from 5-day-old whole plants was extracted using the RNeasy Plant Mini Kit (Qiagen, 74904). For RNA-seq, libraries were constructed with the VAHTS mRNA-seq V6 Library Prep Kit (Vazyme, NR604-01) according to the manufacturer's instructions. The libraries were sequenced at Novogene (UK) via a Novaseq instrument in 150-bp paired-end mode. Two or three biological replicates were performed.

2.9 Isolation of the nuclear matrix

The nuclear matrix was isolated as previously described in (Pathak, Srinivasan, and Mishra 2014). Briefly, Arabidopsis 5-day-old whole plants grown under LD condition (16h at 23 °C under 22 μmol·m^{-2}·s^{-1} continuous white light, 8h at 23 °C dark with 70% humidity) were collected and chopped in 1 ml LB01 buffer (2 mM Na$_2$EDTA, 20 mM NaCl, 2 mM EDTA, 80 mM KCl, 0.5 mM spermine, 15 mM β-mercaptoethanol, 0.1% Triton X-100, pH 7.5). Another 9 ml LB01 buffer was used to wash the nuclei into 1-layer miracloth filter followed by a one-time filter through 30 μm CellTrics (Sysmex, Germany, 04-0042-2316). The nuclei mixture was centrifuged at 1500g for 10 min at 4 °C. The nuclei pellet was further wash with DNase I buffer (20 mM Tris pH 7.4, 20 mM KCl, 70 mM NaCl, 10 mM MgCl2, 0.125 mM spermidine 1 mM PMSF, 0.5% Triton-X 100) until white. After centrifuge, the nuclei were resuspended in 200 μl DNase I buffer, and an aliquot of nuclei was stored for isolation and estimation of total genomic DNA as control. DNase I (Thermo Scientific, EN0525) was added and incubated at 4°C for 1 hr. Nuclei were collected by centrifugation at 3000g for 10 min at 4 °C. Digestion was followed by extraction with 0.4 M NaCl for 5 min twice on ice in Extraction Buffer (10 mM Hepes pH 7.5, 4 mM EDTA, 0.25 mM spermidine, 0.1 mM PMSF, 0.5% (v/v) Triton X-100). Another two times extraction with 2 M NaCl for 5 min on ice in Extraction Buffer. The final nuclear matrix pellet was washed twice with

Wash Buffer (5 mM Tris pH 7.4, 20 mM KCl, 1 mM EDTA, 0.25 mM spermidine, 0.1 mM PMSF).

The nuclei from different steps as indicated were checked by 4',6-diamidino-2-phenylindole (DAPI) staining and analyzed using an LSM780 confocal microscope (Zeiss) to validate DNA content in the nuclei. For protein validation, after chopping, the nuclei mixture was separated into several same-volume nuclei and followed the extraction procedure. Proteins were extracted from supernatant or pellet as indicated. All proteins were separated on 10% Tricine-SDS-PAGE gels (Schagger 2006) followed by Coomassie staining. The gel was visualized by the ChemiDoc (BIO-RAD). LC-MS was performed by Dr. rer. nat. Katja Witzel (Leibniz Institute of Vegetable and Ornamental Crops).

2.10 MAR-qPCR and MAR-seq

DNA was extracted from the isolated nuclear matrix and the input sample. To remove RNA, RNase A (Thermo Scientific, EN0531) was added to a final concentration of 20 µg/ml and incubated for 30 min at 37°C. This was followed by digestion with 100 µg/ml Proteinase K (Ambion, AM2546) at 55°C for 1 hr. DNA was recovered by extraction with phenol:chloroform:isoamyl alcohol (25:24:1) and ethanol precipitation. The isolated input DNA was fragmented by using a Bioruptor® Plus sonication device (Diagenode) to obtain the desired DNA fragment size (enriched at 200 bp). The amount of fragmented DNA was quantified by qPCR. Three biological replicates were performed. Statistical analyses were performed by using one-way ANOVA with Tukey's test ($P < 0.05$), and different letters indicate statistically significant differences. The primers used are listed in Supplementary Table 1. Libraries were prepared using NEBNext® Ultra™ II DNA Library Prep Kit (NEB, E7645) according to the manufacturer's instructions. The libraries were sequenced at Novogene (UK) via a Novaseq instrument in 150-bp paired-end mode. Two biological replicates were performed.

2.11 Bioinformatic analysis

For RNA-seq analysis, Reads were mapped to the TAIR10 wild-type Arabidopsis genome with HISAT2 (Kim et al. 2019) in paired-end mode. Differentially expressed genes were analyzed via the Subread (Liao, Smyth, and Shi 2019) and DESeq2 (Love, Huber, and Anders 2014) R packages with a 0.05 false discovery rate (FDR). The volcano plot and heatmap of DEGs were generated using TBtools (Chen et al. 2020). GO term enrichment was determined at https://david.ncifcrf.gov/summary.jsp.

For MAR-seq analysis, quality control and adapter trimming of MAR-seq reads were performed with Fastp (Chen et al. 2018). Reads were aligned to the TAIR10 reference genome using Bowtie2. Mapped reads were deduplicated using MarkDuplicates

(https://broadinstitute.github.io/picard). Coverage was estimated and normalized to 10 million reads. MAR-seq peaks in wild-type and mutants were called by SCIER2 (Zang et al. 2009). IGB genome browser was used to visualize the data and to generate screenshots. Boxplots and metaplots were generated with R. Kolmogorov-Smirnov tests were performed at https://scistatcalc.blogspot.com. GO term enrichment was determined at https://david.ncifcrf.gov/summary.jsp.

2.12 Fluorescence Recovery After Photobleaching (FRAP) assay

For FRAP of HDA15-GFP or co-transformation of HDA15-GFP and AHL22-3xFLAG assay, the constructs were delivered to *N. benthamiana* by *A. tumefaciens*-mediated transformation. FRAP was performed on Zeiss confocal laser scanning microscope (LSM780. The selected HDA15-GFP signal was photobleached using a 488 nm laser (50% intensity). Time-lapse images of fluorescence recovery were taken every 5 s for at least 2 min.

2.13 Histone extraction and western blot

The histone was extracted by the EpiQuik Total Histone Extraction Kit (EPIGENTEK, OP-0006-100) and followed manufacturer recommendations, using 5-day-old whole plants. Extracted histones were separated on 10% Tricine-SDS-PAGE gels (Schagger 2006). Primary antibodies used included anti-H3 (Sigma/H9289), anti-H3ac (Millipore /06-599), and anti-H4ac (Millipore/06-866). Signals were detected by the ChemiDoc (BIO-RAD).

2.14 ChIP-qPCR

Approximately 1 g of 5-day-old whole plant grown under LD condition (16h at 23 °C under 22 μmol·m^{-2}·s^{-1} continuous white light, 8h at 23 °C dark with 70% humidity) was collected. The ChIP experiments were performed as described by (Moreno-Romero et al. 2016). In brief, fresh tissue was cross-linked in 1x PBS (0.01% Triton, 1% formaldehyde) and vacuum infiltrated for 10 min on ice. The cross-linking was stopped by adding glycine to a final concentration of 125 mM. Cross-linked tissues were ground to a fine powder in liquid nitrogen and resuspended in 6 ml of Honda buffer (0.4 M Sucrose, 2.5% Ficoll, 5% Dextran T40, 25 mM Tris-HCl, pH 7.4, 10 mM MgCl2, 0.5% Triton X-100, 0.5 mM PMSF, 10 mM β-mercaptoethanol, proteinase inhibitor cocktail (Roche, 11836145001)). The mixture was incubated on ice for 20 min followed by two times filter through Miracloth and one time through 30 μm CellTrics (Sysmex, Germany, 04-0042-2316) and centrifuged at 1500g for 10 min at 4 °C. The pellet was resuspended in 150 μl Nuclei lysis buffer (50 mM Tris–HCl, pH 8.0, 10 mM EDTA, 1% SDS, 0.1 mM PMSF, 1 μM pepstatin A, Protease Inhibitor Cocktail) and sonicated by using a Bioruptor® Plus sonication device (Diagenode) to obtain the

desired DNA fragment size (enriched at 500 bp). The following procedures were described by (Moreno-Romero et al. 2016). Immunoprecipitations were performed with anti-H3 (Sigma, H9289) and anti-H3ac (Millipore, 06-599) antibodies. After the de-crosslinking, DNA was purified according to the IPure kit v2 Kit manual (Diagenode, C03010015). The amount of immunoprecipitated DNA was quantified by qPCR. Three biological replicates were performed. Statistical analyses were performed by using one-way ANOVA with Tukey's test ($P < 0.05$), and different letters indicate statistically significant differences. The primers used are listed in Supplementary Table 1.

3 Results

3.1 Purification of AHL complex in Arabidopsis

3.1.1 Tandem affinity purification (TAP) followed by the mass spectrometric analysis of AHL22

To understand how nuclear matrix-associated protein AHLs regulate chromatin and transcriptional activity, I applied the tandem affinity purification (TAP) approach followed by mass spectrometric analysis to identify the interactors of the AHL protein. Given that AHL22 has already shown its role in the development and epigenetic regulation in Arabidopsis (Xiao et al. 2009; Yun et al. 2012), I chose AHL22 as the bait to perform the TAP-MS analysis, from which I identified 14 proteins appearing in both replicates after background filtering (Table 3.1). Among these candidates, several AHL proteins were pulled together with AHL22, including AHLs from Clade A (AHL15, AHL17, AHL13, AHL19, AHL27/ESC, AHL29/SOB) and Clade B (AHL1, AHL3, AHL4). This result confirmed that AHLs usually interact with each other (Zhao et al. 2013). Other than AHLs, I identified a histone H2A protein (HTA7), suggesting that AHLs are highly related to histones, and a transcriptional repressor VRN1, supporting the repressive function of AHLs. I also observed consistent enrichment for a transcription factor FRS12 (FAR1 RELATED SEQUENCE), which acts as a transcriptional repressor. FRS12, together with its paralog FRS7 regulate flowering time and growth by repressing the expression of *GIGANTEA* (*GI*) and *PHYTOCHROME INTERACTING FACTOR 4* (*PIF4*) as well as their downstream signaling targets in a photoperiod manner (Ritter et al. 2017). Moreover, TAP-MS of FRS12 identified AHL9 and AHL14 (Ritter et al. 2017). Together with the function of AHLs in plant development, I hypothesized that AHLs interact with FRS7/12 to regulate chromatin and transcription at the nuclear matrix.

Table 3.1. TAP–mass spectrometry of AHL22

Protein	Annotation	% coverage (rep 1)	No. of peptides (rep 1)	Score (rep 1)	% coverage (rep 2)	No. of peptides (rep 2)	Score (rep 2)
AHL22	AT2G45430	12	9	241	21.5	8	298
AHL15	AT3G55560	49	15	934	52.3	24	1223
AHL17	AT5G49700	44.2	12	476	20.7	6	331
AHL13	AT4G17950	18.7	6	358	305	5	21.2
AHL19	AT3G04570	25.1	5	306	21	5	255
SPFH	AT5G51570	27.7	5	231	19.5	4	273
AHL27	AT1G20900	19.6	4	221	19.6	3	197
AHL3	AT4G25320	15.3	4	215	16.3	4	297
AHL1	AT4G12080	29.2	4	199	39.3	9	425
AHL4	AT5G51590	14.8	4	121	6.9	2	90
HTA7	AT5G27670	34.7	2	119	42.7	3	151
FRS12	AT5G18960	9.1	3	98	4.9	2	78
VRN1	AT3G18990	8.8	3	93	8.5	2	113
AHL29	AT1G76500	10.6	2	88	20.5	4	147

3.1.2 AHLs interact with FRS7 and FRS12 *in vivo*

To further validate the interaction between AHL22 and FRS7/12. I first confirmed the interaction by bimolecular fluorescence complementation (BiFC) assay. Strong YFP signals were only observed in the nuclei with the combination of AHL22-FRS12 and AHL22-FRS7, indicating that AHL22 interacts with FRS7 and FRS12 *in vivo* (Figure 3.1A). Moreover, a Co-immunoprecipitation assay (Co-IP) approach was also used to confirm the interaction. *Nicotiana benthamiana* leaves were infiltrated with *Agrobacterium tumefaciens* (*GV3101*) harboring AHL22-3FLAG or FRS7/12-GFP or both plasmids. GFP-trap was used for immunoprecipitation and an anti-FLAG antibody was then used for immunoblot analysis. As shown in Figures 3.1B and 3.1C, AHL22-3FLAG and FRS12-GFP or FRS7-GFP were co-precipitated, respectively. Taken together, these results demonstrated that AHL22 interacts with FRS7/12 *in vivo*.
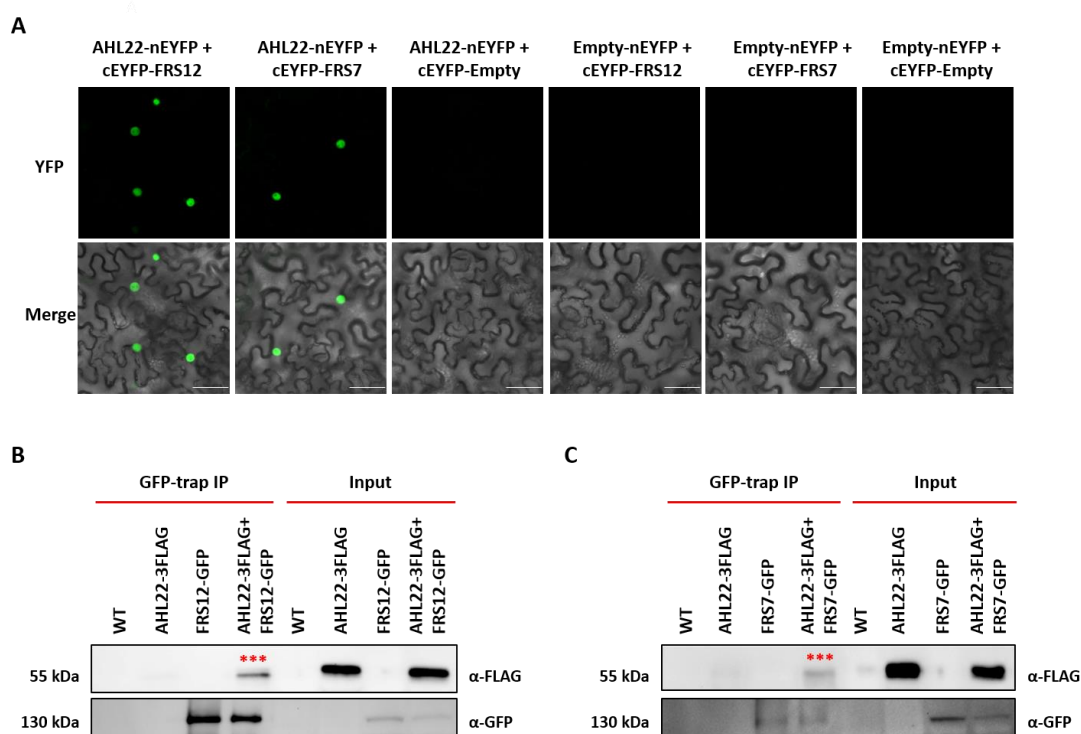

Figure 3.1. AHL22 physically interacts with FRS7 and FRS12 *in vivo*.
(A). Bimolecular fluorescence complementation (BiFC) analysis of AHL22 and FRS7 or FRS12 interaction *in vivo*. AHL22 and FRS7 or FRS12 fused with pSITE-nEYFP-N1 and pSITE-cEYFP-C1 vectors, respectively, were co-transformed into *N. benthamiana*. Scale bar= 50 μm. (B,D). Co-immunoprecipitation assays show interactions between AHL22 and FRS12 or FRS7. AHL22-3FLAG and FRS12-GFP or FRS7-GFP were expressed in *N. benthamiana*. WT, empty leaves. IP, immunoprecipitation. Asterisks indicate targeted proteins.

Given that AHLs usually interact with each other, forming homo- and hetero-complexes in Arabidopsis (Zhao et al. 2013). I further tested the interaction between other AHLs (identified in TAP-MS) and FRSs. AHL29/SOB3 is a well-studied AHL that plays an essential role in hypocotyl elongation and petiole growth (Table 3.1). Similar to AHL22, AHL29 interacted with FRS7 and FRS12 in the BiFC assay (Figure 3.2), supporting that multiple AHLs interact with FRS7 and FRS12 *in vivo*.
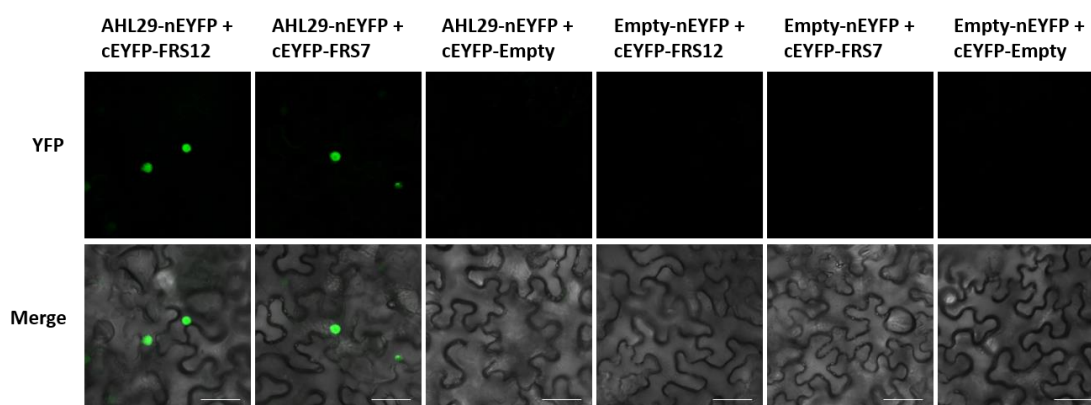

Figure 3.2. AHL29 physically interacts with FRS7 and FRS12 *in vivo*.
Bimolecular fluorescence complementation (BiFC) analysis of AHL29 and FRS7 or FRS12 interaction *in vivo*. AHL29 and FRS7 or FRS12 fused with pSITE-nEYFP-N1 and pSITE-cEYFP-C1 vectors, respectively, were co-transformed into *N. benthamiana*. Scale bar= 50 μm.

3.1.3 The interaction between AHLs and FRSs is independent of the G-R-F-E-I-L region in the PPC domain

The PPC domain of AHL proteins is essential for protein-protein interactions (Zhao et al. 2013). And the conserved six-amino-acid region (G-R-F-E-I-L) is required for the interaction between AHLs and other transcription factors, like TCP4 (Zhao et al. 2013). I then deleted the six-amino-acid region in AHL22 by using point mutagenesis (Figure 3.3A). However, the deleted version of AHL22 (Δ AHL22) still preserved the interaction with FRS7 and FRS12 in the BiFC assay (Figure 3.3B), suggesting that AHL22 interacted with FRS7/12 independent of the PPC domain.
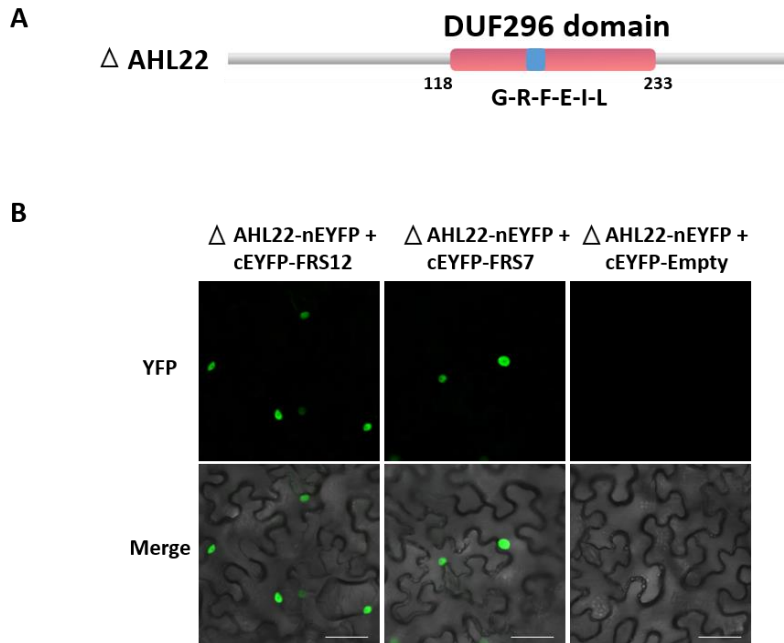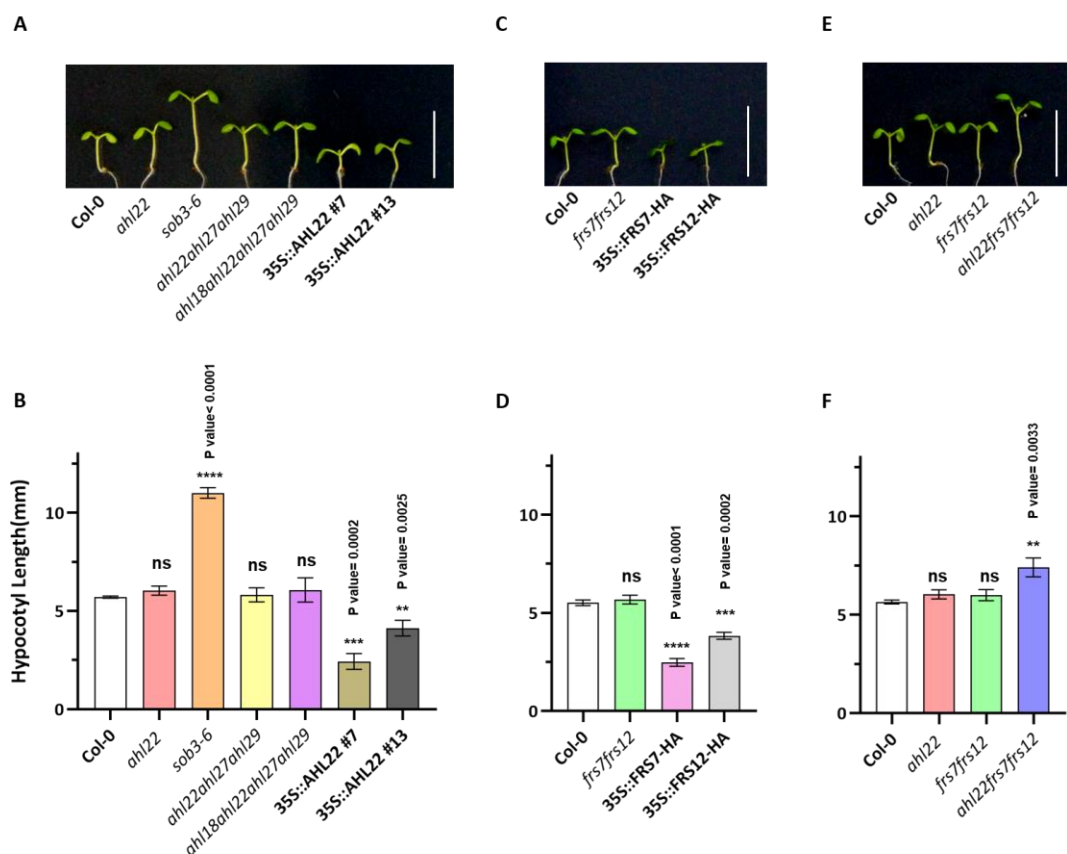
A

△ AHL22

DUF296 domain

118   G-R-F-E-I-L   233

B

△ AHL22-nEYFP +
cEYFP-FRS12

△ AHL22-nEYFP +
cEYFP-FRS7

△ AHL22-nEYFP +
cEYFP-Empty

YFP

Merge

Figure 3.3. AHL22 interacts with FRS7 and FRS12 independently of G-R-F-E-I-L.
(A). Structure of the mutated AHL22 (Δ AHL22). A conserved six-amino-acid region in the PPC/DUF296 domain is highlighted by the blue box. (B). Bimolecular fluorescence complementation (BiFC) analysis of Δ AHL22 and FRS7 or FRS12 interaction *in vivo*. Δ AHL22 and FRS7 or FRS12 fused with pSITE-nEYFP-N1 and pSITE-cEYFP-C1 vectors, respectively, were co-transformed into *N. benthamiana*. Scale bar= 50 μm.

3.1.4 AHL22 and FRS7/12 co-repress hypocotyl elongation

To explore the genetic interaction between AHLs and FRSs, I further analyzed the phenotypes of *ahl* and *frs* mutants. In the AHL family, T-DNA mutant *ahl22-1* (SALK_018866) showed a similar hypocotyl phenotype as Col-0 from three biological experiments with n=30 for each experiment (Figure 3.4A, 3.4B). I then generated an *ahl* triple (*ahl22 ahl27 ahl29*) mutant by crossing *ahl22-1* with *sob3-4 esc-8* (Zhao et al. 2013), further an *ahl* quadruple (*ahl18 ahl22 ahl27 ahl29*) mutant by crossing *ahl18-1* (SAIL_779_H11) with *ahl22-1 sob3-4 esc-8*. Both of the *ahl* triple and *ahl* quadruple mutants exhibited similar hypocotyl length as Col-0 in our growth condition (Figure 3.4A, 3.4B). The dominant-negative mutant *sob3-6* showed an extremely longer hypocotyl phenotype consistent with the previous result (Street et al. 2008; Zhao et al. 2013). Two independent homozygous of T3 *AHL22* overexpression lines exhibited a significantly shorter hypocotyl length than Col-0 (*p-value*<0.5) (Figure 3.4A, 3.4B). Given the functional redundancy of AHL family proteins, AHL22 plays a role in repressing hypocotyl elongation.

The transcriptional repressor complex FRS7-FRS12 also regulates hypocotyl elongation. In line with a similar hypocotyl length as Col-0 under long day (LD) condition (Ritter et al. 2017), the *frs7-1 frs12-1* double mutant had a similar hypocotyl length as Col-0 (Figure 3.4C, 3.4D). The overexpression lines of *FRS7* and *FRS12* showed a significantly shorter hypocotyl phenotype (*p-value*<0.001) (Figure 3.4C, 3.4D), indicating that FRS7 and FRS12 suppress hypocotyl elongation. The *ahl22 frs7 frs12* triple mutant generated from crossing *ahl22-1* with *frs7-1 frs12-1* had a significantly longer hypocotyl length than either single and double mutants (*p-value*<0.05, Figure 3.4E, 3.4F). These results indicate that AHL22 and FRS7/12 act together in the same genetic pathway controlling hypocotyl elongation.

Figure 3.4. Hypocotyl phenotype.
(A, C, E). The hypocotyl phenotype of indicated lines grown vertically under LD condition (16h at 23 °C under 22 µmol·m^{-2}·s^{-1} continuous white light, 8h at 23 °C dark) for 5 days. Scale bar= 1 cm. (B, D, F). Hypocotyl lengths of indicated lines grown under LD condition (16h at 23 °C under 22 µmol·m^{-2}·s^{-1} continuous white light, 8h at 23 °C dark) for 5 days. The average length of three independent measurements ± standard deviations are shown. Each measurement with n=30 plants. Unpaired two-tailed Student's t-test was used to determine significance between wild-type and mutants or overexpression lines. ns *p-value* >0.05, *p-value ≤ 0.05, **p-value ≤ 0.01, ***p-value ≤ = 0.001, ****p-value ≤ = 0.0001.

3.1.5 AHL22 and FRS7/12 are partially redundant in transcriptional regulation

To determine if the phenotypic differences observed in the *ahl22 frs7 frs12* triple mutant were due to transcriptional alterations, we generated transcriptome profiles of 5 days whole plants grown on vertical MS plates. From two biological replicates, I identified 3155, 3108, and 3517 differentially expressed genes (DEGs, log2FC> 1 or log2FC < -1, FDR < 0.05) in *ahl22*, *frs7 frs12*, and *ahl22 frs7 frs12* compared to Col-0, respectively. Among these, I observed that the number of down-regulated genes (DGs) is double that of up-regulated genes (UGs) in all three mutants (Figure 3.5A, 3.5B, and 3.5C), indicating that AHL22 and FRS7/12 have both activation and repression function as previously described (Favero et al. 2020). To examine the molecular pathways affected by *ahl22*, *frs7 frs12,* and *ahl22 frs7 frs12*, I performed a Gene Ontology (GO) enrichment analysis on UGs and DGs. Among the top 6 enrichment GOs, UGs and DGs showed similar pathways in the three mutants. UGs were enriched in "developmental process", "ribosome assembly", "response to auxin", and "cytoplasmic translation" (Figure 3.5D). On the other hand, DGs were enriched in the "oxidation-reduction process", "hydrogen peroxide catabolic process", "plant-type cell wall organization", and "response to oxidative stress" (Figure 3.5E). Overall, the above results suggest that AHL22 and FRS7/12 function in the same pathway and regulate the same subset of genes.

(See figure on next page)

Figure 3.5. Genome-wide transcriptome analysis of Wild type and mutants.
(A, B, C). Volcano plots of DEGs in *ahl22*, *frs7 frs12 and ahl22 frs7 frs12* compared to Col-0. The X-axis and Y-axis represent log2FC and the statistical significance as the negative log10 (*p-value*), respectively. The red dots represent genes that were significantly up-regulated genes (UGs), while the blue dots represent the significantly down-regulated genes (DGs). Genes that were not significantly changed were shown with grey dots. (D). Enriched biological processes of significantly up-regulated genes in *ahl22*, *frs7 frs12 and ahl22 frs7 frs12* compared to Col-0. (E) Enriched biological processes of significantly down-regulated genes in *ahl22*, *frs7 frs12, and ahl22 frs7 frs12* compared to Col-0. The X-axis represents negative log10 (*p-value*). Yellow stars indicate pathway response to auxin.
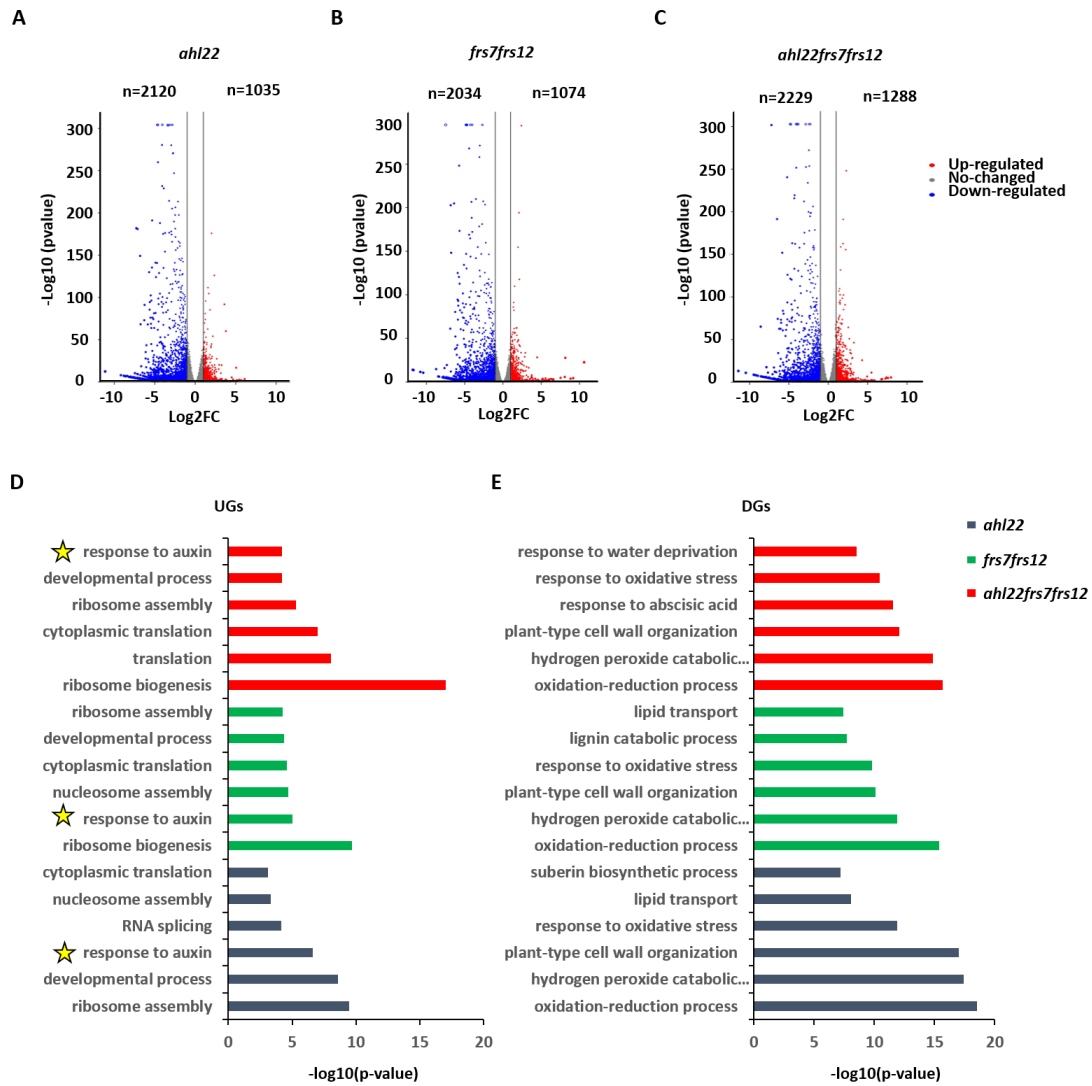
Figure 3.5. (See legend on previous page)

To identify genes responsible for the hypocotyl phenotype in *ahl22 frs7 frs1*2, I examined UGs and DGs and observed a high degree of overlap among *ahl22*, *frs7 frs12*, and *ahl22 frs7 frs1*2, with 537 common up-regulated genes and 1412 common down-regulated genes (Figure 3.6A, 3.6B). I defined genes specifically up- and down-regulated in *ahl22 frs7 frs12* with an increased trend of expression level compared to *ahl22* and *frs7 frs12* (Figure 3.6C, 3.6D), suggesting a redundant role of AHL22 and FRS7/12 at transcriptional regulation. It is known that AHLs inhibit hypocotyl elongation by repressing genes related to auxin and brassinosteroid signaling pathways (Favero et al. 2016; Favero, Le, and Neff 2017; Lee and Seo 2017). Indeed, genes response to auxin (a set of *SAUR* genes) showed increased expression levels in *ahl22 frs7 frs12* compared to *ahl22* and *frs7 frs12*, confirming the redundant function of AHL22 and FRS7/12 at gene repression and hypocotyl elongation (Figure 3.6E, Figure 3.4E, 3.4F).
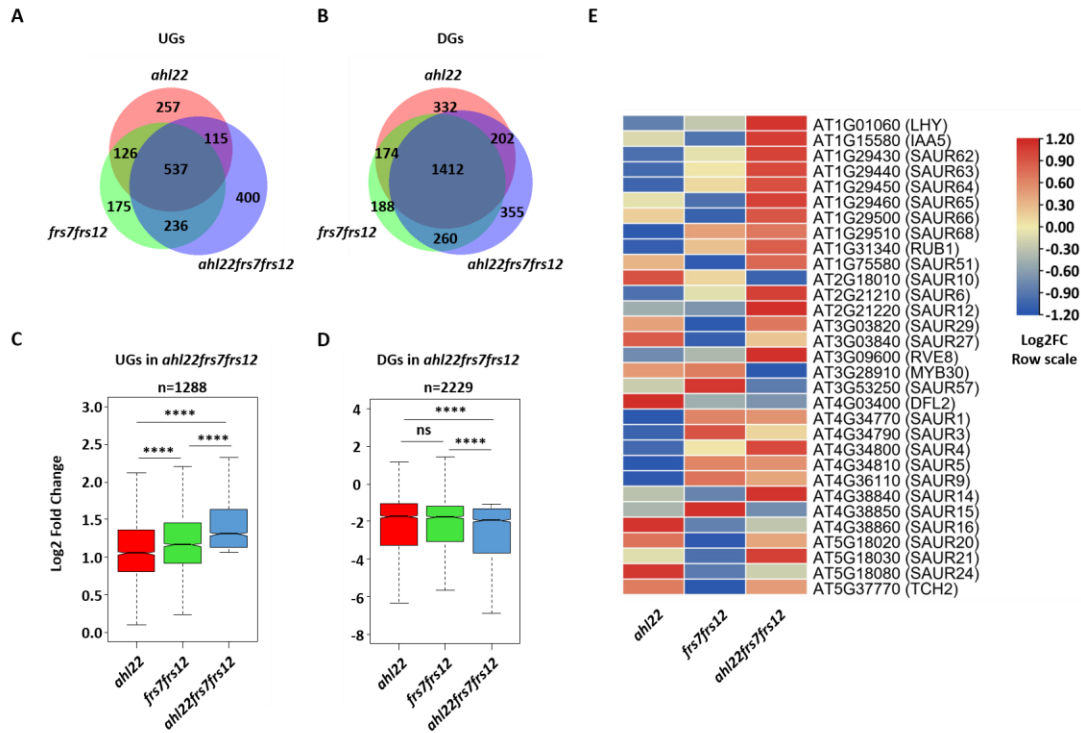
33

Figure 3.6. AHL22 and FRS7/12 act partially redundant in gene regulation.
(A, B). Venn diagrams showing the overlap of UGs (A) and DGs (B) in *ahl22*, *frs7 frs12*, and *ahl22 frs7 frs12* compared to Col-0. (C, D). Box plot showing the Log2 Fold Change levels of *ahl22*, *frs7 frs12*, and *ahl22 frs7 frs12* over UGs, n=1288 (C) and DGs, n=2229 (D) in *ahl22 frs7 frs12* mutant. Unpaired two-tailed Student's t-test was used to determine significance among different mutants. ns *p-value* >0.05, **p-value* ≤ 0.05, ***p-value* ≤ 0.01, ****p-value* ≤ = 0.001, *****p-value* ≤ = 0.0001. (E). Heat map showing the relative mRNA expression levels of genes response to auxin in *ahl22*, *frs7 frs12*, and *ahl22 frs7 frs12,* Log2FC row scale was used.

3.1.6 AHL and FRS directly co-target phytohormone pathways

To determine the direct targets regulated by AHL22 and FRS7/12, I used two published Chromatin immunoprecipitation followed by sequencing (ChIP-seq) data presenting the localization of AHL29/SOB3 (Favero et al. 2020) and FRS12 (Ritter et al. 2017) at the chromatin. Consistent with SOB3 and FRS12 as transcription factors, their distribution shared a similar pattern with a preference at promoter-TSS regions (around 50%) (Figure 3.7A, 3.7B). 7427 SOB3-bound genes and 4624 FRS12-bound genes identified from the published data showed a high degree of overlap with around 2000 common genes (p-value=6.4e^{-294}, Figure 3.7C). These 2000 genes were enriched in phytohormone pathways, including "response to salicylic acid", "response to ethylene", "response to auxin", "response to gibberellin", "response to abscisic acid", "cytokinin-activated signaling pathway", "response to jasmonic acid", "auxin-activated signaling pathway", and "ethylene-activated signaling pathway" by GO enrichment analysis (Figure 3.7D), supporting that AHLs and FRSs function as one complex to regulate the same set of downstream target genes.
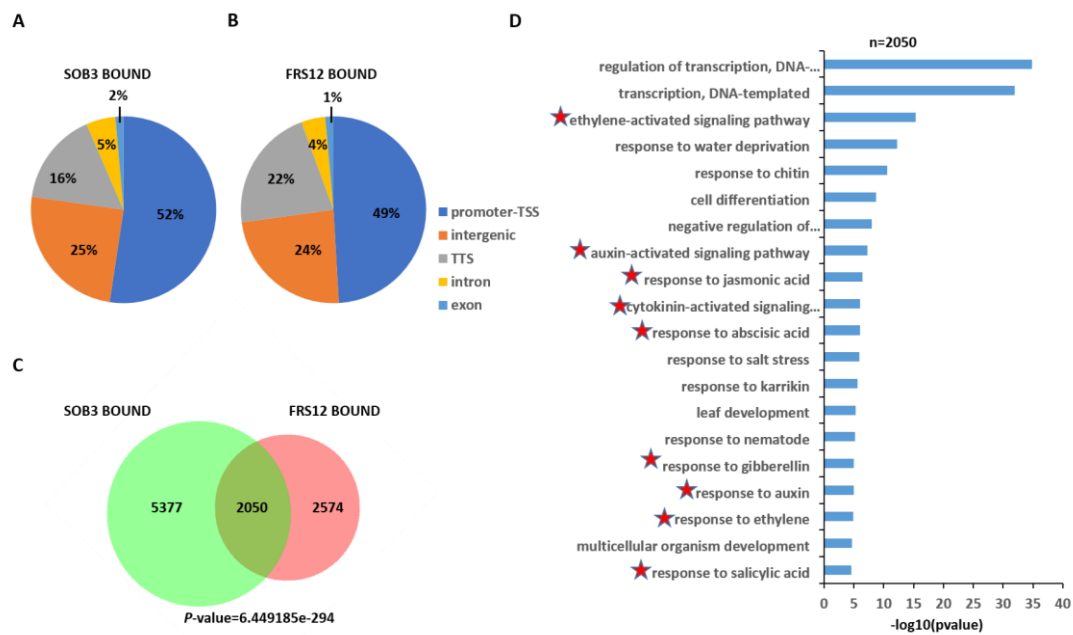

Figure 3.7. AHL22 and FRS7/12 co-target to phytohormone pathways.
(A, B). Distribution of published SOB3 (A) and FRS12 (B) binding sites determined from ChIP-seq data. ''Promoter-TSS'' is defined as -1,000 bp to +100 bp surrounding the transcription start site. ''TTS'' is defined as -100 bp to +1,000 bp surrounding the transcription termination site. (C). Venn diagram showing overlap of SOB3 BOUND and FRS12 BOUND. Significance was tested by a hypergeometric test. (D). Enriched biological processes of commonly targeted genes of SOB3 BOUND and FRS12 BOUND. The X-axis represents negative log10 (*p-value*). Red stars indicate phytohormone pathways.

3.2 Chromatin attaching to the nuclear matrix is essential for transcriptional regulation

3.2.1 Preparation of the nuclear matrix

To isolate the nuclear matrix from Arabidopsis, I adopted the protocol from (Pathak, Srinivasan, and Mishra 2014). This protocol uses DNase I digestion and high salt treatment to remove chromatin and soluble proteins (Figure 3.8). Nuclei were isolated from 5d or 10d Arabidopsis seedlings grown on MS plates. The nuclear matrix was prepared by treating nuclei with DNase I digestion and high salt treatment, with untreated nuclei as control. Protein and DNA were extracted from both nuclear matrix and input nuclei for further LIQUID CHROMATOGRAPHY MASS SPECTROMETRY (LCMS) and whole-genome sequencing analysis, respectively (Figure 3.8).
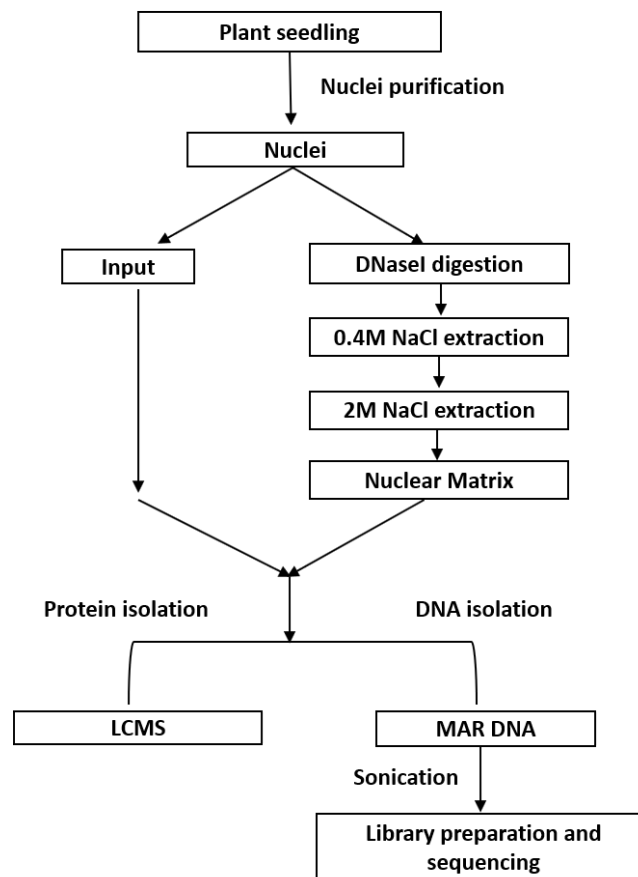

Figure 3.8. Flow diagram representing isolation of nuclear matrix and further DNA and protein extraction.

To validate the preparation of the nuclear matrix, extracted proteins were running in 10% SDS-tricine gel followed by Coomassie staining. After high salt treatment, most of the core histones were removed, indicating the proper removal of soluble and chromatin-bound proteins (Figure 3.9A). The nuclear matrix was further validated by

DAPI staining of the presence of DNA at three stages of the isolation process. The nuclear matrix showed a significant reduction of DAPI fluorescence compared to input and DNase I digested nuclei (Figure 3.9B), indicating the successful removal of genomic DNA during the preparation process.

Coomassie staining, M-Marker, S-Supernant, P-nuclei pellet
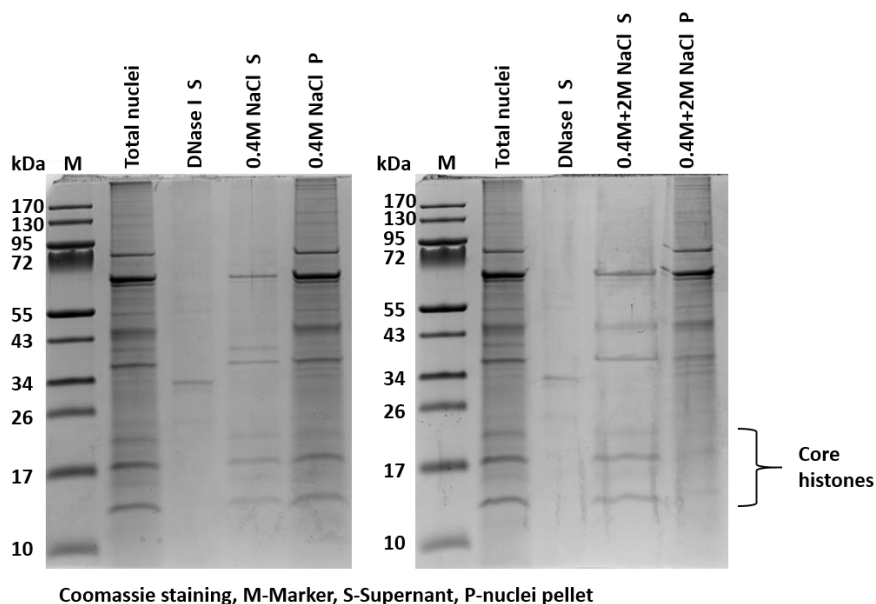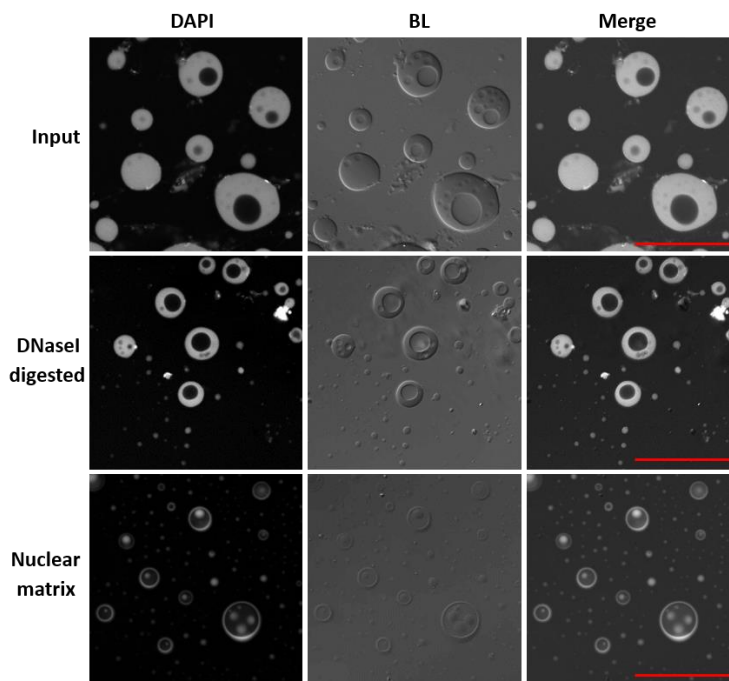

Figure 3.9. Validation of extracted protein and DNA from the nuclear matrix.
(A). Coomassie-stained SDS-tricine gels of proteins during the extraction processes. M-Marker, S-Supernatant, P-nuclei pellet. (B). Confocal images and DAPI staining of nuclei pellet at three stages of nuclear matrix isolation.

3.2.2 AHL22 is a MAR-associated protein

MAR-associated proteins are essential for the function of the nuclear matrix. To identify the MAR-associated proteins in Arabidopsis, proteins were extracted from the nuclear matrix of 10d whole plants grown on vertical MS plates. I collaborated with Dr. Katja Witzel to perform LCMS for input (the whole nuclei) and nuclear matrix proteins. In all three biological replicates, I identified 1535 and 1192 proteins that appeared in at least two replicates from the nuclear matrix and input, respectively (Figure 3.10A). More than 1000 proteins were found in both samples, and 518 proteins were uniquely detected as MAR-associated proteins (Figure 3.10A).
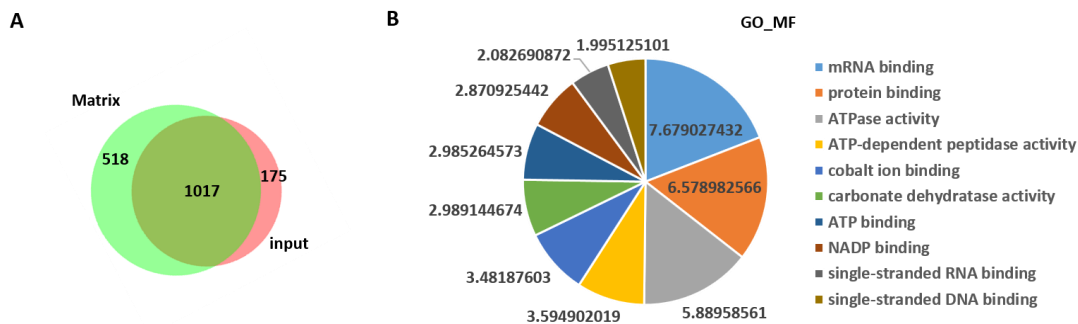

Figure 3.10. Proteomic analysis of Arabidopsis nuclear matrix-associated proteins.
(A). Venn diagram showing overlap of proteins identified in nuclear matrix and input. (B). The enriched molecular function of unique identified proteins (n=518) in nuclear matrix. The number represents a negative log10 (*p-value*).

GO enrichment analysis of the molecular function of these 518 proteins indicated that MAR-associated proteins are involved in "mRNA binding", "protein binding", "ATPase activity", and "single-stranded RNA/DNA binding". Among these pathways, TUBULIN, HEAT SHOCK PROTEIN, and a histone deacetylase were enriched as previous Arabidopsis MAR proteome (Calikowski, Meulia, and Meier 2003) (Table 3.2). Besides these known MAR-associated proteins, AT-hook-containing proteins were also enriched in my proteomic data, such as ARID4 and two AHL proteins (AHL22 and AHL4) (Table 3.2). Moreover, I identified FRS11 and FAR-RED ELONGATED HYPOCOTYLS3 (FHY3) from the FRS family, supporting that FRS proteins function as MAR-associated proteins together with AHLs (Table 3.2).

Table 3.2. LC–mass spectrometry of Arabidopsis MAR-associated proteins

			Matrix						Input					
			rep1		rep2		rep3		rep1		rep2		rep3	
Accession	Protein ID	Annotation	Cov %	# Pep	Cov %	# Pep	Cov %	# Pep	Cov %	# Pep	Cov %	# Pep	Cov %	# Pep
Q9SY66	AT1G10240	FRS11	NA	NA	3	1	6	3	NA	NA	NA	NA	3	1
Q0WNR6	AT1G76510	ARID4	NA	NA	6	2	6	2	NA	NA	NA	NA	3	1
Q9C5X9	AT1G79000	HAC1	NA	NA	2	2	3	5	NA	NA	NA	NA	1	2
O22130	AT2G45430	AHL22	NA	NA	3	1	3	1	NA	NA	NA	NA	3	1
Q9SR02	AT3G04740	MED14	NA	NA	3	2	2	3	NA	NA	NA	NA	NA	NA
Q9LIE5	AT3G22170	FHY3	NA	NA	3	2	6	4	NA	NA	NA	NA	NA	NA
Q8L7U4	AT4G02450	HSP20-like	NA	NA	6	1	15	3	NA	NA	NA	NA	6	1
P29517	AT4G20890	TUB9	NA	NA	27	9	32	13	13	6	NA	NA	NA	NA
O22446	AT4G38130	HDA19	3	1	12	4	13	4	NA	NA	NA	NA	13	4
P29516	AT5G23860	TUB8	9	3	NA	NA	33	15	NA	NA	NA	NA	23	8
P34881	AT5G49160	MET1	NA	NA	1	1	3	4	NA	NA	NA	NA	1	2
Q9FHM5	AT5G51590	AHL4	NA	NA	4	1	8	2	NA	NA	NA	NA	4	1

Cov. Coverage; Pep, peptide; NA, not detected

3.2.3 Distribution of MARs in *Arabidopsis* genome

To investigate the relationship between MARs and transcriptional regulation, I generated genome profiles for DNA extracted from the nuclear matrix of *ahl22 frs7 frs12* and *sob3-6*, along with WT Col-0 as the control, followed by whole genome sequence (MAR-seq). To characterize the MARs in the genome, I first focused on the distribution of MARs in Col-0. Using SCIER (FDR<0.05), 16629 MAR peaks were identified from two biological replicates. The distribution of all MAR peaks showed a preference for gene and promoter (82%), with only 18% for TEs (Figure 3.11A). Metagene plots of MAR-seq signal over protein-coding genes revealed two major MAR peaks, one over regions just downstream of the TSS and a smaller peak just at 3' of the transcription end site (TES) (Figure 3.11B). Similarly, a previous report shows that MARs identified from Arabidopsis Chr 4 have a preference to transcription start sites, leading to an increased expression of genes (Pascuzzi et al. 2014). Consistent with the distribution of MAR, no obvious peaks were observed over TE (Figure 3.11C). A randomly selected region (Chr1: 5250000-5450000) showed an overview of MAR peaks over genes rather than TE (Figure 3.11D). Together, these results indicate that MAR prefers to distribute at genes.
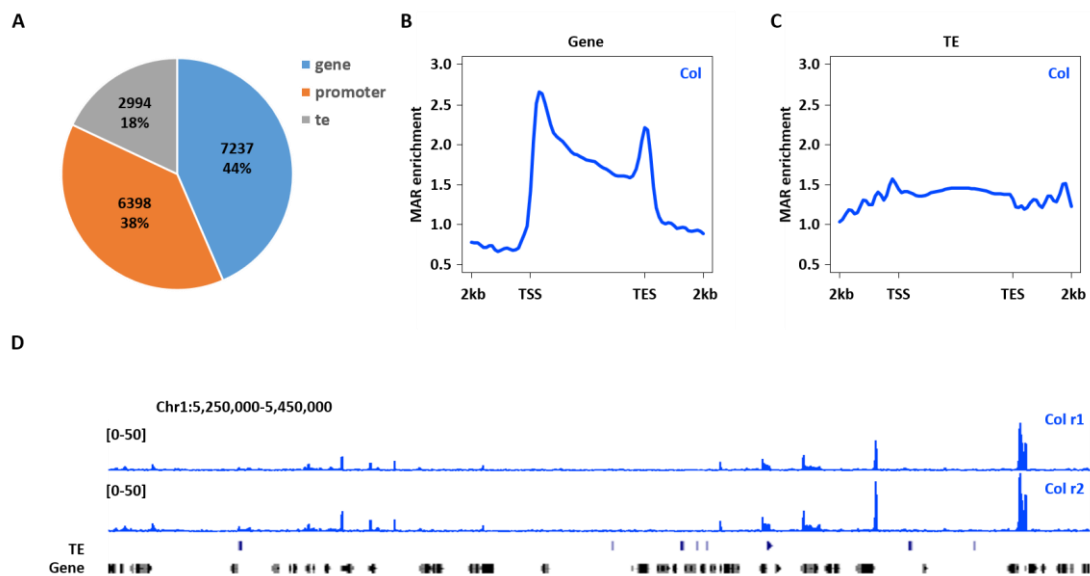

Figure 3.11. Distribution of MARs in Col-0.

(A). Distribution of MARs determined from MAR-seq data. (B). Metagene plot showing the MAR enrichment of Columbia over genes. (C). Metagene plot showing the MAR enrichment of Col-0 over TEs. (D). Genome browser view of a randomly selected region (Chr1: 5250000-5450000) showing MAR peaks in 2 replicates of Col-0.

3.2.4 MARs are relative with active epigenetic marks and high expression genes

To determine if specific epigenetic features mark the regions (protein-coding genes) that are enriched with MARs. I investigated the preferences of different epigenetic marks on these genes using previously published data (Liu et al. 2016). In general, MAR enriched genes were highly correlated with active histone marks, including H3K4me3, H3K36me3, and histone acetylation, with a preference for 5' end of coding genes (Figure 3.12). Accordingly, MARs-enriched genes had low levels of silenced marks, such as H3K27me1/3, H3K9me1/2, and DNA methylation (Figure 3.12). In addition, MAR-enriched genes preferred two histone variants H3.3 and H2A.Z at the 3' end and 5' end of genes (Figure 3.12), which usually correlated with gene activation (Stroud et al. 2012; Dai et al. 2017; Sura et al. 2017). Furthermore, MAR-enriched genes exhibited a similar pattern to DNase I hypersensitive sites with two peaks at the transcription start sites (TSSs) and transcription end sites (TESs) of genes, suggesting that MAR-enriched genes tended to have a more open chromatin state (Figure 3.12). In summary, MAR-enriched genes preferentially localize to the open chromatin regions of actively transcribing genes with active epigenetic marks.
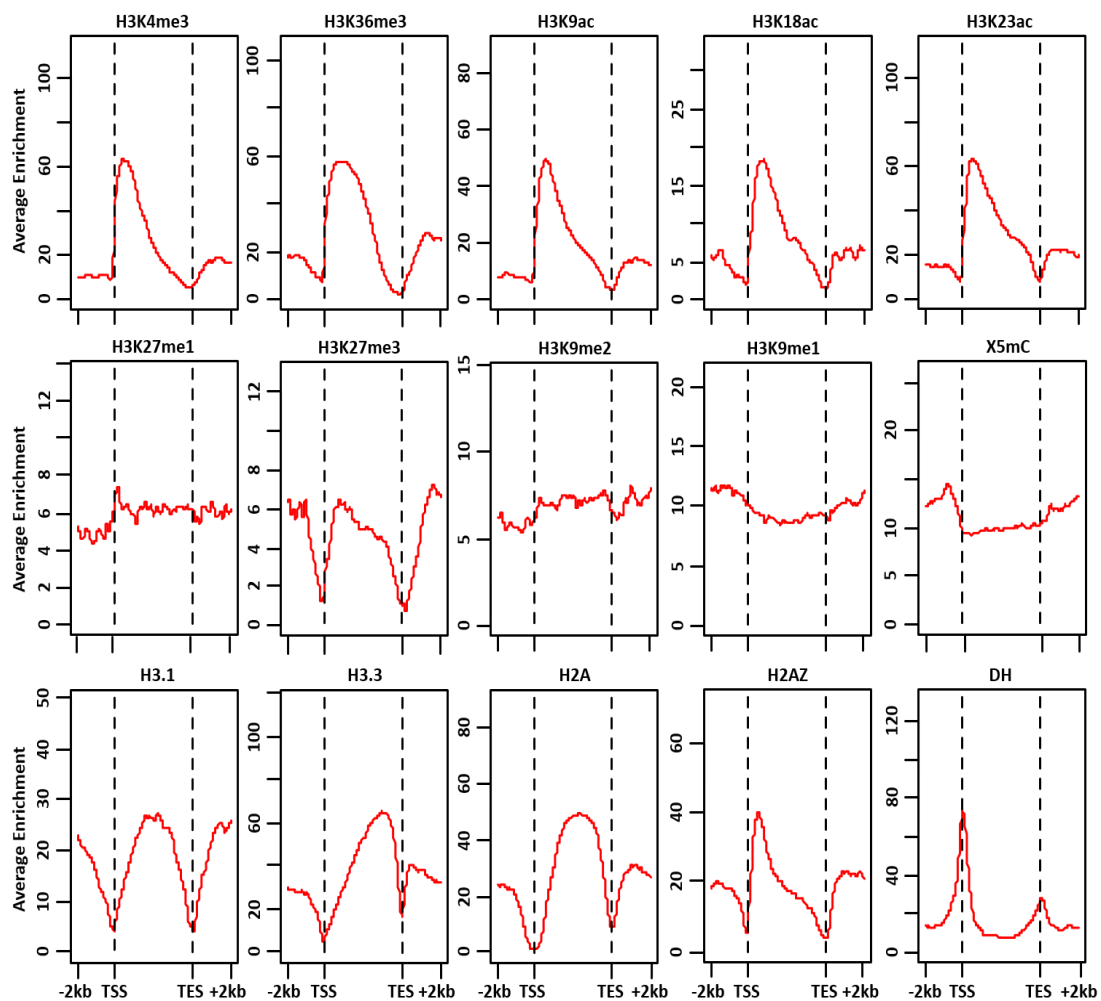

Figure 3.12. Distribution of average epigenetic features across MARs over genes.

Since MAR-enriched genes are usually associated with active epigenetic marks, I further analyzed the expression levels of MAR-enriched genes. Boxplot showed that MAR-enriched genes have a significantly higher expression level (RPKM) than other genes (*p-value*<0.001) (Figure 3.13A). The increased expression levels were contributed by a higher number of highly transcriptional active genes (RPKM>10) and a significantly lower number of genes with an RPKM less than 1 compared to the pattern of all genes (Figure 3.13B). Metagene plot showed that highly transcriptional active genes have a higher MAR enrichment level, especially for the genes with an RPKM of more than 50 (Figure 3.13C). Taken together, these data indicated that MARs-enriched genes preferred active epigenetic marks and highly transcriptional active genes.
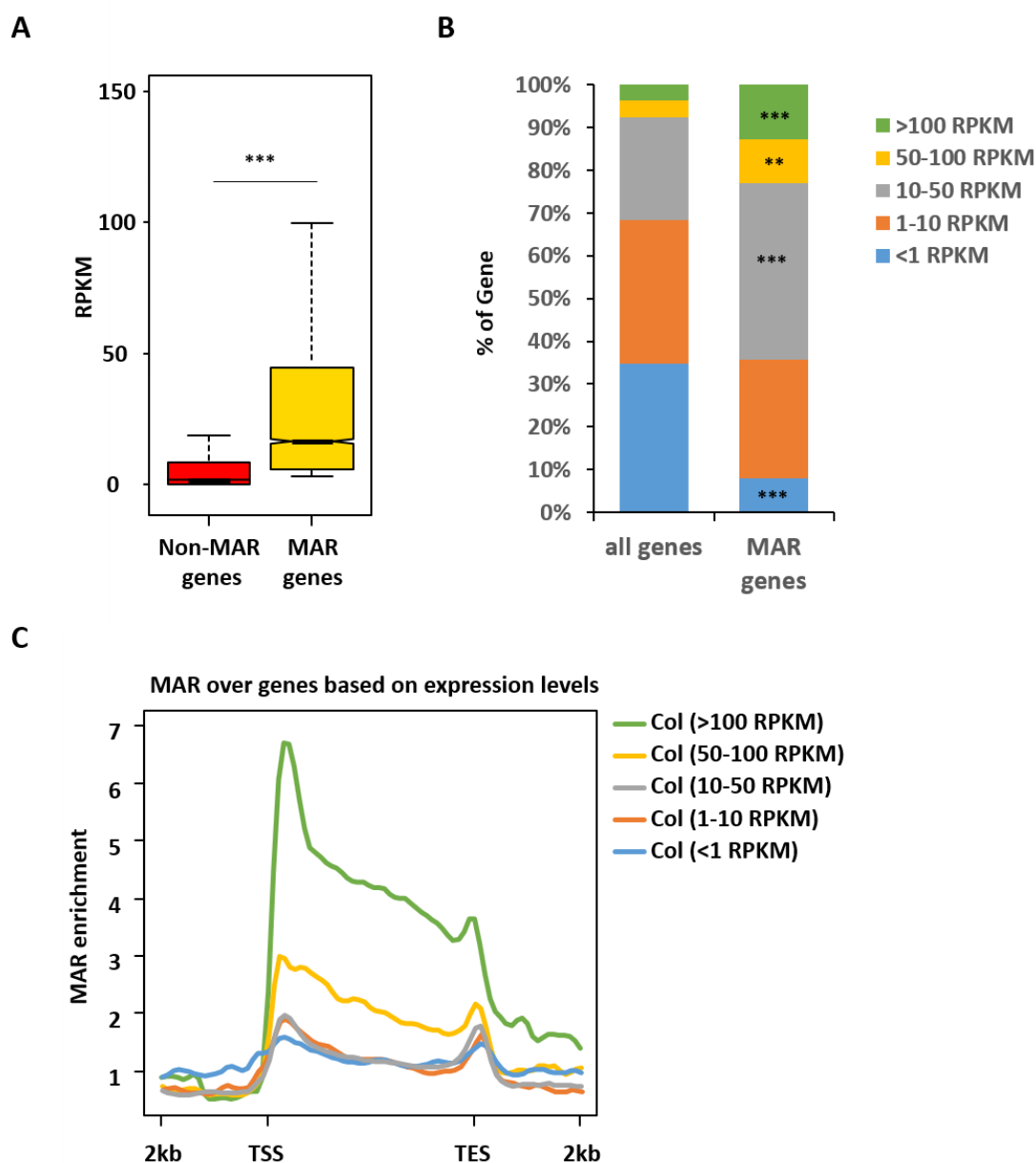

Figure 3.13. (See legend on next page)

(See figure on previous page)

Figure 3.13. Expression levels of MARs in Col-0.

(A). Box plot showing the expression level (RPKM) of non-MAR enriched and MAR enriched genes N.S. *p-value* >0.05, *p-value ≤0.05, **p-value ≤ 0.01, ***p-value ≤0.001. (Kolmogorov-Smirnov test). (B). The distribution of genes over expression ranges from less than 1 RPKM, 1-10 RPKM, 10-50 RPKM, 50-100 RPKM, and larger than 100 RPKM in MAR enriched genes and all genes. Fisher 's exact test, **$P<0.01$, ***$P<0.001$. (C). Metagene plot showing the average distribution of MAR enrichment over protein-coding genes grouped by their expression levels (RPKM).

3.2.5 AHL-FRS complex is required for MARs enrichment

Arabidopsis AHL proteins have been shown to bind to Matrix Attachment Regions (Fujimoto et al. 2004; Lim et al. 2007; Xu et al. 2013). LCMS data from my study also identified AHLs as nuclear matrix-associated proteins (Table 3). To investigate the relationship between AHL proteins and MAR enrichment, I compared the MAR-seq data from *ahl22 frs7 frs12* (*triple*) and *sob3-6* to Col-0. In total, by using SCIER (FDR <0.05), I identified 10416, 12099, and 16626 MAR peaks in the *triple*, *sob3-6*, and Col-0, respectively (Figure 3.14A). The distribution of MAR peaks shared a similar pattern, with around 80% of MAR peaks belonging to gene and promoter regions (Figure 3.14A).

I further focused on the MARs at genes from *triple*. A total of 5576 genes showed a different MAR peak between Col and *triple* with a general decreased MAR enrichment over protein-coding genes from TSS to TES in *triple* (Figure 3.14B). Most of the different peaks on genes (n=5457) showed a decreased MAR enrichment in *triple* (Figure 3.14C). However, those genes with increased MAR enrichment (n=119) showed a random increase in the genome (Figure 3.14D). These results indicated that the AHL-FRS complex is required for MARs binding at the nuclear matrix.
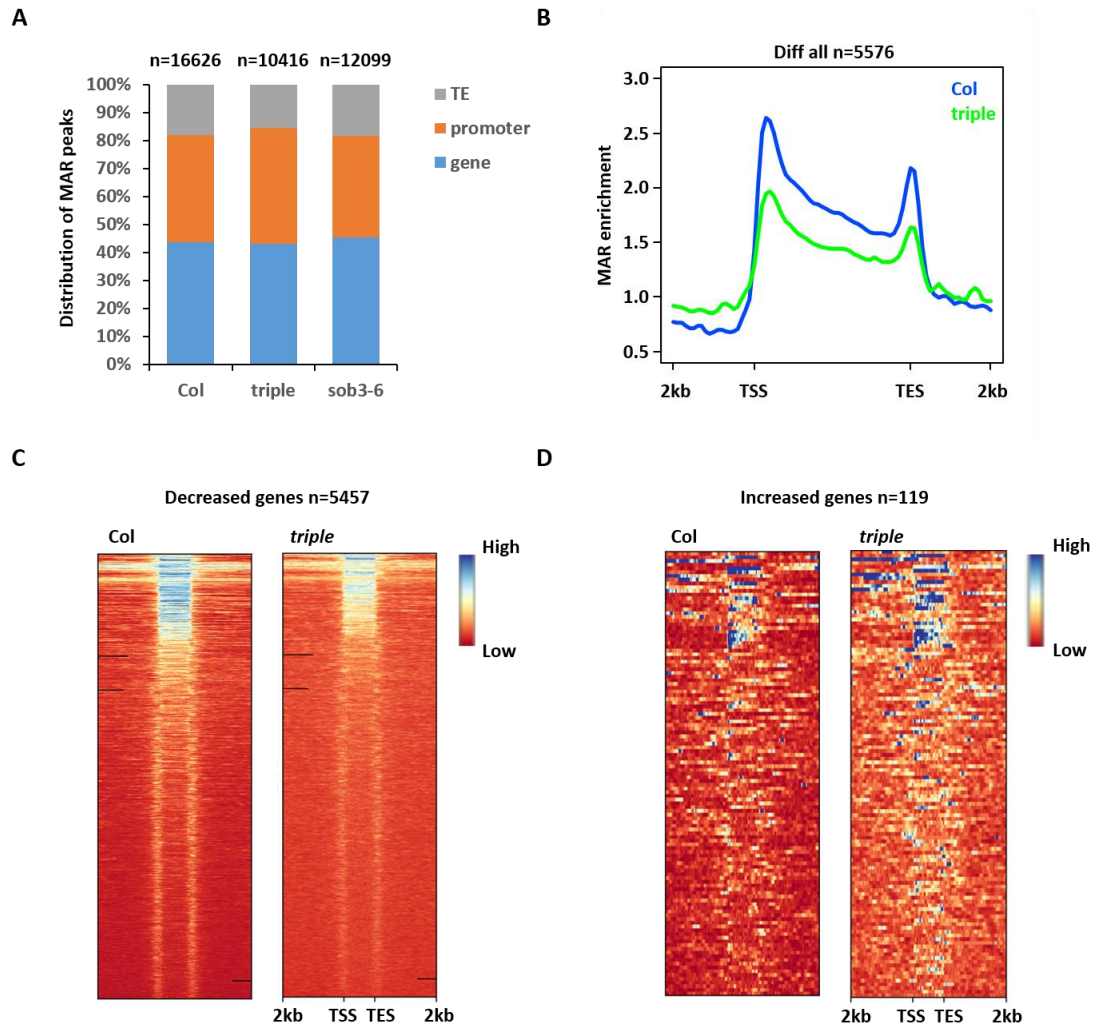
Figure 3.14. AHL22 and FRS7/12 are required for MAR enrichment.
(A). Distribution of MARs determined from MAR-seq data from Col-0, *triple*, and *sob3-6*. (B). Metagene plot showing the MAR enrichment of all differential peaks (n=5576) in *triple* compared to Col-0. (C, D). Heatmap of normalized MAR signal over MAR decreased genes (n=5457, C) and MAR increased genes (n=119, D) in Col-0 and *triple*. TSS: transcription start site, TES: transcription end site. The profiles were generated after merging two biological replicates at each sample.

3.2.6 Decreased MARs are mainly at short genes

To uncover the distribution of decreased MARs on different gene lengths, I separated all genes into 6 groups by size and plotted MAR enrichment over them. The distribution of the different sizes of decreased MAR genes shared a similar pattern with all genes (Figure 3.15A), indicating the loss of MAR is genome-wide. However, genes less than 2kb had a higher decreased MAR enrichment than those more than 2kb and contributed to the overall decrease of MAR enrichment (Figure 3.15B). Genes less than 2kb had a sharp peak downstream of TSS, whereas genes with more than 2kb had a higher peak at TES rather than TSS (Figure 3.15B). Thus, small genes exhibited more MARs and contributed to the overall loss of MAR enrichment in *triple*.
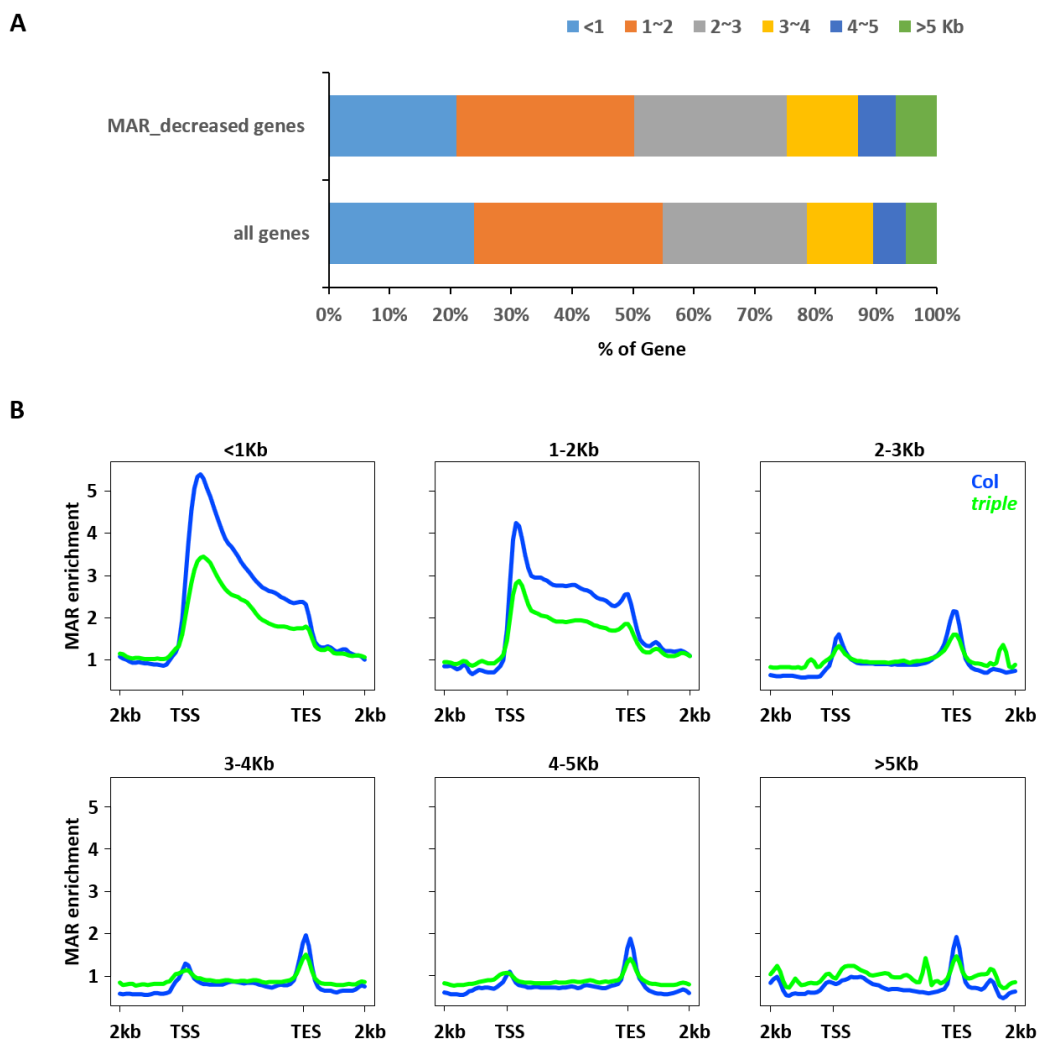

Figure 3.15. Distribution of decreased MAR at different sizes of genes.
(A). Distribution of genes over gene size ranging from less than 1 kb, 1-2 kb, 2-3 kb, 3-4 kb, 4-5 kb and larger than 5 kb in MAR decreased genes and all genes. (B). Metagene plot showing the average distribution of MAR enrichment over protein-coding genes grouped by gene size. TSS: transcription start site, TES: transcription end site.

45

3.2.7 Dual roles of reduced MARs in transcriptional regulation

Given that MAR-enriched genes are associated with active epigenetic marks and highly transcriptional active genes, I hypothesized that the reduced MARs might cause gene repression. To investigate the effect of decreased MAR on gene expression, I first compared the expression levels of MAR increased (n=119), decreased (n=5457), and unaltered (n=1661) genes. Boxplot showed that genes with reduced MARs had significantly lower expression levels (RPKM) in *triple* compared to Col-0 (Figure 3.16A). However, both UGs and DGs from 5-d-old whole plants showed a significant overlap with MAR-reduced genes, with a *p-value*=0.03 and 1.3e^{-6}, respectively (Figure 3.16B), suggesting that reduced MAR might have both active and repressive effects on gene expression with a dominant effect on gene repression. Gene ontology (GO) enrichment analysis indicated that among common genes (n=443) between MAR decreased genes and DGs, the term "cellular response to hypoxia", "response to water deprivation" and "response to cold" are the most highly enriched (Figure 3.16D). On the other hand, the most enriched GO terms for common genes (n=232) between MAR decreased genes and UGs include "response to auxin", "regulation of growth", and "auxin-activated signaling pathway" (Figure 3.16C).
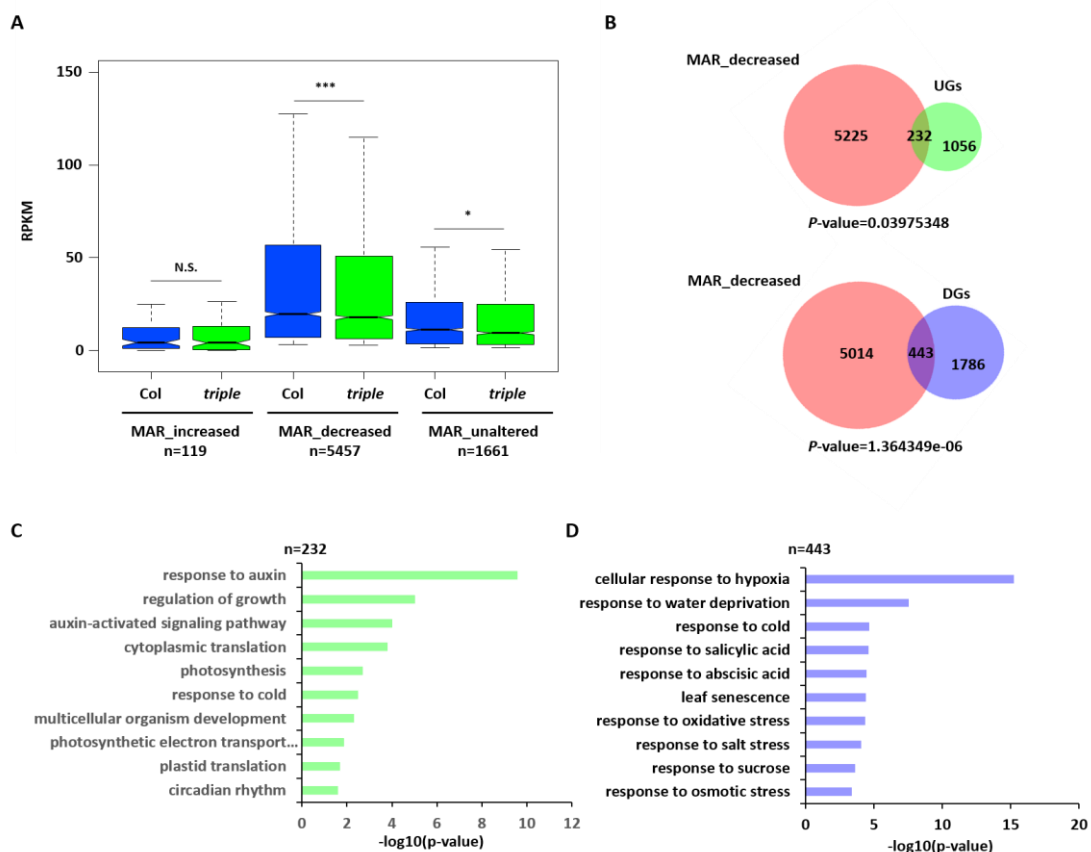

Figure 3.16. (See legend on next page)

(See figure on the previous page)

Figure 3.16. Decreased MAR in gene expression.

(A). Box plot showing the expression level (RPKM) of MAR increased (n=119), MAR decreased (n=5457), and MAR unaltered (n=1661) genes. N.S. *p-value* >0.05, **p-value* ≤0.05, ***p-value* ≤0.01, ****p-value* ≤0.001. (Kolmogorov-Smirnov test). (B). Venn diagrams showing overlap of MAR decreased genes and UGs or DGs identified in *triple* compared to Col-0. Significance was tested using a hypergeometric test. (C, D). Enriched biological processes of common genes identified from MAR decreased genes and UGs (C) and DGs (D) in the *triple* mutant. The X-axis represents negative log10 (*p-value*).

Arabidopsis AHLs inhibit hypocotyl elongation by repressing genes involved in both auxin and brassinosteroid signaling pathways, including *YUC8*, *YUC9*, and members of the *SMALL AUXIN UP-REGULATED RNA19* (*SAUR19*) subfamily (Favero et al. 2016; Favero, Le, and Neff 2017; Lee and Seo 2017). Decreased MAR-induced gene activation was highly enriched in genes response to auxin (Figure 3.16C). In this pathway, several *SAUR* genes showed a decrease in MAR enrichment and a higher expression level (RPKM) in *triple* compared to Col-0, including *SAUR6*, *SAUR14/15/16*, *SAUR20/21*, and *SAUR62/63/64*, which are direct targets of SOB3-GFP (Favero et al. 2020) (Figure 3.17A and 3.17B). The reduction in MAR enrichment was also observed in the *sob3-6* mutant (Figure 3.17A and 3.17B). Other auxin response genes, such as *SAUR50/51*, *SAUR72*, *SAUR78*, *YUC8*, and *IAA29*, are direct targets of both SOB3-GFP and FRS12-HBH (Ritter et al. 2017; Favero et al. 2020), had a reduced level of MAR enrichment and most of the genes showed an increased expression level (RPKM) in the *triple* mutant (Figure 3.18A and 3.18B). These *SAUR* genes are short genes less than 1kb, which were highly enriched with MAR levels compared to long genes and exhibited a noticeable decrease of MAR occupancy in the *triple* mutant (Figure 3.15B).
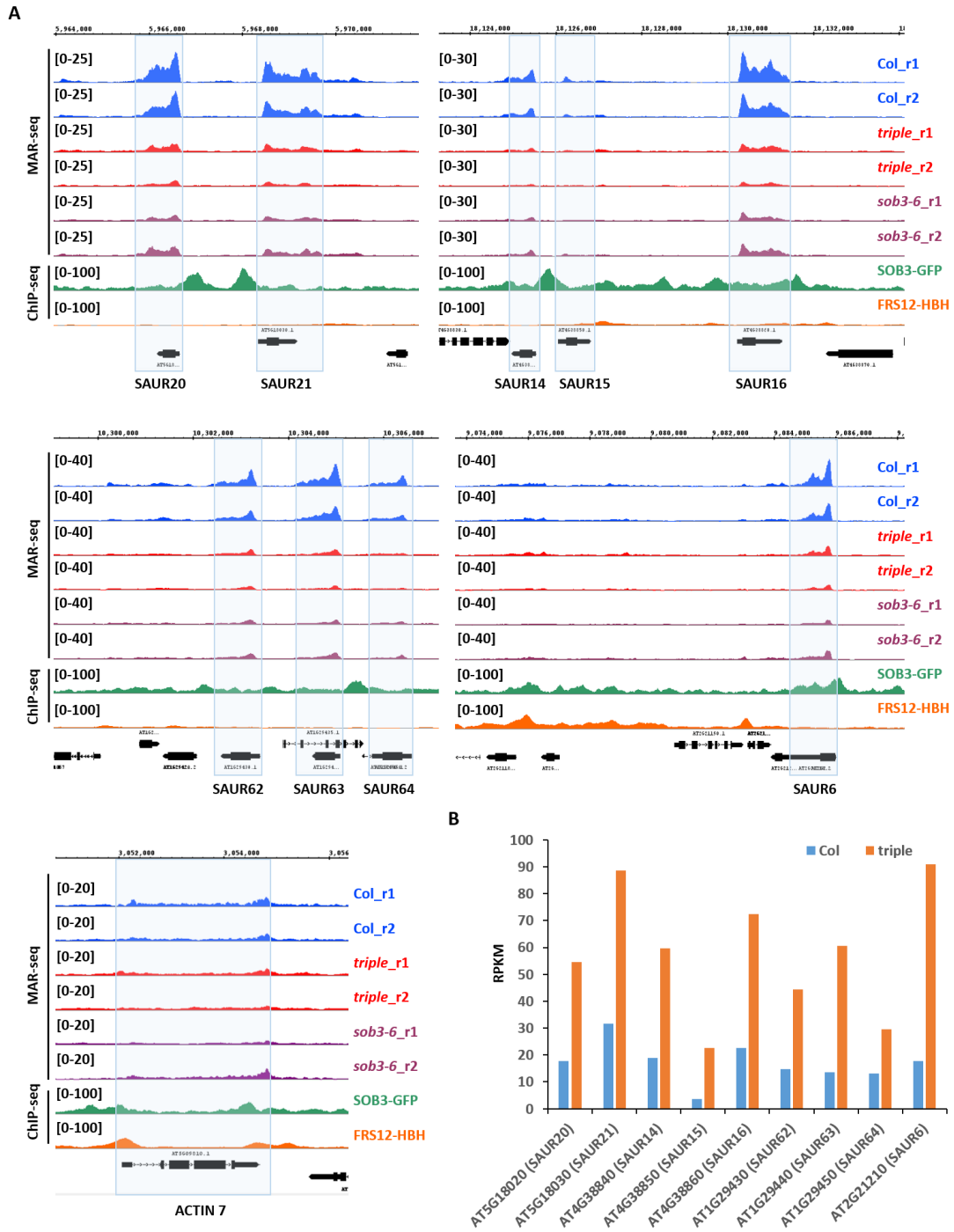
Figure 3.17. Decreased MAR at genes response to auxin targeted by SOB3.
(A). Genome browser views of two replicates of auxin response genes indicated in the blue box in Col-0, *triple*, and *sob3-6*. ACTIN 7 was used as a control. (B). The relative expression levels (RPKM) of targeted genes from RNA-seq data of Col-0 and *triple*.
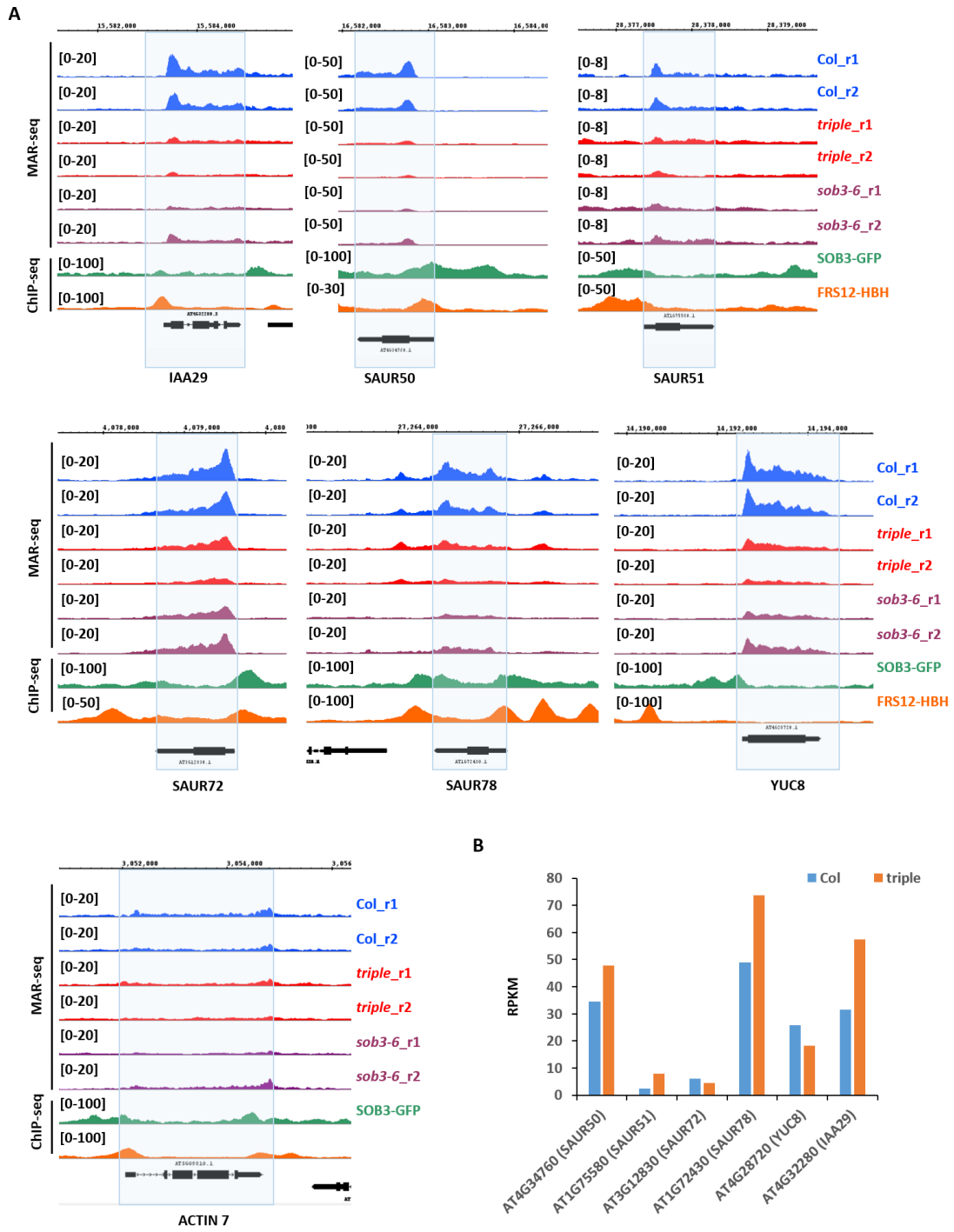
Figure 3.18. Decreased MAR at genes response to auxin targeted by both SOB3 and FRS12. (A). Genome browser views of two replicates of auxin response genes indicated in the blue box in Col-0, *triple*, and *sob3-6*. ACTIN 7 was used as a control. (B). The relative expression levels (RPKM) of targeted genes from RNA-seq data of Col-0 and *triple*.

I further validated the results of MAR-seq by qPCR at selected *SAUR* genes. Given that MAR enrichment had a sharp peak in the TSS region for those small genes (Figure 3.15B), I focused on the TSS regions as indicated in Figure 3.19A. The analysis showed that compared to Col-0, both *triple* and *sob3-6* displayed significantly lower occupancy of MAR at the regions of *SAUR* genes (Figure 3.19B), except for *SAUR15* might be due to the low MAR enrichment (Figure 3.17A). These data indicated that the AHL-FRS complex is responsible for the MAR attachment at auxin response genes, suppressing multiple *SAUR* genes to inhibit hypocotyl elongation.
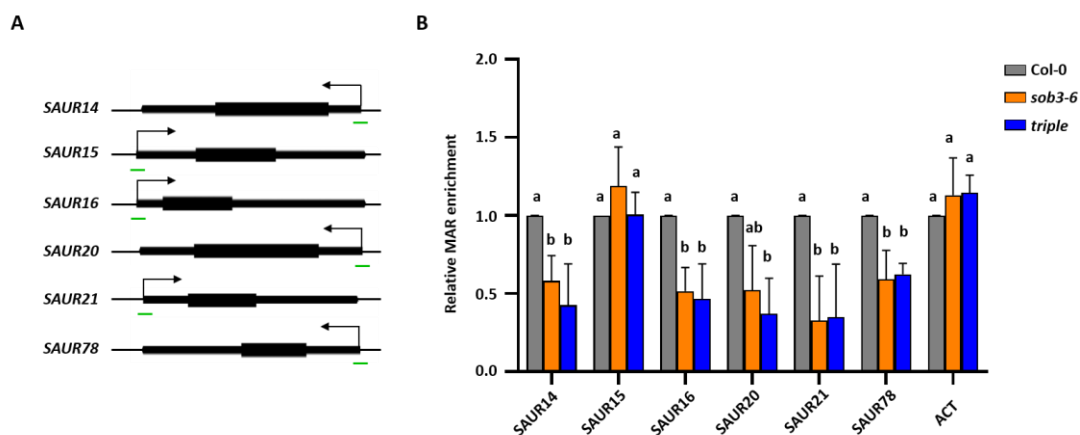
Figure 3.19. Decreased MAR at genes response to auxin.

(A). Schematic structures of selected genes. Arrows indicate transcription start sites. Green lines indicate regions examined by MAR-qPCR. (B). Relative MAR enrichment at selected genes determined by MAR-qPCR in Col-0, *sob3-6*, and *triple*. Values are means ± SD of three biological repeats. The significance of differences in each gene was tested using one-way ANOVA with Tukey's test ($P < 0.05$), and different letters indicate statistically significant differences.

3.3 AHL22 cooperates with HDA15 to repress the expression of auxin response genes

3.3.1 AHL22 interacts with HDA15

My results showed that nuclear matrix binding protein AHL22 could interact with FRS proteins to suppress hypocotyl elongation by repressing the expression of auxin response genes (Figure 3.1, 3.4 and 3.6). This repression depends on AHL-FRS-mediated MAR attachment to the nuclear matrix (Figure 3.17 and 3.18). However, a molecular mechanism for this coordination has not been clearly established. Given that in the flowering time regulation, overexpression of AHL22 delays flowering time by decreasing H3 acetylation and increasing H3K9me2 level in the FT chromatin through the interaction with histone deacetylases (HDA6, HDA9, HDA19), resulting in a reduced *FT* expression (Yun et al. 2012). Another AHL, AHL16/TEK can interact with retinoblastoma-associated protein (FVE and MSI5) and mediate H3 acetylation levels at *FLC* loci (Xu et al. 2013). So I hypothesized that in hypocotyl elongation, AHL22 interacts with histone deacetylases and regulates the expression of auxin response genes by modulating histone acetylation levels.

Multiple HDACs are involved in different aspects of plant development (reviewed in Introduction). One of the HDACs, HDA15 from the RPD3 subgroup, has been shown to interact with HY5 and NF-YCs and repress hypocotyl elongation by modulating H4 hypoacetylation and transcription repression at target loci (Tang et al. 2017; Zhao, Peng, et al. 2019). Therefore, I further focused on the relationship between AHL22 and HDA15. In BiFC, the YFP signal was only observed in the combination of AHL22 and HDA15 (Figure 3.20A). Around 40% of the nuclei showed the colocalization of the YFP signal and H3.3-RFP signal, indicating that AHL22 can interact with HDA15 *in vivo* (Figure 3.20A and 3.20B). The T-DNA insertion mutant of *hda15-1* (SALK_004027) displayed a significantly longer hypocotyl phenotype under the same growth condition as *ahl22 frs7 frs12* and *sob3-6* (Figure 3.20C and 3.20D). Together, these data suggested that the AHL complex and HDA15 acted in a similar pathway to regulate hypocotyl elongation.

A

AHL22-nEYFP + cEYFP-HDA15 | Empty-nEYFP + cEYFP-HDA15 | AHL22-nEYFP + cEYFP-Empty | Empty-nEYFP + cEYFP-Empty

YFP

H3.3-RFP

Merge

B

Percentage of nuclei with YFP (%)

n=120

***

Empty-nEYFP + cEYFP-Empty
AHL22-nEYFP + cEYFP-Empty
Empty-nEYFP + cEYFP-HDA15
AHL22-nEYFP + cEYFP-HDA15

C

Col-0   Hda15-1

D

P value= 0.0003

***

Hypocotyl Length (mm)
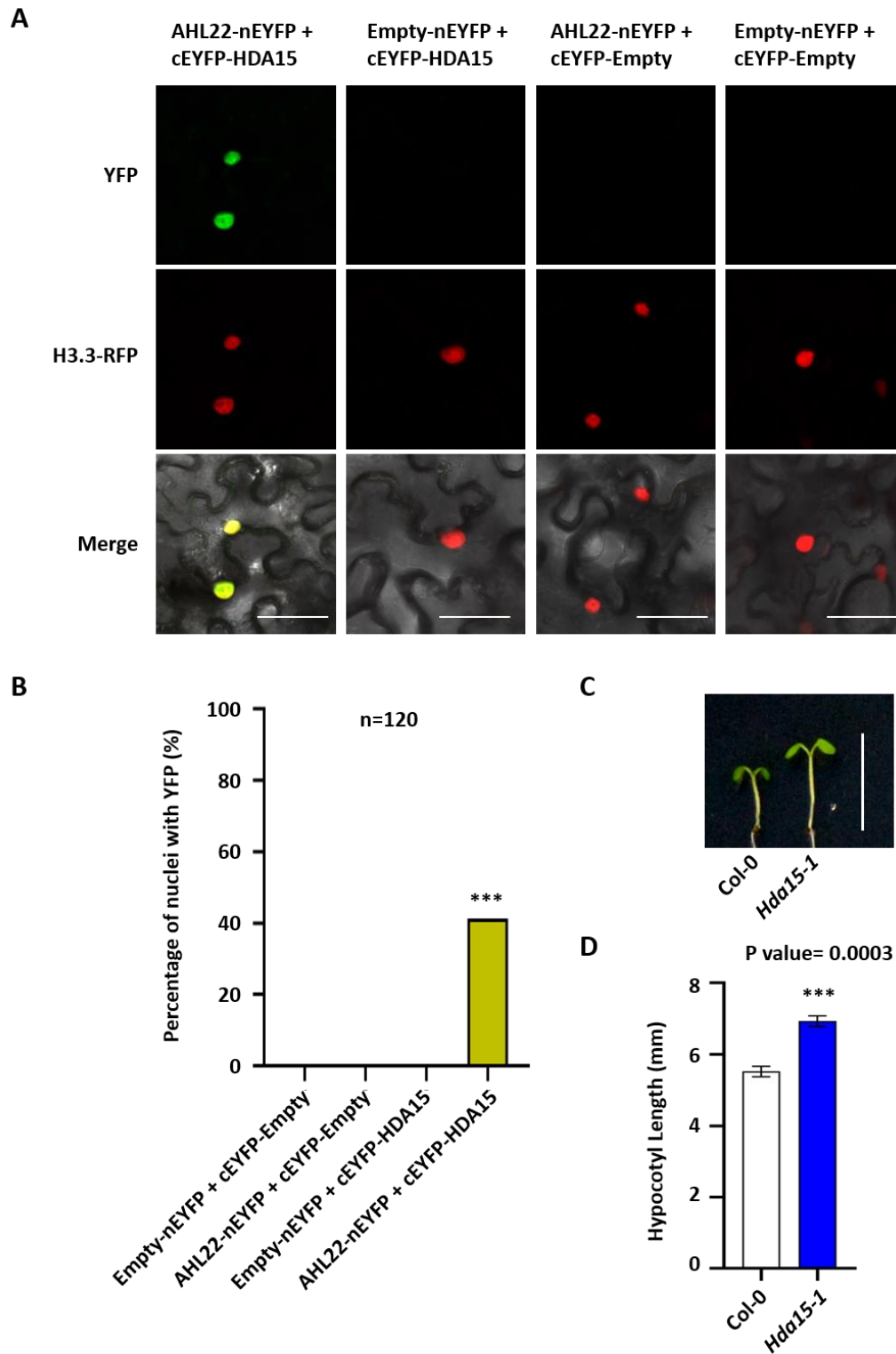
Col-0   Hda15-1

Figure 3.20. (See legend on next page)

(See figure on previous page)

Figure 3.20. AHL22 and HDA15 interaction.

(A). Bimolecular fluorescence complementation (BiFC) analysis of AHL22 and HDA15 interaction in vivo. AHL22 and HDA15 fused with pSITE-nEYFP-N1 and pSITE-cEYFP-C1 vectors, respectively, were co-transformed into *N. benthamiana*. H3.3 RFP was used to indicate the nuclei. Scale bar= 50 μm. (B). Quantification of the nuclei with both YFP and RFP signals from different pairwise BiFC experiments. n=120. (C). The hypocotyl phenotype of *hda15-1* grown vertically under LD condition (16h at 23 °C under 22 μmol·m^{-2}·s^{-1} continuous white light, 8h at 23 °C dark) for 5 days. Scale bar= 1 cm. (D). Hypocotyl lengths of Col-0 and *hda15-1*. The average length of three independent measurements ± standard deviations are shown. Each measurement with n=30 plants. Unpaired two-tailed Student's t-test was used to determine significance between wild-type and mutants or overexpression lines. ns *p-value* >0.05, **p-value* ≤ 0.05, ***p-value* ≤ 0.01, ****p-value* ≤ = 0.001, *****p-value* ≤ = 0.0001.

Since AHL and FRS form a complex to regulate hypocotyl growth, I further tested whether FRS7 and FRS12 could also interact with HDA15 by using BiFC. The results showed that HDA15 was found only interacting with AHL22, as the YFP signal can only be detected in the combination of AHL22-HDA15 but not in the combination of FRS7-HDA15 and FRS12-HDA15 (Figure 3.21). Furthermore, HDA15 can interact with itself to form a dimer in the nuclei, with the YFP signal predominantly distributed in the nucleolus (Figure 3.21). Thus, I concluded that HDA15 interacted only with AHL22.
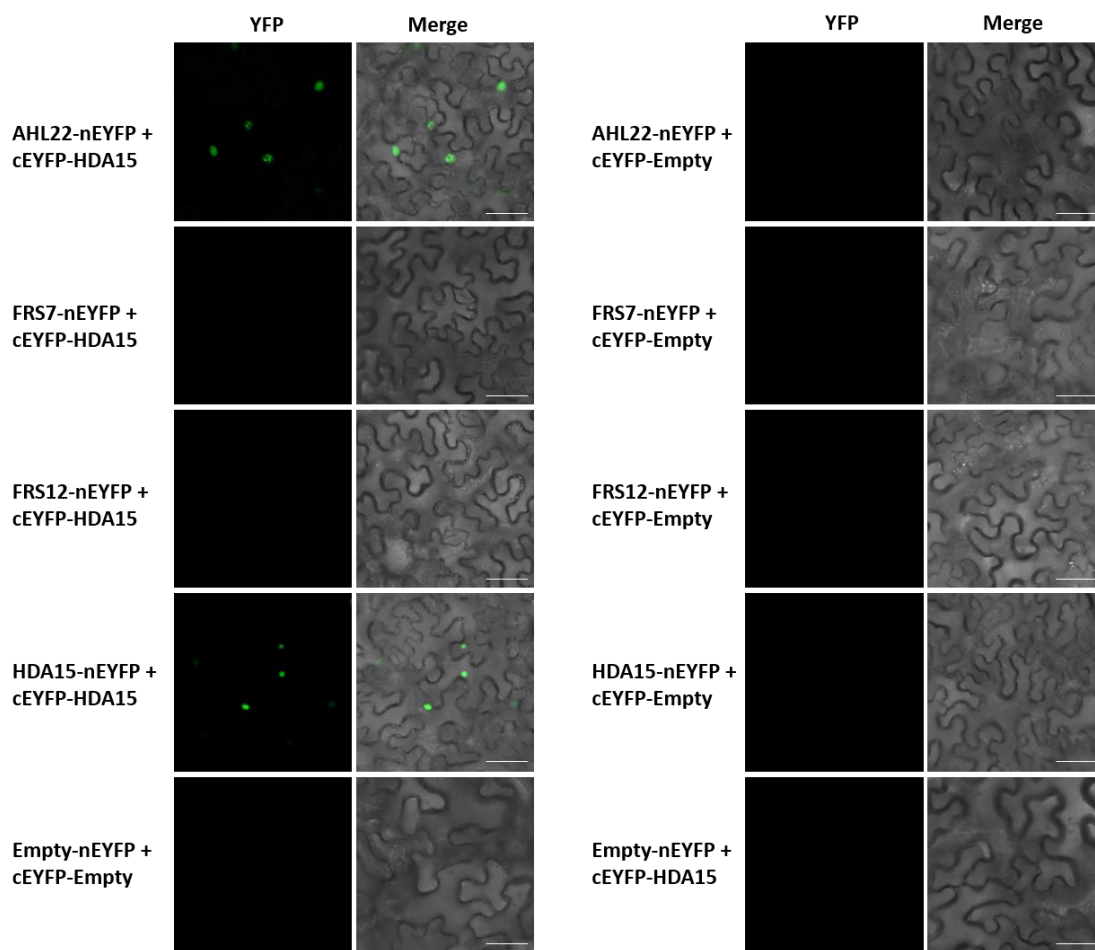

Figure 3.21. BiFC analysis of FRS7/12 and HDA15 interaction *in vivo*.
AHL22/FRS7/FRS12/HDA15 and HDA15 fused with pSITE-nEYFP-N1 and pSITE-cEYFP-C1 vector, respectively, were co-transformed into *N. benthamiana*. Scale bar= 50 μm.

3.3.2 AHL22 and HDA15 form speckles in the nucleoplasm independently of phase separation

The localization of HDA15 is dependent on light. When exposed to light, HDA15 signals are in the nucleus, whereas shuttles out of the nucleus in the absence of light (Alinsug et al. 2012). From my BiFC results, in the absence of AHL22 co-expression, the HDA15 signal exhibited uniform distribution in the nucleolus under light (Figure 3.22A). However, when HDA15 was co-expressed with AHL22 as the BiFC pairs, the reconstituted yellow fluorescent protein (YFP) fluorescence resulting from the physical interaction between HDA15 and AHL22 is distributed in discrete nuclear speckles in the nucleoplasm under light (Figure 3.22A). This was further confirmed by expressing a single HDA15 protein and co-expressing HDA15 and AHL22 proteins in *Nicotiana benthamiana* leaves. Around 80% of HDA15 proteins showed a single nucleolus signal when only expressed HDA15. This number was reduced to around 30% with an increased number (around 70%) of multiple speckles signal in the nucleoplasm when co-expressed HDA15 and AHL22 (Figure 3.22B and 3.22C). These results suggested that the interaction between AHL22 and HDA15 results in the distribution of discrete speckles of HDA15 from the nucleolus to the nucleoplasm.

(See figure on next page)

Figure 3.22. AHL22 and HDA15 form speckles *in vivo*.
(A). AHL22/HDA15 and HDA15 fused with pSITE-nEYFP-N1 and pSITE-cEYFP-C1 vector, respectively, were co-transformed into *N. benthamiana*. Scale bar= 5 μm. (B). 35S::HDA15-GFP and a combination of 35S-HDA15-GFP and 35S-AHL22-3FLAG were co-transformed into *N. benthamiana*. Scale bar=*5* μm or 10 μm. (C). Quantification of the nuclei with single or multiple GFP signals in 35S::HDA15-GFP and combination of 35S::HDA15-GFP and 35S::AHL22-3FLAG.

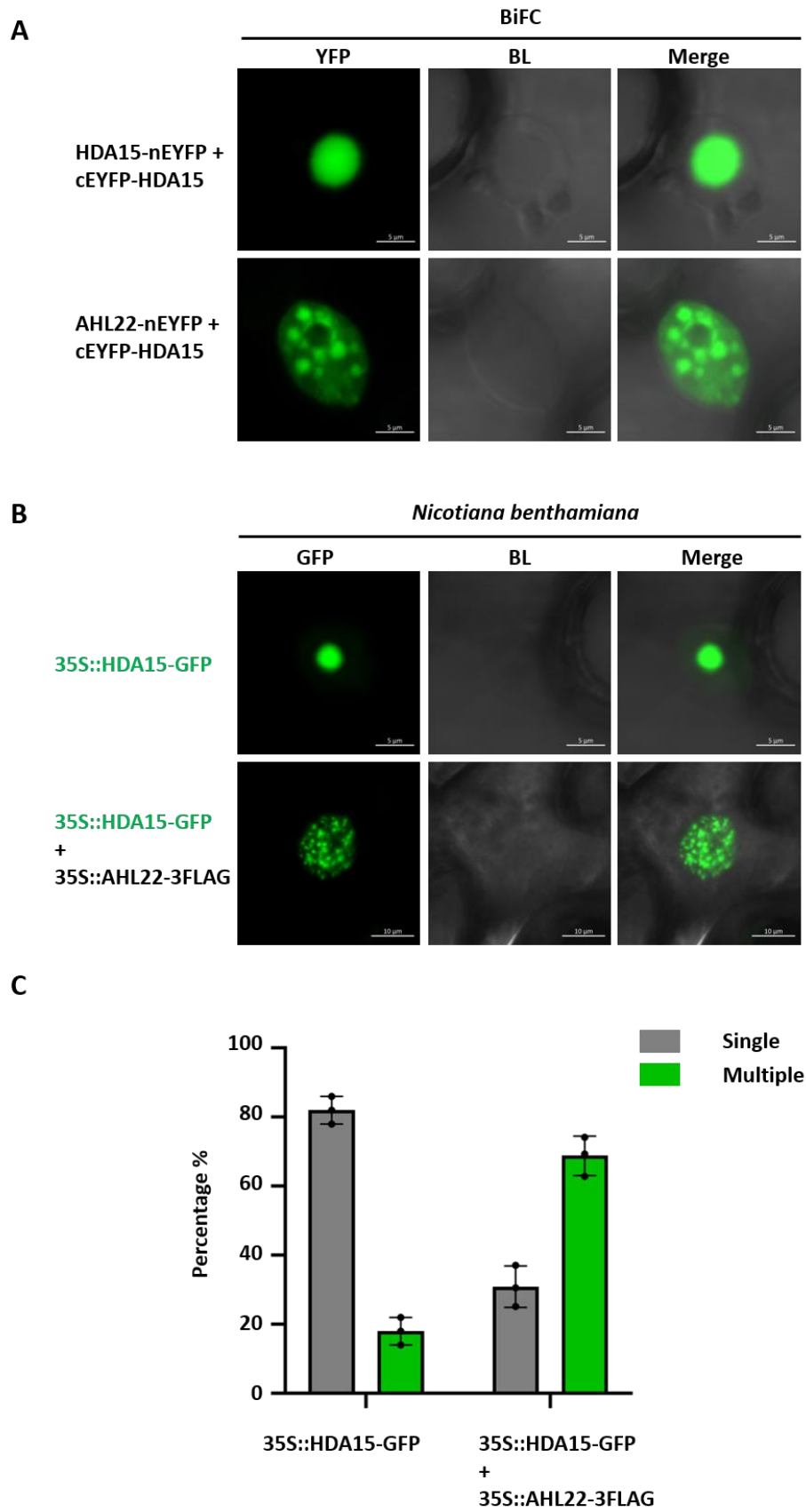A

BiFC

| YFP | BL | Merge |

HDA15-nEYFP +
cEYFP-HDA15

AHL22-nEYFP +
cEYFP-HDA15

B

Nicotiana benthamiana

| GFP | BL | Merge |

35S::HDA15-GFP

35S::HDA15-GFP
+
35S::AHL22-3FLAG

C

Figure 3.22. (See legend on previous page)

Liquid-liquid phase separation (LLPS) is known to be essential in many aspects of cellular processes, including the formation of classical membrane-less organelles (Boeynaems et al. 2018; Emenecker, Holehouse, and Strader 2020). To investigate whether the nuclear speckles formed by the combination of AHL22 and HDA15 in the nuclear undergo LLPS, I carried out a Fluorescence Recovery After Photobleaching (FRAP) assay followed by time-lapse imaging for the *in vivo* signal of HDA15-GFP. The results showed that the HDA15-GFP signal did not diffuse from the unbleached area to the bleached area in both single expressed HDA15-GFP and co-expressed HDA15-GFP with AHL22 signals (Figure 3.23A and 3.23B), suggesting that the nuclear speckles form gel-like condensates rather than liquid-like droplets.
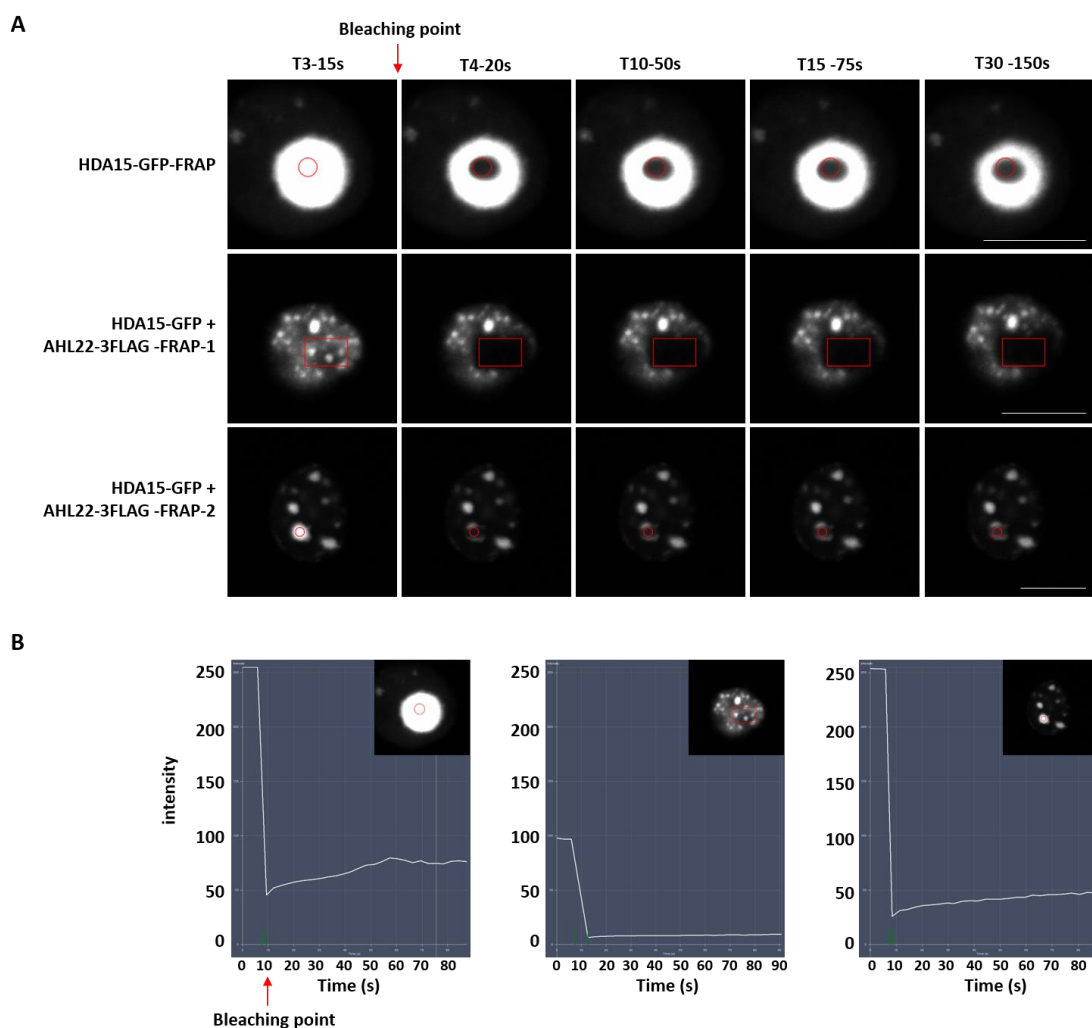

Figure 3.23. The formation of speckles is independent of LLPS.
(A). Fluorescence recovery after photobleaching (FRAP) assay of HDA15-GFP protein. The red arrow indicates the bleaching point. Scale bar= 10 μm. (B). Time course of the recovery of HDA15-GFP droplets after bleaching. The red arrow indicates the bleaching point.

3.3.3 HDA15 suppresses the expression of auxin-responsive genes

To further investigate the gene regulation responsible for the longer hypocotyl phenotype in the *hda15-1* mutant, I generated transcriptome profiles of 5-d-old seedlings grown on vertical MS plates under the same condition as *ahl22 frs7 frs12* transcriptome analysis. From three biological replicates, I identified in total 1179 differentially expressed genes (DEGs, log2FC > 1 or log2FC < -1, FDR < 0.05) in *hda15* compared to Col-0, with 556 DGs and 623 UGs (Figure 3.24A). These DGs and UGs in *hda15* showed a high overlap with the DGs and UGs in *ahl22 frs7 frs12*, with a p-value of $6.8e^{-305}$ and $2.2e^{-183}$, respectively (Figure 3.24B). Further GO enrichment analysis indicated that UGs in *hda15* were involved in phytohormone pathways, including "response to jasmonic acid", "response to abscisic acid", "response to gibberellin" as well as "response to auxin" (Figure 3.24C). By contrast, DGs were involved in the "starch catabolic process", "circadian rhythm", and "carbohydrate metabolic process" (Figure 3.24D). Overall, these data demonstrated that HDA15 and AHL-FRS complex act in a similar pathway.
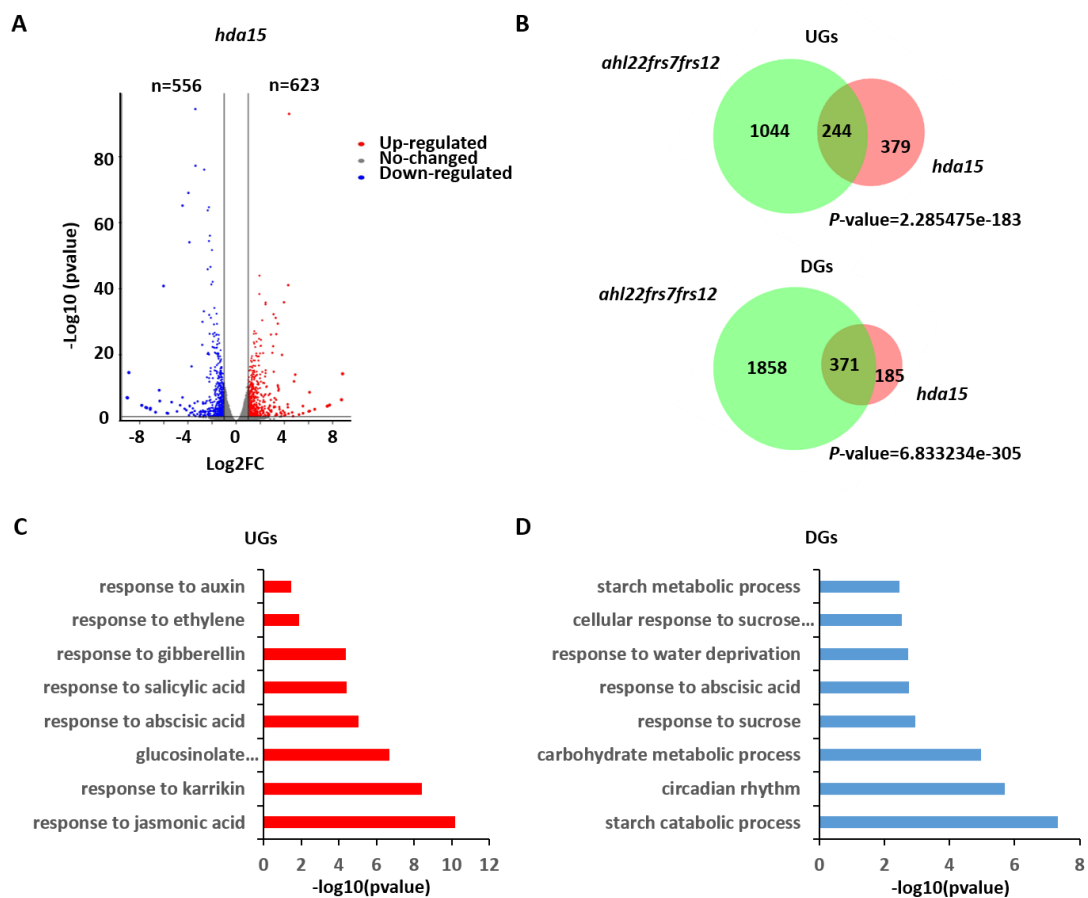
Figure 3.24. RNA-seq of *hda15-1*.

(A). Volcano plots of DEGs in *hda15-1* compared to Col-0. The X and Y axes represent log2FC and the statistical significance as the negative log10 (*p-value*). The red dots represent genes that were significantly up-regulated genes (UGs), while the blue dots represent the significantly down-regulated genes (DGs). Genes that were not significantly changed were shown with grey dots. (B). Venn diagrams showing overlap of UGs and DGs in *triple* and *hda15-1*. Significance was tested using a hypergeometric test. (C, D). Enriched biological processes of common genes identified from UGs (C) and DGs (D) in *triple* and *hda15-1* mutants. The X-axis represents negative log10 (*p-value*).

Transcriptome data revealed that HDA15 and AHL-FRS complex co-repress a number of genes involved in auxin response, such as *SAUR* family genes. The qRT-PCR analysis confirmed that the expression of *SAUR6*, *SAUR14*, *SAUR15*, *SAUR16*, *SAUR20*, *SAUR21*, *SAUR51*, and *SAUR78* was significantly increased in both *triple* and *hda15-1* (Figure 3.25A and 3.25B), supporting the repressive function of HDA15 and AHL-FRS complex in hypocotyl elongation via the auxin signaling pathway.
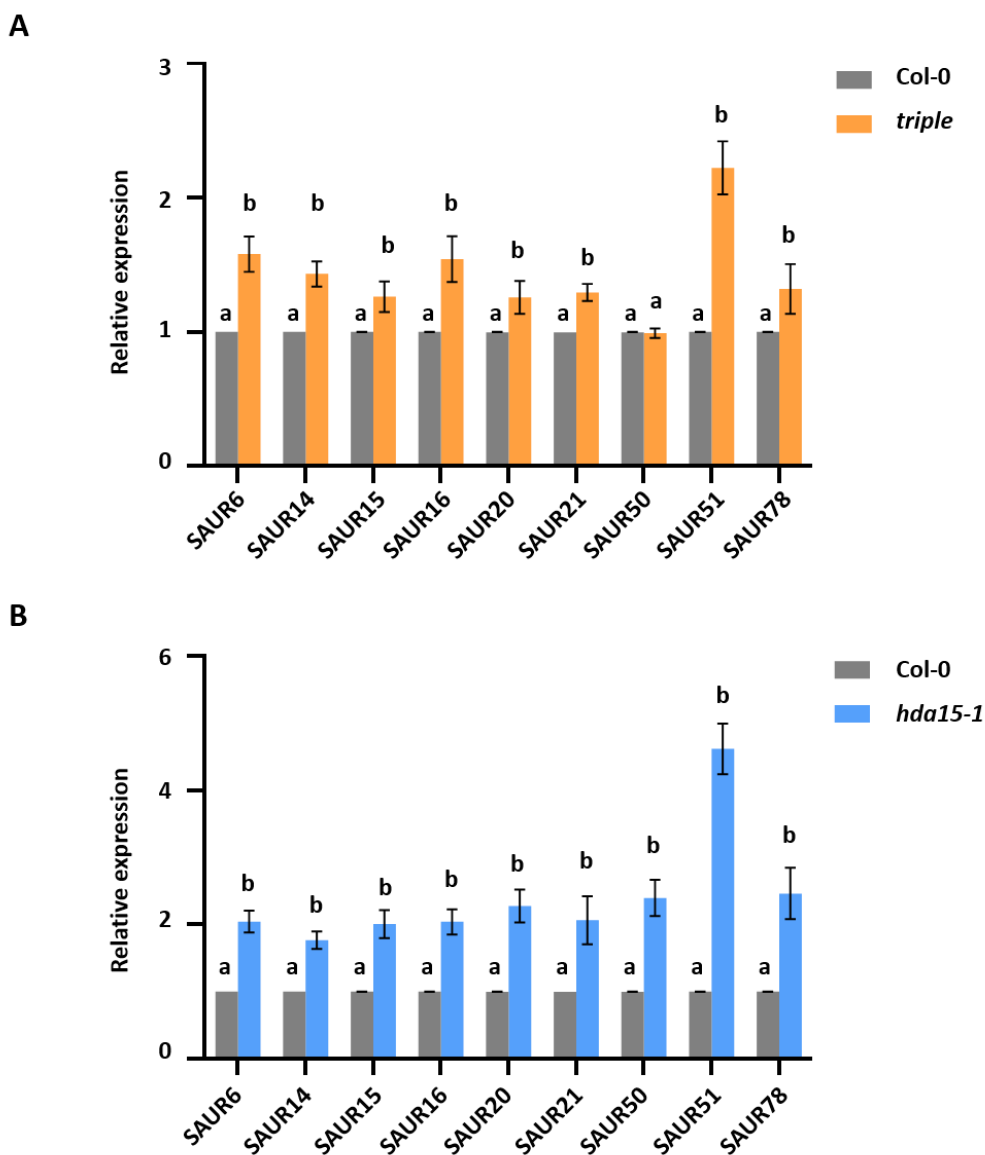
Figure 3.25. HDA15 and AHL-FRS complex co-repress the expression of genes' response to auxin.

(A, B). The relative expression level of the selected genes by qRT-PCR from 5-d-old whole plants in *triple* (A) and *hda15-1* (B). Values are means ± SD of three biological repeats. The significance of differences in each gene was tested using one-way ANOVA with Tukey's test ($P < 0.05$), and different letters indicate statistically significant differences.

3.3.4 AHL complex and HDA15 decrease the H3ac levels of the target genes

As a histone deacetylase, HDA15 negatively controls hypocotyl elongation. To examine the histone acetylation levels of the HDA15 and AHL-FRS complex coregulated genes, I first performed a western blot on total extracts of Col-0, *ahl22 frs7 frs12*, and *hda15-1* from 5-d-old seedlings, and observed a slight increase of H3 acetylation (H3ac) in the *hda15-1* mutant but not in the *ahl22 frs7 frs12* mutant (Figure 3.26A). This might be because of the low sensitive detection by western blot for total protein level from total extracts in the *ahl22 frs7 frs12* mutant. The level of H4ac and H3 did not show a difference among Col-0, *ahl22 frs7 frs12*, and *hda15-1* in our experiments (Figure 26A). I then validated the H3ac levels by ChIP-qPCR assay at the promoter regions of selected *SAUR* genes, including *SAUR14/15*, *SAUR16*, *SAUR20*, *SAUR21*, and *SAUR78* (Figure 3.26B). A significant increase in H3ac levels in the promoter regions of these genes was detected in *hda15-1* and *ahl22 frs7 frs12* compared to wild type (Figure 3.26C). These data indicated that HDA15 and AHL-FRS complex might repress the expression of auxin response genes by removing H3 acetylation at promoter regions.
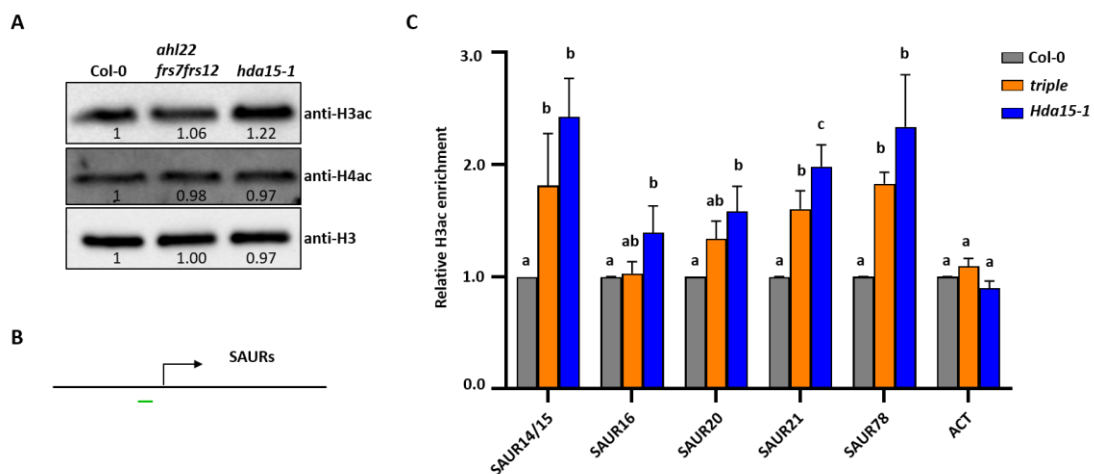
Figure 3.26. HDA15 and AHL-FRS complex decreases the histone H3ac levels of the target genes.

(A). Western blot for H3ac, H4ac and H3 levels in total extracts from 5-d-old whole plants of Col-0, *ahl22 frs7 frs12* and *hda15-1*. (B). Schematic structure of selected genes. Arrows indicate transcription start sites. The green line indicates regions examined by ChIP-qPCR. (C). Relative H3ac enrichment at selected genes determined by ChIP-qPCR in Col-0, *triple* and *hda15-1*. Values are means ± SD of three biological repeats. The significance of differences in each gene was tested using one-way ANOVA with Tukey's test ($P < 0.05$), and different letters indicate statistically significant differences.

4 Discussion

Chromatin structure and dynamics influence DNA accessibility to regulate gene expression (Allis and Jenuwein 2016). The nuclear matrix, a supporting structure of nuclei responsible for DNA compartment and chromatin organization, has been studied to affect DNA replication and transcription (Nelson et al. 1986). However, *in vivo* genome-wide analysis of nuclear matrix on transcriptional control is poorly understood in plants. In this thesis, I isolated Arabidopsis nuclear matrix and extracted the DNA and proteins, followed by whole genome sequencing and LIQUID CHROMATOGRAPHY MASS SPECTROMETRY (LCMS) analysis to study the function of matrix attachment regions and nuclear matrix-associated proteins, respectively. I provided evidence to show that AT-hook Motif Nuclear Localized proteins (AHLs) are nuclear matrix-associated proteins (Table 3.2), such as AHL22 and AHL4. Tandem affinity purification (TAP) followed by the mass spectrometric analysis of AHL22 revealed that AHLs form a complex with other transcription factors (FRS12). Interestingly, FRS11 and FHY3, from the same family of FRS12, were candidates of the nuclear matrix-associated proteins (Table 3.2), suggesting that AHLs and FRSs shared a strong interaction. Indeed, the AHLs and FRSs together as a negative regulator in hypocotyl elongation by repressing the expression of auxin-responsive genes. This repression depends on the AHL complex-mediated nuclear matrix attachment. Moreover, AHL-mediated histone deacetylation inhibited auxin response genes by interacting with a histone deacetylase, HDA15. Thus, this thesis provides insight into how nuclear matrix attachment and histone deacetylation regulate gene expression in hypocotyl elongation.

4.1 AHLs form a complex with non-AHL proteins in plant development

AT-hook Motif Nuclear Localized proteins (AHLs) are conserved in all sequenced land plants (Zhao et al. 2013; Zhao et al. 2014). 29 Arabidopsis AHLs have been classified into two clades based on the existence of intron (Zhao et al. 2013). Previous studies showed that AHL proteins interact with each other and function redundantly in many aspects of plant development (Street et al. 2008; Zhao et al. 2013). Indeed, my TAP-MS data supported the interaction among the AHL family. Several AHLs from both clades were enriched in the candidates of AHL22 interactors (Table 3.1). Besides the AHL proteins, AHLs can interact with other non-AHL proteins *in vitro* and *in vivo*. Such the proteins, TCP transcription factors were proved to interact with AHL29/SOB3 (Zhao et al. 2013). In my study, I identified new interactors of the AHL family, including transcription factor FRS12/FRS7 (Table 3.1, Figure 3.1, 3.2) and histone protein HTA7 (Table 3.1).

As sessile organisms, plants heavily rely on the plasticity of growth and development to adaptively respond to external challenges. In *Arabidopsis thaliana*, the AT-hook motif nuclear-localized (AHL) transcription factor family have been implicated in

hypocotyl elongation. Hypocotyl growth is strongly influenced by both external and internal cues, such as temperature and light, as well as phytohormones, including auxin, brassinosteroid, gibberellins, and ethylene, respectively (Vandenbussche, Verbelen, and Van Der Straeten 2005). AHL family represses hypocotyl growth by modulating the expression of *YUC* genes and the *SAUR19* subfamily (Favero et al. 2016; Favero, Le, and Neff 2017; Lee and Seo 2017). The FRS7-FRS12 complex was reported to inhibit hypocotyl growth by directly binding to the PIF4 transcription factor and repressing its expression, further repressing PIF4-downstream targets in a photoperiod manner (Ritter et al. 2017). My analysis of the genetic interaction between *ahl22* and *frs7 frs12* suggests that the *ahl22 frs7 frs12* triple mutant displays a longer hypocotyl phenotype resulting from increased gene expression accumulation response to auxin, such as *SAUR* family genes (Figure 3.4, 3.6, 3.25). SAURs promote cell expansion by activating H^+-ATPases to lower apoplastic pH (Rayle and Cleland 1980; Spartz et al. 2014; Li et al. 2022). Similar to the direct binding of FRSs to PIF4, AHL29/SOB3 direct binds to PIFs in the regulation of petiole growth. Unlike the direct repression of PIF4-downstream targets from FRSs, AHL29/SOB3 antagonizes PIF-mediated transcriptional activation of genes related to growth and hormone pathways (Favero et al. 2020). This raises one possibility that the AHL-FRS complex represses hypocotyl elongation by redundantly regulating PIF-mediated downstream genes.

Arabidopsis AHLs contain one or two AT-hook motif(s) and act as DNA-binding proteins to modify epigenetic modifications. In the flowering time control, AHL22 and AHL16 modulate histone acetylation and H3K9me2 level at two key flower genes, *FT* and *FLC*, respectively (Yun et al. 2012; Xu et al. 2013). Recent studies showed that multiple AHLs function at different plant developments. For instance, AHL29/SOB3 restricts petiole growth by antagonizing PIF4-mediated transcriptional activation related to growth and phytohormones (Favero et al. 2020). AHL16 contributes to pollen wall exine patterning by regulating the expression of AGPs and CalS5 (Jia et al. 2014; Xiong et al. 2020). AHL15 promotes plant longevity by repressing *SPL* gene expression (Rahimi et al. 2022). However, the exact molecular mechanism of how histone modifications influence AHL-mediated transcription in plant developments is still elusive. In addition, AHL proteins bind to Matrix Attachment Regions (MARs) (Fujimoto et al. 2004; Lim et al. 2007; Xu et al. 2013). However, the contribution of the nuclear matrix to their transcriptional regulation remains undiscovered.

My study first provides evidence of how nuclear matrix and histone modification contribute to AHL complex-mediated transcription in hypocotyl elongation. By performing genome-wide proteomic and MAR-seq analysis, I have found that AHL and FRS proteins are enriched as nuclear matrix-associated proteins and are required for matrix attachment regions enrichment, especially for the short genes, including auxin-responsive genes (Table 3.2, Figure 3.14, 3.15, 3.16, 3.17, 3.18, 3.19). The reduced MAR enrichment in *ahl22 frs7 frs12* results in the increased expression of *SAUR* genes (Figure 3.16, 3.17, 3.18). This activation was further reasoned by an

increased H3 acetylation level resulting from the interaction between AHL and a histone deacetylase, HDA15 (Figure 3.20, 3.26).

4.2 MARs contribute to both repressive and active transcription

Matrix attachment regions (MARs) are found in all mammals and plants. They are DNA elements that bind to the nuclear matrix or copurified along with nuclear matrix isolation (Michalowski et al. 1999). MARs are crucial for chromatin organization and act as positive and/or negative regulators of gene expression (Cockerill, Yuen, and Garrard 1987; Allen, Spiker, and Thompson 2000; Heng et al. 2004; Chavali, Funa, and Chavali 2011). In this study, I report the first *in vivo* genome-wide distribution of MARs in the Arabidopsis genome. I identified 16629 MAR elements in Wild-type (Col-0) (Figure 3.11). These MARs prefer coding genes over TEs and accumulate around TSS and TES sites (Figure 3.11). The peak downstream of the TSS site is consistent with the previous study on plants and animals (Pascuzzi et al. 2014; Pathak, Srinivasan, and Mishra 2014), supporting that MARs are highly related to gene expression. Further characterization of MARs revealed that MAR-enriched genes are highly correlated with active epigenetic marks and exhibit a higher expression level than non-MARs marked genes (Figure 3.12 3.13). Moreover, MARs have a higher enrichment at short genes (less than 2 kb) (Figure 3.15). Collectively, the genome-wide distribution of MARs indicates that Arabidopsis MARs are highly associated with gene expression.

By correlating the differential MARs with transcriptomic data in *ahl22 frs7 frs12* compared to Col-0, I found that decreased MARs dependent on AHL-complex play dual roles in transcriptional control (Figure 3.16). As nuclear matrix proteins, the RNA-seq and ChIP-seq data of AHL29/SOB3 in petiole growth revealed that AHLs has both positive and negative function in transcription (Favero et al. 2020). Previous studies showed that the AHL and FRS family function as repressors in many aspects of plant development. However, how the AHL complex activates gene expression remains unknown.

AHL complex-dependent MARs negatively regulate gene expression.
AHL22 and AHL16 modulate gene expression by affecting histone acetylation levels (Yun et al. 2012; Xu et al. 2013). Together with a correlation of histone acetylation on MARs (Figure 3.12), histone acetylation may be required for the repressive function of AHL complex-mediated MARs. In this study, I identified a histone deacetylase, HDA15, which shares a phenotype and transcription pattern similar to the AHL complex by interacting predominantly with AHL22 in the hypocotyl regulation (Figure 3.20, 3.24, 3.25). Indeed, auxin-responsive genes (*SAURs*) exhibit an increased H3 acetylation level in both *ahl22 frs7 frs12* and *hda15* mutants compared to Col-0 (Figure 3.26). These genes are direct targets of AHLs and/or FRSs and have a lower MAR enrichment in the *ahl22 frs7 frs12* and *sob3-6* mutants (Figure 3.17, 3.18). Taken together, these data suggest that AHL complex-dependent MARs repress gene

expression by altering the histone acetylation levels. This active histone modification promotes transcription by reducing the compaction of DNA-histone and promoting RNA polymerase and transcription factors binding to genes to initial transcription (Eberharter and Becker 2002; Clayton, Hazzalin, and Mahadevan 2006). Furthermore, it will be interesting to investigate, for example, whether other active epigenetic marks can also influence the repressive function of AHL-dependent MARs in transcriptional control, as MARs are highly associated with other active epigenetic marks (Figure 3.12).

AHL complex-dependent MARs positively regulate gene expression.
Although I have bridged the connection of MARs and histone modification in AHL/FRS-mediated transcriptional repression in hypocotyl regulation, little is known about how MAR and AHL activate gene expression. My study shows a significant correlation between decreased MARs enrichment and down-regulated genes in *ahl22 frs7 frs12* compared to Col-0 (Figure 3.16). Moreover, transcriptome data also showed that numerous genes had a reduced level in *ahl* and *frs* (Figure 3.5). Based on our knowledge, there are a few potential ways in which pathways could contribute to this activation by AHL complex-dependent MARs.

Other transcription factors contribute to transcription activation by AHL complex-dependent MARs. Proteomic data of AHL revealed that AHL proteins not only interact with each other but also interact with other non-AHL proteins, like TCP and FRS. In addition, ChIP-seq data of both AHL29/SOB3 and FRS12 co-targets are highly involved in transcriptional regulation (Figure 3.7), indicating a complicated regulatory network of AHL proteins in transcription. PHYTOCHROME-INTERACTING FACTORs (PIFs), the key positive plant growth regulators, are involved in the AHL-FRS regulatory network. The FRS7-FRS12 complex function as a repressor by directly binding to the PIF4 transcription factor and repressing its expression, further repressing PIF4-downstream targets in a photoperiod manner (Ritter et al. 2017). AHL29/SOB3 represses petiole growth by antagonizing PIFs-mediated transcriptional activation of genes (Favero et al. 2020). However, no evidence showed that PIFs could interact with AHLs or FRSs. I have found that the decreased MAR enrichment at PIFs results in a lower expression level compared to Col-0 (Figure 4.1). Interestingly, the distribution of MAR at PIFs is mainly outside the coding regions instead of two major peaks around TSS and TES (Figure 4.1, 3.11), indicating that different MARs locations may have different transcription functions. Therefore, AHL complex-dependent MARs positively regulate gene expression by increasing positive transcription factors' activity, indirectly activating gene expression.
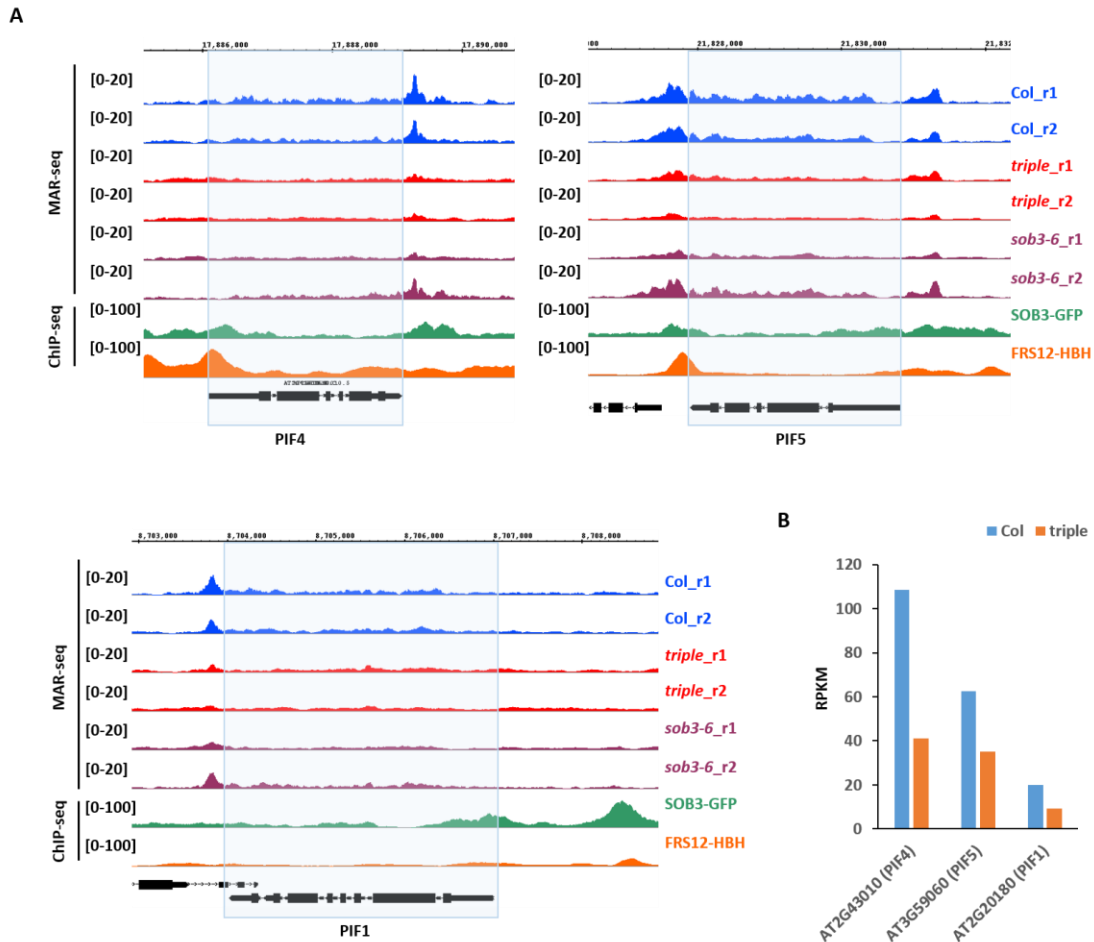
Figure 4.1. Decreased MAR at PIFs targeted by both SOB3 and FRS12.
(A). Genome browser views of two replicates of PIFs indicated in the blue box in Col, *triple* and *sob3-6*. (B). The relative expression levels (RPKM) of PIFs from RNA-seq data of Col and *triple*.

Pol II pausing may be involved in transcription activation by AHL complex-dependent MARs. Pol II pausing, also known as Pol II poised, happens 30-50 bp downstream of the transcription start site (TSS) and requires further activation to proceed to transcription elongation (Adelman and Lis 2012; Jonkers and Lis 2015). In *Drosophila melanogaster*, paused Pol II can inhibit transcription reinitiation and should be released before new initiation can occur (Shao and Zeitlinger 2017; Zlotorynski 2017). MARs are associated with the ends of some DNaseI-sensitive (transcriptionally poised) domains (Bonifer et al. 1991). My findings showed that MARs localize downstream of the TSS site (Figure 3.11), suggesting that MARs may play a role in Pol II pausing. I hypothesize that reduced MAR enrichment to the nuclear matrix in *ahl22 frs7 frs12* mutant may result in more Pol II pausing at targets genes, further inhibiting transcription elongation. Therefore, an important topic for future studies is investigating the genome-wide profile of Pol II distributions to measure the extent of poising in the mutant.

4.3 Histone acetylation is required for the activation of hypocotyl-related genes

Histone modifications are essential for chromatin structure and transcription, which are dynamically controlled by specific "writers", "erasers", and "readers". These modifications influence transcription by directly affecting DNA accessibility or indirectly recruiting histone readers for other regulatory mechanisms (Kouzarides 2007; Musselman et al. 2012). Histone acetylation functions as a hallmark of transcriptional activation by reducing the affinity of DNA and histone, which promotes the binding of RNA polymerase and transcription factors (Eberharter and Becker 2002; Clayton, Hazzalin, and Mahadevan 2006). Histone acetylation plays a vital role in AHL-mediated transcription. AHL22 and AHL16 modulate certain flower genes expression by affecting histone acetylation levels in the flower time control (Yun et al. 2012; Xu et al. 2013). In this study, I identified a histone deacetylase, HDA15, which shares a similar function with AHL22 and FRS7/12 in hypocotyl elongation (Figure 3.20, 3.24, 3.25). HDA15 represses hypocotyl elongation by interacting with HY5 and NF-YCs and directly targeting auxin signaling genes, causing hypoacetylation and transcription repression (Tang et al. 2017; Zhao, Peng, et al. 2019). I also observed an increased H3 acetylation level at *SAUR* genes in *ahl22 frs7frs12* and *hda15* (Figure 3.26). Although I have shown that MARs binding to the nuclear matrix is essential for the proper expression of *SAURs*, whether these targets bear a more open chromatin state remains unknown. Detailed studies on chromatin accessibility, for example, Assay for Transposase-Accessible Chromatin with high-throughput sequencing (ATAC-seq) will provide more insight into the function of nuclear matrix and histone acetylation on transcriptional control.

The localization of HDA15 in the nuclear is driven by light from nuclear to cytoplasm (Alinsug et al. 2012). From my observation, overexpression of AHL22 could distribute the HDA15 signal from nucleolus to nucleoplasm as speckles (Figure 3.22). And this distribution is independent of phase separation (Figure 3.23). It remains to be determined whether this signal distribution is caused by the compaction of DNA to the nuclear matrix and influences the genome-wide acetylation landscape. Moreover, Further identification and characterization of other HDACs in different AHL complex-mediated plant development could help incorporate new insight into the function of AHL complex-dependent nuclear matrix and histone modifications in transcriptional regulation.

5 Summary

The nuclear matrix, a supporting structure of nuclei, influences transcription states by regulating chromatin structure and histone modifications. Compartments of the nuclear matrix, such as matrix attachment regions (MARs) and matrix-associated proteins, act in DNA replication and transcription in mammals. However, *in vivo* genome-wide analysis of nuclear matrix on transcriptional regulation is poorly understood in plants.

In this thesis, I isolated Arabidopsis nuclear matrix and extracted the DNA and proteins followed by whole genome sequencing and LIQUID CHROMATOGRAPHY MASS SPECTROMETRY (LCMS) analysis to study the function of matrix attachment regions and nuclear matrix-associated proteins, respectively. I first provided evidence to show that AT-hook Motif Nuclear Localized proteins (AHLs) are nuclear matrix-associated proteins, including AHL22. Tandem affinity purification (TAP) followed by the mass spectrometric analysis of AHL22 revealed that AHLs form a complex not only with other AHLs but also with non-AHL transcription factors, such as FRS12. Interestingly, FRS11 and FHY3, from the same family of FRS12, were candidates of the nuclear matrix-associated proteins, suggesting that AHLs and FRSs shared a strong interaction. Indeed, AHLs and FRSs interact physically and genetically and function as a negative regulator of hypocotyl elongation by repressing the expression of auxin-responsive genes *SAURs*.

Genome-wide analysis of MARs revealed that MARs prefer coding genes rather than TEs in the genome and accumulate at around both TSS and TES sites. The peak downstream of the TSS site is consistent with the previous study in both plants and animals, supporting that MARs are highly associated with gene expression. Indeed, the correlation between MAR-enriched genes and different epigenetic modifications showed that MAR-enriched genes are correlated with active histone marks. Moreover, MAR-enriched genes exhibit a higher expression level than other genes and are enriched at short genes less than 2 kb. AHL complex-dependent MARs contribute to both active and repressive transcription.

This repression further depends on AHL-mediated histone deacetylation by interacting with a histone deacetylase, HDA15. The *hda15* mutant shares a phenotype and transcription pattern similar to the mutant of the AHL complex in the hypocotyl regulation. Supportively, HDA15 and AHL-FRS complex represses the expression of auxin response genes by decreasing the levels of histone H3 acetylation. In addition, overexpression of AHL22 could distribute the HDA15 signal from the nucleolus to the nucleoplasm and form speckles.

Taken together, the present study identified components of the nuclear matrix in

Arabidopsis and shed light on the role of a nuclear matrix binding protein AHL22 in repressing hypocotyl elongation, by attaching DNA to the nuclear matrix and reducing histone H3 acetylation levels. Thus, this thesis provides insights into how Arabidopsis AHL-dependent nuclear matrix attachment and histone modifications contribute to transcriptional regulation and plant development.

6 Reference

Adelman, K., and J. T. Lis. 2012. 'Promoter-proximal pausing of RNA polymerase II: emerging roles in metazoans', *Nat Rev Genet*, 13: 720-31.

Albrethsen, J., J. C. Knol, and C. R. Jimenez. 2009. 'Unravelling the nuclear matrix proteome', *J Proteomics*, 72: 71-81.

Alinsug, M. V., F. F. Chen, M. Luo, R. Tai, L. Jiang, and K. Wu. 2012. 'Subcellular localization of class II HDAs in Arabidopsis thaliana: nucleocytoplasmic shuttling of HDA15 is driven by light', *PLoS One*, 7: e30846.

Allen, G. C., S. Spiker, and W. F. Thompson. 2000. 'Use of matrix attachment regions (MARs) to minimize transgene silencing', *Plant Mol Biol*, 43: 361-76.

Allis, C. D., and T. Jenuwein. 2016. 'The molecular hallmarks of epigenetic control', *Nat Rev Genet*, 17: 487-500.

Amankwah, K. S., and U. De Boni. 1994. 'Ultrastructural localization of filamentous actin within neuronal interphase nuclei in situ', *Exp Cell Res*, 210: 315-25.

An, Z., L. Yin, Y. Liu, M. Peng, W. H. Shen, and A. Dong. 2020. 'The histone methylation readers MRG1/MRG2 and the histone chaperones NRP1/NRP2 associate in fine-tuning Arabidopsis flowering time', *Plant J*, 103: 1010-24.

Anzola, J. M., T. Sieberer, M. Ortbauer, H. Butt, B. Korbei, I. Weinhofer, A. E. Mullner, and C. Luschnig. 2010. 'Putative Arabidopsis transcriptional adaptor protein (PROPORZ1) is required to modulate histone acetylation in response to auxin', *Proc Natl Acad Sci U S A*, 107: 10308-13.

Arabidopsis Genome, Initiative. 2000. 'Analysis of the genome sequence of the flowering plant Arabidopsis thaliana', *Nature*, 408: 796-815.

Aravind, L., and D. Landsman. 1998. 'AT-hook motifs identified in a wide variety of DNA-binding proteins', *Nucleic Acids Res*, 26: 4413-21.

Avramova, Z., P. SanMiguel, E. Georgieva, and J. L. Bennetzen. 1995. 'Matrix attachment regions and transcribed sequences within a long chromosomal continuum containing maize Adh1', *Plant Cell*, 7: 1667-80.

Bannister, A. J., and T. Kouzarides. 2011. 'Regulation of chromatin by histone modifications', *Cell Res*, 21: 381-95.

Benhamed, M., C. Bertrand, C. Servet, and D. X. Zhou. 2006. 'Arabidopsis GCN5, HD1, and TAF1/HAF2 interact to regulate histone acetylation required for light-responsive gene expression', *Plant Cell*, 18: 2893-903.

Berezney, R., and D. S. Coffey. 1974. 'Identification of a nuclear protein matrix', *Biochem Biophys Res Commun*, 60: 1410-7.

———. 1977. 'Nuclear matrix. Isolation and characterization of a framework structure from rat liver nuclei', *J Cell Biol*, 73: 616-37.

Berezney, R., M. J. Mortillaro, H. Ma, X. Wei, and J. Samarabandu. 1995. 'The nuclear matrix: a structural milieu for genomic function', *Int Rev Cytol*, 162A: 1-65.

Bernatavichute, Y. V., X. Zhang, S. Cokus, M. Pellegrini, and S. E. Jacobsen. 2008. 'Genome-wide association of histone H3 lysine nine methylation with CHG DNA methylation in Arabidopsis thaliana', *PLoS One*, 3: e3156.

Berr, A., E. J. McCallum, R. Menard, D. Meyer, J. Fuchs, A. Dong, and W. H. Shen. 2010. 'Arabidopsis

SET DOMAIN GROUP2 is required for H3K4 trimethylation and is crucial for both sporophyte and gametophyte development', *Plant Cell*, 22: 3232-48.

Berr, A., S. Shafiq, V. Pinon, A. Dong, and W. H. Shen. 2015. 'The trxG family histone methyltransferase SET DOMAIN GROUP 26 promotes flowering via a distinctive genetic pathway', *Plant J*, 81: 316-28.

Berrios, M., N. Osheroff, and P. A. Fisher. 1985. 'In situ localization of DNA topoisomerase II, a major polypeptide component of the Drosophila nuclear matrix fraction', *Proc Natl Acad Sci U S A*, 82: 4142-6.

Bjerling, P., R. A. Silverstein, G. Thon, A. Caudy, S. Grewal, and K. Ekwall. 2002. 'Functional divergence between histone deacetylases in fission yeast by distinct cellular localization and in vivo specificity', *Mol Cell Biol*, 22: 2170-81.

Bode, J., T. Schlake, M. Rios-Ramirez, C. Mielke, M. Stengert, V. Kay, and D. Klehr-Wirth. 1995. 'Scaffold/matrix-attached regions: structural properties creating transcriptionally active loci', *Int Rev Cytol*, 162A: 389-454.

Bode, J., M. Stengert-Iber, V. Kay, T. Schlake, and A. Dietz-Pfeilstetter. 1996. 'Scaffold/matrix-attached regions: topological switches with multiple regulatory functions', *Crit Rev Eukaryot Gene Expr*, 6: 115-38.

Boeynaems, S., S. Alberti, N. L. Fawzi, T. Mittag, M. Polymenidou, F. Rousseau, J. Schymkowitz, J. Shorter, B. Wolozin, L. Van Den Bosch, P. Tompa, and M. Fuxreiter. 2018. 'Protein Phase Separation: A New Phase in Cell Biology', *Trends Cell Biol*, 28: 420-35.

Bonifer, C., A. Hecht, H. Saueressig, D. M. Winter, and A. E. Sippel. 1991. 'Dynamic chromatin: the regulatory domain organization of eukaryotic gene loci', *J Cell Biochem*, 47: 99-108.

Boycheva, I., V. Vassileva, and A. Iantcheva. 2014. 'Histone acetyltransferases in plant development and plasticity', *Curr Genomics*, 15: 28-37.

Bu, Z., Y. Yu, Z. Li, Y. Liu, W. Jiang, Y. Huang, and A. W. Dong. 2014. 'Regulation of arabidopsis flowering by the histone mark readers MRG1/2 via interaction with CONSTANS to modulate FT expression', *PLoS Genet*, 10: e1004617.

Bustin, M. 2001. 'Revised nomenclature for high mobility group (HMG) chromosomal proteins', *Trends Biochem Sci*, 26: 152-3.

Cai, S., H. J. Han, and T. Kohwi-Shigematsu. 2003. 'Tissue-specific nuclear architecture and gene expression regulated by SATB1', *Nat Genet*, 34: 42-51.

Cairns, B. R., A. Schlichter, H. Erdjument-Bromage, P. Tempst, R. D. Kornberg, and F. Winston. 1999. 'Two functionally distinct forms of the RSC nucleosome-remodeling complex, containing essential AT hook, BAH, and bromodomains', *Mol Cell*, 4: 715-23.

Calikowski, T. T., T. Meulia, and I. Meier. 2003. 'A proteomic study of the arabidopsis nuclear matrix', *J Cell Biochem*, 90: 361-78.

Caro, E., H. Stroud, M. V. Greenberg, Y. V. Bernatavichute, S. Feng, M. Groth, A. A. Vashisht, J. Wohlschlegel, and S. E. Jacobsen. 2012. 'The SET-domain protein SUVR5 mediates H3K9me2 deposition and silencing at stimulus response genes in a DNA methylation-independent manner', *PLoS Genet*, 8: e1002995.

Cartagena, J. A., S. Matsunaga, M. Seki, D. Kurihara, M. Yokoyama, K. Shinozaki, S. Fujimoto, Y. Azumi, S. Uchiyama, and K. Fukui. 2008. 'The Arabidopsis SDG4 contributes to the regulation of pollen tube growth by methylation of histone H3 lysines 4 and 36 in mature pollen', *Dev Biol*, 315: 355-68.

Casanova-Saez, R., and U. Voss. 2019. 'Auxin Metabolism Controls Developmental Decisions in Land Plants', *Trends Plant Sci*, 24: 741-54.

Chavali, P. L., K. Funa, and S. Chavali. 2011. 'Cis-regulation of microRNA expression by scaffold/matrix-attachment regions', *Nucleic Acids Res*, 39: 6908-18.

Chen, C., H. Chen, Y. Zhang, H. R. Thomas, M. H. Frank, Y. He, and R. Xia. 2020. 'TBtools: An Integrative Toolkit Developed for Interactive Analyses of Big Biological Data', *Mol Plant*, 13: 1194-202.

Chen, S., Y. Zhou, Y. Chen, and J. Gu. 2018. 'fastp: an ultra-fast all-in-one FASTQ preprocessor', *Bioinformatics*, 34: i884-i90.

Chen, X., L. Lu, K. S. Mayer, M. Scalf, S. Qian, A. Lomax, L. M. Smith, and X. Zhong. 2016. 'POWERDRESS interacts with HISTONE DEACETYLASE 9 to promote aging in Arabidopsis', *Elife*, 5.

Clayton, A. L., C. A. Hazzalin, and L. C. Mahadevan. 2006. 'Enhanced histone acetylation and transcription: a dynamic perspective', *Mol Cell*, 23: 289-96.

Clough, S. J., and A. F. Bent. 1998. 'Floral dip: a simplified method for Agrobacterium-mediated transformation of Arabidopsis thaliana', *Plant J*, 16: 735-43.

Cockerill, P. N., M. H. Yuen, and W. T. Garrard. 1987. 'The enhancer of the immunoglobulin heavy chain locus is flanked by presumptive chromosomal loop anchorage elements', *J Biol Chem*, 262: 5394-7.

Collett, C. E., N. P. Harberd, and O. Leyser. 2000. 'Hormonal interactions in the control of Arabidopsis hypocotyl elongation', *Plant Physiol*, 124: 553-62.

Cremer, T., G. Kreth, H. Koester, R. H. Fink, R. Heintzmann, M. Cremer, I. Solovei, D. Zink, and C. Cremer. 2000. 'Chromosome territories, interchromatin domain compartment, and nuclear matrix: an integrated view of the functional nuclear architecture', *Crit Rev Eukaryot Gene Expr*, 10: 179-212.

Croft, J. A., J. M. Bridger, S. Boyle, P. Perry, P. Teague, and W. A. Bickmore. 1999. 'Differences in the localization and morphology of chromosomes in the human nucleus', *J Cell Biol*, 145: 1119-31.

Cutter, A. R., and J. J. Hayes. 2015. 'A brief review of nucleosome structure', *FEBS Lett*, 589: 2914-22.

Dai, X., Y. Bai, L. Zhao, X. Dou, Y. Liu, L. Wang, Y. Li, W. Li, Y. Hui, X. Huang, Z. Wang, and Y. Qin. 2017. 'H2A.Z Represses Gene Expression by Modulating Promoter Nucleosome Structure and Enhancer Histone Modifications in Arabidopsis', *Mol Plant*, 10: 1274-92.

Davarinejad, H., Y. C. Huang, B. Mermaz, C. LeBlanc, A. Poulet, G. Thomson, V. Joly, M. Munoz, A. Arvanitis-Vigneault, D. Valsakumar, G. Villarino, A. Ross, B. H. Rotstein, E. I. Alarcon, J. S. Brunzelle, P. Voigt, J. Dong, J. F. Couture, and Y. Jacob. 2022. 'The histone H3.1 variant regulates TONSOKU-mediated DNA repair during replication', *Science*, 375: 1281-86.

de la Paz Sanchez, M., and C. Gutierrez. 2009. 'Arabidopsis ORC1 is a PHD-containing H3K4me3 effector that regulates transcription', *Proc Natl Acad Sci U S A*, 106: 2065-70.

Dharmasiri, N., S. Dharmasiri, and M. Estelle. 2005. 'The F-box protein TIR1 is an auxin receptor', *Nature*, 435: 441-5.

Dickinson, L. A., T. Joh, Y. Kohwi, and T. Kohwi-Shigematsu. 1992. 'A tissue-specific MAR/SAR DNA-binding protein with unusual binding site recognition', *Cell*, 70: 631-45.

Dong, G., D. P. Ma, and J. Li. 2008. 'The histone methyltransferase SDG8 regulates shoot branching in Arabidopsis', *Biochem Biophys Res Commun*, 373: 659-64.

Dong, J., C. LeBlanc, A. Poulet, B. Mermaz, G. Villarino, K. M. Webb, V. Joly, J. Mendez, P. Voigt, and Y.

Jacob. 2021. 'H3.1K27me1 maintains transcriptional silencing and genome stability by preventing GCN5-mediated histone acetylation', *Plant Cell*, 33: 961-79.

Dutta, A., P. Choudhary, J. Caruana, and R. Raina. 2017. 'JMJ27, an Arabidopsis H3K9 histone demethylase, modulates defense against Pseudomonas syringae and flowering time', *Plant J*, 91: 1015-28.

Eberharter, A., and P. B. Becker. 2002. 'Histone acetylation: a switch between repressive and permissive chromatin. Second in review series on chromatin dynamics', *EMBO Rep*, 3: 224-9.

Emenecker, R. J., A. S. Holehouse, and L. C. Strader. 2020. 'Emerging Roles for Phase Separation in Plants', *Dev Cell*, 55: 69-83.

Fan, H., P. Lv, X. Huo, J. Wu, Q. Wang, L. Cheng, Y. Liu, Q. Q. Tang, L. Zhang, F. Zhang, X. Zheng, H. Wu, and B. Wen. 2018. 'The nuclear matrix protein HNRNPU maintains 3D genome architecture globally in mouse hepatocytes', *Genome Res*, 28: 192-202.

Favero, D. S., C. N. Jacques, A. Iwase, K. N. Le, J. Zhao, K. Sugimoto, and M. M. Neff. 2016. 'SUPPRESSOR OF PHYTOCHROME B4-#3 Represses Genes Associated with Auxin Signaling to Modulate Hypocotyl Growth', *Plant Physiol*, 171: 2701-16.

Favero, D. S., A. Kawamura, M. Shibata, A. Takebayashi, J. H. Jung, T. Suzuki, K. E. Jaeger, T. Ishida, A. Iwase, P. A. Wigge, M. M. Neff, and K. Sugimoto. 2020. 'AT-Hook Transcription Factors Restrict Petiole Growth by Antagonizing PIFs', *Curr Biol*, 30: 1454-66 e6.

Favero, D. S., K. N. Le, and M. M. Neff. 2017. 'Brassinosteroid signaling converges with SUPPRESSOR OF PHYTOCHROME B4-#3 to influence the expression of SMALL AUXIN UP RNA genes and hypocotyl growth', *Plant J*, 89: 1133-45.

Feister, H. A., J. E. Onyia, R. R. Miles, X. Yang, R. Galvin, J. M. Hock, and J. P. Bidwell. 2000. 'The expression of the nuclear matrix proteins NuMA, topoisomerase II-alpha, and -beta in bone and osseous cell culture: regulation by parathyroid hormone', *Bone*, 26: 227-34.

Fuchs, J., D. Demidov, A. Houben, and I. Schubert. 2006. 'Chromosomal histone modification patterns--from conservation to diversity', *Trends Plant Sci*, 11: 199-208.

Fujimoto, S., S. Matsunaga, M. Yonemura, S. Uchiyama, T. Azuma, and K. Fukui. 2004. 'Identification of a novel plant MAR DNA binding protein localized on chromosomal surfaces', *Plant Mol Biol*, 56: 225-39.

Gallavotti, A., S. Malcomber, C. Gaines, S. Stanfield, C. Whipple, E. Kellogg, and R. J. Schmidt. 2011. 'BARREN STALK FASTIGIATE1 is an AT-hook protein required for the formation of maize ears', *Plant Cell*, 23: 1756-71.

Gallinari, P., S. Di Marco, P. Jones, M. Pallaoro, and C. Steinkuhler. 2007. 'HDACs, histone deacetylation and gene transcription: from molecular biology to cancer therapeutics', *Cell Res*, 17: 195-211.

Gan, E. S., Y. Xu, J. Y. Wong, J. G. Goh, B. Sun, W. Y. Wee, J. Huang, and T. Ito. 2014. 'Jumonji demethylases moderate precocious flowering at elevated temperature via regulation of FLC in Arabidopsis', *Nat Commun*, 5: 5098.

Gasser, S. M., B. B. Amati, M. E. Cardenas, and J. F. Hofmann. 1989. 'Studies on scaffold attachment sites and their relation to genome function', *Int Rev Cytol*, 119: 57-96.

Gendreau, E., J. Traas, T. Desnos, O. Grandjean, M. Caboche, and H. Hofte. 1997. 'Cellular basis of hypocotyl growth in Arabidopsis thaliana', *Plant Physiol*, 114: 295-305.

Gibcus, J. H., and J. Dekker. 2013. 'The hierarchy of the 3D genome', *Mol Cell*, 49: 773-82.

Gindullis, F., N. J. Peffer, and I. Meier. 1999. 'MAF1, a novel plant protein interacting with matrix

attachment region binding protein MFP1, is located at the nuclear envelope', *Plant Cell*, 11: 1755-68.

Girod, P. A., D. Q. Nguyen, D. Calabrese, S. Puttini, M. Grandjean, D. Martinet, A. Regamey, D. Saugy, J. S. Beckmann, P. Bucher, and N. Mermod. 2007. 'Genome-wide prediction of matrix attachment regions that increase gene expression in mammalian cells', *Nat Methods*, 4: 747-53.

Goodrich, J., P. Puangsomlee, M. Martin, D. Long, E. M. Meyerowitz, and G. Coupland. 1997. 'A Polycomb-group gene regulates homeotic gene expression in Arabidopsis', *Nature*, 386: 44-51.

Gray, W. M., S. Kepinski, D. Rouse, O. Leyser, and M. Estelle. 2001. 'Auxin regulates SCF(TIR1)-dependent degradation of AUX/IAA proteins', *Nature*, 414: 271-6.

Grossniklaus, U., J. P. Vielle-Calzada, M. A. Hoeppner, and W. B. Gagliano. 1998. 'Maternal control of embryogenesis by MEDEA, a polycomb group gene in Arabidopsis', *Science*, 280: 446-50.

Gu, D., C. Y. Chen, M. Zhao, L. Zhao, X. Duan, J. Duan, K. Wu, and X. Liu. 2017. 'Identification of HDA15-PIF1 as a key repression module directing the transcriptional network of seed germination in the dark', *Nucleic Acids Res*, 45: 7137-50.

Hacisuleyman, E., L. A. Goff, C. Trapnell, A. Williams, J. Henao-Mejia, L. Sun, P. McClanahan, D. G. Hendrickson, M. Sauvageau, D. R. Kelley, M. Morse, J. Engreitz, E. S. Lander, M. Guttman, H. F. Lodish, R. Flavell, A. Raj, and J. L. Rinn. 2014. 'Topological organization of multichromosomal regions by the long intergenic noncoding RNA Firre', *Nat Struct Mol Biol*, 21: 198-206.

Hagen, G., and T. Guilfoyle. 2002. 'Auxin-responsive gene expression: genes, promoters and regulatory factors', *Plant Mol Biol*, 49: 373-85.

Han, H. J., J. Russo, Y. Kohwi, and T. Kohwi-Shigematsu. 2008. 'SATB1 reprogrammes gene expression to promote breast tumour growth and metastasis', *Nature*, 452: 187-93.

Hancock, R. 2000. 'A new look at the nuclear matrix', *Chromosoma*, 109: 219-25.

Harris, C. J., and S. E. Jacobsen. 2019. 'ADCP1: a novel plant H3K9me2 reader', *Cell Res*, 29: 6-7.

He, D. C., T. Martin, and S. Penman. 1991. 'Localization of heterogeneous nuclear ribonucleoprotein in the interphase nuclear matrix core filaments and on perichromosomal filaments at mitosis', *Proc Natl Acad Sci U S A*, 88: 7469-73.

He, Y., S. D. Michaels, and R. M. Amasino. 2003. 'Regulation of flowering time by histone acetylation in Arabidopsis', *Science*, 302: 1751-4.

Helbig, R., and F. O. Fackelmayer. 2003. 'Scaffold attachment factor A (SAF-A) is concentrated in inactive X chromosome territories through its RGG domain', *Chromosoma*, 112: 173-82.

Heng, H. H., S. Goetze, C. J. Ye, G. Liu, J. B. Stevens, S. W. Bremer, S. M. Wykes, J. Bode, and S. A. Krawetz. 2004. 'Chromatin loops are selectively anchored using scaffold/matrix-attachment regions', *J Cell Sci*, 117: 999-1008.

Hozak, P., A. B. Hassan, D. A. Jackson, and P. R. Cook. 1993. 'Visualization of replication factories attached to nucleoskeleton', *Cell*, 73: 361-73.

Hozak, P., A. M. Sasseville, Y. Raymond, and P. R. Cook. 1995. 'Lamin proteins form an internal nucleoskeleton as well as a peripheral lamina in human cells', *J Cell Sci*, 108 (Pt 2): 635-44.

Hu, Z., N. Song, M. Zheng, X. Liu, Z. Liu, J. Xing, J. Ma, W. Guo, Y. Yao, H. Peng, M. Xin, D. X. Zhou, Z. Ni, and Q. Sun. 2015. 'Histone acetyltransferase GCN5 is essential for heat stress-responsive gene activation and thermotolerance in Arabidopsis', *Plant J*, 84: 1178-91.

Hung, F. Y., F. F. Chen, C. Li, C. Chen, J. H. Chen, Y. Cui, and K. Wu. 2019. 'The LDL1/2-HDA6 Histone Modification Complex Interacts With TOC1 and Regulates the Core Circadian Clock Components in Arabidopsis', *Front Plant Sci*, 10: 233.

Hung, F. Y., F. F. Chen, C. Li, C. Chen, Y. C. Lai, J. H. Chen, Y. Cui, and K. Wu. 2018. 'The Arabidopsis LDL1/2-HDA6 histone modification complex is functionally associated with CCA1/LHY in regulation of circadian clock genes', *Nucleic Acids Res*, 46: 10669-81.

Hung, F. Y., Y. C. Lai, J. Wang, Y. R. Feng, Y. H. Shih, J. H. Chen, H. C. Sun, S. Yang, C. Li, and K. Wu. 2021. 'The Arabidopsis histone demethylase JMJ28 regulates CONSTANS by interacting with FBH transcription factors', *Plant Cell*, 33: 1196-211.

Huo, X., L. Ji, Y. Zhang, P. Lv, X. Cao, Q. Wang, Z. Yan, S. Dong, D. Du, F. Zhang, G. Wei, Y. Liu, and B. Wen. 2020. 'The Nuclear Matrix Protein SAFB Cooperates with Major Satellite RNAs to Stabilize Heterochromatin Architecture Partially through Phase Separation', *Mol Cell*, 77: 368-83 e7.

Iborra, F. J., A. Pombo, D. A. Jackson, and P. R. Cook. 1996. 'Active RNA polymerases are localized within discrete transcription "factories" in human nuclei', *J Cell Sci*, 109 (Pt 6): 1427-36.

Jackson, J. P., L. Johnson, Z. Jasencakova, X. Zhang, L. PerezBurgos, P. B. Singh, X. Cheng, I. Schubert, T. Jenuwein, and S. E. Jacobsen. 2004. 'Dimethylation of histone H3 lysine 9 is a critical mark for DNA methylation and gene silencing in Arabidopsis thaliana', *Chromosoma*, 112: 308-15.

Jackson, J. P., A. M. Lindroth, X. Cao, and S. E. Jacobsen. 2002. 'Control of CpNpG DNA methylation by the KRYPTONITE histone H3 methyltransferase', *Nature*, 416: 556-60.

Jacob, Y., S. Feng, C. A. LeBlanc, Y. V. Bernatavichute, H. Stroud, S. Cokus, L. M. Johnson, M. Pellegrini, S. E. Jacobsen, and S. D. Michaels. 2009. 'ATXR5 and ATXR6 are H3K27 monomethyltransferases required for chromatin structure and gene silencing', *Nat Struct Mol Biol*, 16: 763-8.

Jacob, Y., H. Stroud, C. Leblanc, S. Feng, L. Zhuo, E. Caro, C. Hassel, C. Gutierrez, S. D. Michaels, and S. E. Jacobsen. 2010. 'Regulation of heterochromatic DNA replication by histone H3 lysine 27 methyltransferases', *Nature*, 466: 987-91.

Jenuwein, T., and C. D. Allis. 2001. 'Translating the histone code', *Science*, 293: 1074-80.

Jia, Q. S., J. Zhu, X. F. Xu, Y. Lou, Z. L. Zhang, Z. P. Zhang, and Z. N. Yang. 2014. 'Arabidopsis AT-hook protein TEK positively regulates the expression of arabinogalactan proteins in controlling nexine layer formation in the pollen wall', *Mol Plant*.

Jiang, D., X. Gu, and Y. He. 2009. 'Establishment of the winter-annual growth habit via FRIGIDA-mediated histone methylation at FLOWERING LOCUS C in Arabidopsis', *Plant Cell*, 21: 1733-46.

Jiang, D., W. Yang, Y. He, and R. M. Amasino. 2007. 'Arabidopsis relatives of the human lysine-specific Demethylase1 repress the expression of FWA and FLOWERING LOCUS C and thus promote the floral transition', *Plant Cell*, 19: 2975-87.

Jiang, H., J. Moreno-Romero, J. Santos-Gonzalez, G. De Jaeger, K. Gevaert, E. Van De Slijke, and C. Kohler. 2017. 'Ectopic application of the repressive histone modification H3K9me2 establishes post-zygotic reproductive isolation in Arabidopsis thaliana', *Genes Dev*, 31: 1272-87.

Jiang, J., A. B. Ding, F. Liu, and X. Zhong. 2020. 'Linking signaling pathways to histone acetylation dynamics in plants', *J Exp Bot*, 71: 5179-90.

Johnson, L., S. Mollah, B. A. Garcia, T. L. Muratore, J. Shabanowitz, D. F. Hunt, and S. E. Jacobsen.

2004. 'Mass spectrometry analysis of Arabidopsis histone H3 reveals distinct combinations of post-translational modifications', *Nucleic Acids Res*, 32: 6511-8.

Jonkers, I., and J. T. Lis. 2015. 'Getting up to speed with transcription elongation by RNA polymerase II', *Nat Rev Mol Cell Biol*, 16: 167-77.

Kagale, S., M. G. Links, and K. Rozwadowski. 2010. 'Genome-wide analysis of ethylene-responsive element binding factor-associated amphiphilic repression motif-containing transcriptional regulators in Arabidopsis', *Plant Physiol*, 152: 1109-34.

Karami, O., A. Rahimi, M. Khan, M. Bemer, R. R. Hazarika, P. Mak, M. Compier, V. van Noort, and R. Offringa. 2020. 'A suppressor of axillary meristem maturation promotes longevity in flowering plants', *Nat Plants*, 6: 368-76.

Karami, O., A. Rahimi, P. Mak, A. Horstman, K. Boutilier, M. Compier, B. van der Zaal, and R. Offringa. 2021. 'An Arabidopsis AT-hook motif nuclear protein mediates somatic embryogenesis and coinciding genome duplication', *Nat Commun*, 12: 2508.

Kaufmann, S. H., and J. H. Shaper. 1984. 'A subset of non-histone nuclear proteins reversibly stabilized by the sulfhydryl cross-linking reagent tetrathionate. Polypeptides of the internal nuclear matrix', *Exp Cell Res*, 155: 477-95.

Keaton, M. A., C. M. Taylor, R. M. Layer, and A. Dutta. 2011. 'Nuclear scaffold attachment sites within ENCODE regions associate with actively transcribed genes', *PLoS One*, 6: e17912.

Kepinski, S., and O. Leyser. 2005. 'The Arabidopsis F-box protein TIR1 is an auxin receptor', *Nature*, 435: 446-51.

Kerppola, T. K. 2006. 'Design and implementation of bimolecular fluorescence complementation (BiFC) assays for the visualization of protein interactions in living cells', *Nat Protoc*, 1: 1278-86.

Kim, D., J. M. Paggi, C. Park, C. Bennett, and S. L. Salzberg. 2019. 'Graph-based genome alignment and genotyping with HISAT2 and HISAT-genotype', *Nat Biotechnol*, 37: 907-15.

Kim, J. Y., W. Yang, J. Forner, J. U. Lohmann, B. Noh, and Y. S. Noh. 2018. 'Epigenetic reprogramming by histone acetyltransferase HAG1/AtGCN5 is required for pluripotency acquisition in Arabidopsis', *EMBO J*, 37.

Kim, K. C., Z. Lai, B. Fan, and Z. Chen. 2008. 'Arabidopsis WRKY38 and WRKY62 transcription factors interact with histone deacetylase 19 in basal defense', *Plant Cell*, 20: 2357-71.

Kim, Y. J., R. Wang, L. Gao, D. Li, C. Xu, H. Mang, J. Jeon, X. Chen, X. Zhong, J. M. Kwak, B. Mo, L. Xiao, and X. Chen. 2016. 'POWERDRESS and HDA9 interact and promote histone H3 deacetylation at specific genomic sites in Arabidopsis', *Proc Natl Acad Sci U S A*, 113: 14858-63.

Kohwi-Shigematsu, T., Y. Kohwi, K. Takahashi, H. W. Richards, S. D. Ayers, H. J. Han, and S. Cai. 2012. 'SATB1-mediated functional packaging of chromatin into loops', *Methods*, 58: 243-54.

Kouzarides, T. 2007. 'Chromatin modifications and their function', *Cell*, 128: 693-705.

Kumar, P. P., O. Bischof, P. K. Purbey, D. Notani, H. Urlaub, A. Dejean, and S. Galande. 2007. 'Functional interaction between PML and SATB1 regulates chromatin-loop architecture and transcription of the MHC class I locus', *Nat Cell Biol*, 9: 45-56.

Kumar, V., J. K. Thakur, and M. Prasad. 2021. 'Histone acetylation dynamics regulating plant development and stress responses', *Cell Mol Life Sci*, 78: 4467-86.

Kumpf, R., T. Thorstensen, M. A. Rahman, J. Heyman, H. Z. Nenseth, T. Lammens, U. Herrmann, R. Swarup, S. V. Veiseth, G. Emberland, M. J. Bennett, L. De Veylder, and R. B. Aalen. 2014. 'The ASH1-RELATED3 SET-domain protein controls cell division competence of the meristem and

the quiescent center of the Arabidopsis primary root', *Plant Physiol*, 166: 632-43.

Lavy, M., and M. Estelle. 2016. 'Mechanisms of auxin signaling', *Development*, 143: 3226-9.

Lee, H. G., and P. J. Seo. 2019. 'MYB96 recruits the HDA15 protein to suppress negative regulators of ABA signaling in Arabidopsis', *Nat Commun*, 10: 1713.

Lee, K., P. Mas, and P. J. Seo. 2019. 'The EC-HDA9 complex rhythmically regulates histone acetylation at the TOC1 promoter in Arabidopsis', *Commun Biol*, 2: 143.

Lee, K., and P. J. Seo. 2017. 'Coordination of matrix attachment and ATP-dependent chromatin remodeling regulate auxin biosynthesis and Arabidopsis hypocotyl elongation', *PLoS One*, 12: e0181804.

Lee, W. Y., D. Lee, W. I. Chung, and C. S. Kwon. 2009. 'Arabidopsis ING and Alfin1-like protein families localize to the nucleus and bind to H3K4me3/2 via plant homeodomain fingers', *Plant J*, 58: 511-24.

Li, M., C. Liu, S. R. Hepworth, C. Ma, H. Li, J. Li, S. M. Wang, and H. Yin. 2022. 'SAUR15 interaction with BRI1 activates plasma membrane H+-ATPase to promote organ development of Arabidopsis', *Plant Physiol*.

Li, X., C. J. Harris, Z. Zhong, W. Chen, R. Liu, B. Jia, Z. Wang, S. Li, S. E. Jacobsen, and J. Du. 2018. 'Mechanistic insights into plant SUVH family H3K9 methyltransferases and their binding to context-biased non-CG DNA methylation', *Proc Natl Acad Sci U S A*, 115: E8793-E802.

Li, X., X. Wang, K. He, Y. Ma, N. Su, H. He, V. Stolc, W. Tongprasit, W. Jin, J. Jiang, W. Terzaghi, S. Li, and X. W. Deng. 2008. 'High-resolution mapping of epigenetic modifications of the rice genome uncovers interplay between DNA methylation, histone methylation, and gene expression', *Plant Cell*, 20: 259-76.

Li, Z., X. Fu, Y. Wang, R. Liu, and Y. He. 2018. 'Polycomb-mediated gene silencing by the BAH-EMF1 complex in plants', *Nat Genet*, 50: 1254-61.

Liao, Y., G. K. Smyth, and W. Shi. 2019. 'The R package Rsubread is easier, faster, cheaper and better for alignment and quantification of RNA sequencing reads', *Nucleic Acids Res*, 47: e47.

Lim, P. O., Y. Kim, E. Breeze, J. C. Koo, H. R. Woo, J. S. Ryu, D. H. Park, J. Beynon, A. Tabrett, V. Buchanan-Wollaston, and H. G. Nam. 2007. 'Overexpression of a chromatin architecture-controlling AT-hook protein extends leaf longevity and increases the post-harvest storage life of plants', *Plant J*, 52: 1140-53.

Lincoln, C., J. H. Britton, and M. Estelle. 1990. 'Growth and development of the axr1 mutants of Arabidopsis', *Plant Cell*, 2: 1071-80.

Lindroth, A. M., D. Shultis, Z. Jasencakova, J. Fuchs, L. Johnson, D. Schubert, D. Patnaik, S. Pradhan, J. Goodrich, I. Schubert, T. Jenuwein, S. Khorasanizadeh, and S. E. Jacobsen. 2004. 'Dual histone H3 methylation marks at lysines 9 and 27 required for interaction with CHROMOMETHYLASE3', *EMBO J*, 23: 4286-96.

Linnemann, A. K., A. E. Platts, and S. A. Krawetz. 2009. 'Differential nuclear scaffold/matrix attachment marks expressed genes', *Hum Mol Genet*, 18: 645-54.

Lippman, Z., A. V. Gendrel, M. Black, M. W. Vaughn, N. Dedhia, W. R. McCombie, K. Lavine, V. Mittal, B. May, K. D. Kasschau, J. C. Carrington, R. W. Doerge, V. Colot, and R. Martienssen. 2004. 'Role of transposable elements in heterochromatin and epigenetic control', *Nature*, 430: 471-6.

Liu, C., F. Lu, X. Cui, and X. Cao. 2010. 'Histone methylation in higher plants', *Annu Rev Plant Biol*, 61: 395-420.

Liu, C., C. Wang, G. Wang, C. Becker, M. Zaidem, and D. Weigel. 2016. 'Genome-wide analysis of chromatin packing in Arabidopsis thaliana at single-gene resolution', *Genome Res*, 26: 1057-68.

Liu, F., V. Quesada, P. Crevillen, I. Baurle, S. Swiezewski, and C. Dean. 2007. 'The Arabidopsis RNA-binding protein FCA requires a lysine-specific demethylase 1 homolog to downregulate FLC', *Mol Cell*, 28: 398-407.

Liu, X., C. Y. Chen, K. C. Wang, M. Luo, R. Tai, L. Yuan, M. Zhao, S. Yang, G. Tian, Y. Cui, H. L. Hsieh, and K. Wu. 2013. 'PHYTOCHROME INTERACTING FACTOR3 associates with the histone deacetylase HDA15 in repression of chlorophyll biosynthesis and photosynthesis in etiolated Arabidopsis seedlings', *Plant Cell*, 25: 1258-73.

Liu, X., S. Yang, M. Zhao, M. Luo, C. W. Yu, C. Y. Chen, R. Tai, and K. Wu. 2014. 'Transcriptional repression by histone deacetylases in plants', *Mol Plant*, 7: 764-72.

Liu, X., C. W. Yu, J. Duan, M. Luo, K. Wang, G. Tian, Y. Cui, and K. Wu. 2012. 'HDA6 directly interacts with DNA methyltransferase MET1 and maintains transposable element silencing in Arabidopsis', *Plant Physiol*, 158: 119-29.

Long, J. A., C. Ohno, Z. R. Smith, and E. M. Meyerowitz. 2006. 'TOPLESS regulates apical embryonic fate in Arabidopsis', *Science*, 312: 1520-3.

Lopez-Gonzalez, L., A. Mouriz, L. Narro-Diego, R. Bustos, J. M. Martinez-Zapater, J. A. Jarillo, and M. Pineiro. 2014. 'Chromatin-dependent repression of the Arabidopsis floral integrator genes involves plant specific PHD-containing proteins', *Plant Cell*, 26: 3922-38.

Lou, Y., X. F. Xu, J. Zhu, J. N. Gu, S. Blackmore, and Z. N. Yang. 2014. 'The tapetal AHL family protein TEK determines nexine formation in the pollen wall', *Nat Commun*, 5: 3855.

Love, M. I., W. Huber, and S. Anders. 2014. 'Moderated estimation of fold change and dispersion for RNA-seq data with DESeq2', *Genome Biol*, 15: 550.

Lu, F., X. Cui, S. Zhang, T. Jenuwein, and X. Cao. 2011. 'Arabidopsis REF6 is a histone H3 lysine 27 demethylase', *Nat Genet*, 43: 715-9.

Lu, F., X. Cui, S. Zhang, C. Liu, and X. Cao. 2010. 'JMJ14 is an H3K4 demethylase regulating flowering time in Arabidopsis', *Cell Res*, 20: 387-90.

Lu, F., G. Li, X. Cui, C. Liu, X. J. Wang, and X. Cao. 2008. 'Comparative analysis of JmjC domain-containing proteins reveals the potential histone demethylases in Arabidopsis and rice', *J Integr Plant Biol*, 50: 886-96.

Lu, H., Y. Zou, and N. Feng. 2010. 'Overexpression of AHL20 negatively regulates defenses in Arabidopsis', *J Integr Plant Biol*, 52: 801-8.

Lu, S. X., S. M. Knowles, C. J. Webb, R. B. Celaya, C. Cha, J. P. Siu, and E. M. Tobin. 2011. 'The Jumonji C domain-containing protein JMJ30 regulates period length in the Arabidopsis circadian clock', *Plant Physiol*, 155: 906-15.

Luger, K., and J. C. Hansen. 2005. 'Nucleosome and chromatin fiber dynamics', *Curr Opin Struct Biol*, 15: 188-96.

Luger, K., A. W. Mader, R. K. Richmond, D. F. Sargent, and T. J. Richmond. 1997. 'Crystal structure of the nucleosome core particle at 2.8 A resolution', *Nature*, 389: 251-60.

Luger, K., T. J. Rechsteiner, A. J. Flaus, M. M. Waye, and T. J. Richmond. 1997. 'Characterization of nucleosome core particles containing histone proteins made in bacteria', *J Mol Biol*, 272: 301-11.

Mao, Y., K. A. Pavangadkar, M. F. Thomashow, and S. J. Triezenberg. 2006. 'Physical and functional

interactions of Arabidopsis ADA2 transcriptional coactivator proteins with the acetyltransferase GCN5 and with the cold-induced transcription factor CBF1', *Biochim Biophys Acta*, 1759: 69-79.

Maraschin Fdos, S., J. Memelink, and R. Offringa. 2009. 'Auxin-induced, SCF(TIR1)-mediated poly-ubiquitination marks AUX/IAA proteins for degradation', *Plant J*, 59: 100-9.

Margueron, R., and D. Reinberg. 2011. 'The Polycomb complex PRC2 and its mark in life', *Nature*, 469: 343-9.

Marmorstein, R. 2001. 'Protein modules that manipulate histone tails for chromatin regulation', *Nat Rev Mol Cell Biol*, 2: 422-32.

Martelli, A. M., E. Falcieri, P. Gobbi, L. Manzoli, R. S. Gilmour, and L. Cocco. 1991. 'Heat-induced stabilization of the nuclear matrix: a morphological and biochemical analysis in murine erythroleukemia cells', *Exp Cell Res*, 196: 216-25.

Martens, J. H., M. Verlaan, E. Kalkhoven, J. C. Dorsman, and A. Zantema. 2002. 'Scaffold/matrix attachment region elements interact with a p300-scaffold attachment factor A complex and are bound by acetylated nucleosomes', *Mol Cell Biol*, 22: 2598-606.

Matsushita, A., T. Furumoto, S. Ishida, and Y. Takahashi. 2007. 'AGF1, an AT-hook protein, is necessary for the negative feedback of AtGA3ox1 encoding GA 3-oxidase', *Plant Physiol*, 143: 1152-62.

Mattern, K. A., B. M. Humbel, A. O. Muijsers, L. de Jong, and R. van Driel. 1996. 'hnRNP proteins and B23 are the major proteins of the internal nuclear matrix of HeLa S3 cells', *J Cell Biochem*, 62: 275-89.

Mattern, K. A., R. E. van Goethem, L. de Jong, and R. van Driel. 1997. 'Major internal nuclear matrix proteins are common to different human cell types', *J Cell Biochem*, 65: 42-52.

Mayer, K. S., X. Chen, D. Sanders, J. Chen, J. Jiang, P. Nguyen, M. Scalf, L. M. Smith, and X. Zhong. 2019. 'HDA9-PWR-HOS15 Is a Core Histone Deacetylase Complex Regulating Transcription and Development', *Plant Physiol*, 180: 342-55.

Meier, I., T. Phelan, W. Gruissem, S. Spiker, and D. Schneider. 1996. 'MFP1, a novel plant filament-like protein with affinity for matrix attachment region DNA', *Plant Cell*, 8: 2105-15.

Michalowski, S. M., G. C. Allen, G. E. Hall, Jr., W. F. Thompson, and S. Spiker. 1999. 'Characterization of randomly-obtained matrix attachment regions (MARs) from higher plants', *Biochemistry*, 38: 12795-804.

Mika, S., and B. Rost. 2005. 'NMPdb: Database of Nuclear Matrix Proteins', *Nucleic Acids Res*, 33: D160-3.

Miura, A., M. Nakamura, S. Inagaki, A. Kobayashi, H. Saze, and T. Kakutani. 2009. 'An Arabidopsis jmjC domain protein protects transcribed genes from DNA methylation at CHG sites', *EMBO J*, 28: 1078-86.

Molitor, A. M., Z. Bu, Y. Yu, and W. H. Shen. 2014. 'Arabidopsis AL PHD-PRC1 complexes promote seed germination through H3K4me3-to-H3K27me3 chromatin state switch in repression of seed developmental genes', *PLoS Genet*, 10: e1004091.

Moreno-Romero, J., H. Jiang, J. Santos-Gonzalez, and C. Kohler. 2016. 'Parental epigenetic asymmetry of PRC2-mediated histone modifications in the Arabidopsis endosperm', *EMBO J*, 35: 1298-311.

Morisawa, G., A. Han-Yama, I. Moda, A. Tamai, M. Iwabuchi, and T. Meshi. 2000. 'AHM1, a novel type of nuclear matrix-localized, MAR binding protein with a single AT hook and a J domain-homologous region', *Plant Cell*, 12: 1903-16.

Mozgova, I., C. Kohler, and L. Hennig. 2015. 'Keeping the gate closed: functions of the polycomb repressive complex PRC2 in development', *Plant J*, 83: 121-32.

Murfett, J., X. J. Wang, G. Hagen, and T. J. Guilfoyle. 2001. 'Identification of Arabidopsis histone deacetylase HDA6 mutants that affect transgene expression', *Plant Cell*, 13: 1047-61.

Musselman, C. A., M. E. Lalonde, J. Cote, and T. G. Kutateladze. 2012. 'Perceiving the epigenetic landscape through histone readers', *Nat Struct Mol Biol*, 19: 1218-27.

Mylne, J. S., L. Barrett, F. Tessadori, S. Mesnage, L. Johnson, Y. V. Bernatavichute, S. E. Jacobsen, P. Fransz, and C. Dean. 2006. 'LHP1, the Arabidopsis homologue of HETEROCHROMATIN PROTEIN1, is required for epigenetic silencing of FLC', *Proc Natl Acad Sci U S A*, 103: 5012-7.

Nakayasu, H., and R. Berezney. 1991. 'Nuclear matrins: identification of the major nuclear matrix proteins', *Proc Natl Acad Sci U S A*, 88: 10312-6.

Narwade, N., S. Patel, A. Alam, S. Chattopadhyay, S. Mittal, and A. Kulkarni. 2019. 'Mapping of scaffold/matrix attachment regions in human genome: a data mining exercise', *Nucleic Acids Res*, 47: 7247-61.

Nelson, W. G., K. J. Pienta, E. R. Barrack, and D. S. Coffey. 1986. 'The role of the nuclear matrix in the organization and function of DNA', *Annu Rev Biophys Biophys Chem*, 15: 457-75.

Ng, D. W., T. Wang, M. B. Chandrasekharan, R. Aramayo, S. Kertbundit, and T. C. Hall. 2007. 'Plant SET domain-containing proteins: structure, function and regulation', *Biochim Biophys Acta*, 1769: 316-29.

Nickerson, J. 2001. 'Experimental observations of a nuclear matrix', *J Cell Sci*, 114: 463-74.

Nickerson, J. A. 1998. 'Nuclear dreams: the malignant alteration of nuclear architecture', *J Cell Biochem*, 70: 172-80.

Noh, B., S. H. Lee, H. J. Kim, G. Yi, E. A. Shin, M. Lee, K. J. Jung, M. R. Doyle, R. M. Amasino, and Y. S. Noh. 2004. 'Divergent roles of a pair of homologous jumonji/zinc-finger-class transcription factor proteins in the regulation of Arabidopsis flowering time', *Plant Cell*, 16: 2601-13.

Oh, E., J. Y. Zhu, H. Ryu, I. Hwang, and Z. Y. Wang. 2014. 'TOPLESS mediates brassinosteroid-induced transcriptional repression through interaction with BZR1', *Nat Commun*, 5: 4140.

Oudet, P., M. Gross-Bellard, and P. Chambon. 1975. 'Electron microscopic and biochemical evidence that chromatin structure is a repeating unit', *Cell*, 4: 281-300.

Pandey, R., A. Muller, C. A. Napoli, D. A. Selinger, C. S. Pikaard, E. J. Richards, J. Bender, D. W. Mount, and R. A. Jorgensen. 2002. 'Analysis of histone acetyltransferase and histone deacetylase families of Arabidopsis thaliana suggests functional diversification of chromatin modification among multicellular eukaryotes', *Nucleic Acids Res*, 30: 5036-55.

Paponov, I. A., M. Paponov, W. Teale, M. Menges, S. Chakrabortee, J. A. Murray, and K. Palme. 2008. 'Comprehensive transcriptome analysis of auxin responses in Arabidopsis', *Mol Plant*, 1: 321-37.

Park, H. J., D. Baek, J. Y. Cha, X. Liao, S. H. Kang, C. R. McClung, S. Y. Lee, D. J. Yun, and W. Y. Kim. 2019. 'HOS15 Interacts with the Histone Deacetylase HDA9 and the Evening Complex to Epigenetically Regulate the Floral Activator GIGANTEA', *Plant Cell*, 31: 37-51.

Pascuzzi, P. E., M. A. Flores-Vergara, T. J. Lee, B. Sosinski, M. W. Vaughn, L. Hanley-Bowdoin, W. F. Thompson, and G. C. Allen. 2014. 'In vivo mapping of arabidopsis scaffold/matrix attachment regions reveals link to nucleosome-disfavoring poly(dA:dT) tracts', *Plant Cell*, 26: 102-20.

Pathak, R. U., A. Srinivasan, and R. K. Mishra. 2014. 'Genome-wide mapping of matrix attachment regions in Drosophila melanogaster', *BMC Genomics*, 15: 1022.

Peters, A. H., S. Kubicek, K. Mechtler, R. J. O'Sullivan, A. A. Derijck, L. Perez-Burgos, A. Kohlmaier, S. Opravil, M. Tachibana, Y. Shinkai, J. H. Martens, and T. Jenuwein. 2003. 'Partitioning and plasticity of repressive histone methylation states in mammalian chromatin', *Mol Cell*, 12: 1577-89.

Pien, S., and U. Grossniklaus. 2007. 'Polycomb group and trithorax group proteins in Arabidopsis', *Biochim Biophys Acta*, 1769: 375-82.

Potok, M. E., Y. Wang, L. Xu, Z. Zhong, W. Liu, S. Feng, B. Naranbaatar, S. Rayatpisheh, Z. Wang, J. A. Wohlschlegel, I. Ausin, and S. E. Jacobsen. 2019. 'Arabidopsis SWR1-associated protein methyl-CpG-binding domain 9 is required for histone H2A.Z deposition', *Nat Commun*, 10: 3352.

Probst, A. V., M. Fagard, F. Proux, P. Mourrain, S. Boutet, K. Earley, R. J. Lawrence, C. S. Pikaard, J. Murfett, I. Furner, H. Vaucheret, and O. Mittelsten Scheid. 2004. 'Arabidopsis histone deacetylase HDA6 is required for maintenance of transcriptional gene silencing and determines nuclear organization of rDNA repeats', *Plant Cell*, 16: 1021-34.

Qian, S., X. Lv, R. N. Scheid, L. Lu, Z. Yang, W. Chen, R. Liu, M. D. Boersma, J. M. Denu, X. Zhong, and J. Du. 2018. 'Dual recognition of H3K4me3 and H3K27me3 by a plant histone reader SHL', *Nat Commun*, 9: 2425.

Rahimi, A., O. Karami, A. D. Lestari, T. de Werk, P. Amakorova, D. Shi, O. Novak, T. Greb, and R. Offringa. 2022. 'Control of cambium initiation and activity in Arabidopsis by the transcriptional regulator AHL15', *Curr Biol*.

Rayle, D. L., and R. Cleland. 1970. 'Enhancement of wall loosening and elongation by Acid solutions', *Plant Physiol*, 46: 250-3.

Rayle, D. L., and R. E. Cleland. 1980. 'Evidence that Auxin-induced Growth of Soybean Hypocotyls Involves Proton Excretion', *Plant Physiol*, 66: 433-7.

———. 1992. 'The Acid Growth Theory of auxin-induced cell elongation is alive and well', *Plant Physiol*, 99: 1271-4.

Razin, S. V., V. V. Borunova, O. V. Iarovaia, and Y. S. Vassetzky. 2014. 'Nuclear matrix and structural and functional compartmentalization of the eucaryotic cell nucleus', *Biochemistry (Mosc)*, 79: 608-18.

Rice, J. C., S. D. Briggs, B. Ueberheide, C. M. Barber, J. Shabanowitz, D. F. Hunt, Y. Shinkai, and C. D. Allis. 2003. 'Histone methyltransferases direct different degrees of methylation to define distinct chromatin domains', *Mol Cell*, 12: 1591-8.

Ritter, A., S. Inigo, P. Fernandez-Calvo, K. S. Heyndrickx, S. Dhondt, H. Shi, L. De Milde, R. Vanden Bossche, R. De Clercq, D. Eeckhout, M. Ron, D. E. Somers, D. Inze, K. Gevaert, G. De Jaeger, K. Vandepoele, L. Pauwels, and A. Goossens. 2017. 'The transcriptional repressor complex FRS7-FRS12 regulates flowering time and growth in Arabidopsis', *Nat Commun*, 8: 15235.

Rosa, S., and P. Shaw. 2013. 'Insights into chromatin structure and dynamics in plants', *Biology (Basel)*, 2: 1378-410.

Rudd, S., M. Frisch, K. Grote, B. C. Meyers, K. Mayer, and T. Werner. 2004. 'Genome-wide in silico mapping of scaffold/matrix attachment regions in Arabidopsis suggests correlation of intragenic scaffold/matrix attachment regions with gene expression', *Plant Physiol*, 135: 715-22.

Ryu, H., H. Cho, W. Bae, and I. Hwang. 2014. 'Control of early seedling development by BES1/TPL/HDA19-mediated epigenetic regulation of ABI3', *Nat Commun*, 5: 4138.

Saleh, A., R. Alvarez-Venegas, M. Yilmaz, O. Le, G. Hou, M. Sadder, A. Al-Abdallat, Y. Xia, G. Lu, I. Ladunga, and Z. Avramova. 2008. 'The highly similar Arabidopsis homologs of trithorax ATX1 and ATX2 encode proteins with divergent biochemical functions', *Plant Cell*, 20: 568-79.

Saze, H., A. Shiraishi, A. Miura, and T. Kakutani. 2008. 'Control of genic DNA methylation by a jmjC domain-containing protein in Arabidopsis thaliana', *Science*, 319: 462-5.

Schagger, H. 2006. 'Tricine-SDS-PAGE', *Nat Protoc*, 1: 16-22.

Sequeira-Mendes, J., I. Araguez, R. Peiro, R. Mendez-Giraldez, X. Zhang, S. E. Jacobsen, U. Bastolla, and C. Gutierrez. 2014. 'The Functional Topography of the Arabidopsis Genome Is Organized in a Reduced Number of Linear Motifs of Chromatin States', *Plant Cell*, 26: 2351-66.

Servet, C., N. Conde e Silva, and D. X. Zhou. 2010. 'Histone acetyltransferase AtGCN5/HAG1 is a versatile regulator of developmental and inducible gene expression in Arabidopsis', *Mol Plant*, 3: 670-7.

Shao, W., and J. Zeitlinger. 2017. 'Paused RNA polymerase II inhibits new transcriptional initiation', *Nat Genet*, 49: 1045-51.

Shi, Y., F. Lan, C. Matson, P. Mulligan, J. R. Whetstine, P. A. Cole, R. A. Casero, and Y. Shi. 2004. 'Histone demethylation mediated by the nuclear amine oxidase homolog LSD1', *Cell*, 119: 941-53.

Singh, M., L. D'Silva, and T. A. Holak. 2006. 'DNA-binding properties of the recombinant high-mobility-group-like AT-hook-containing region from human BRG1 protein', *Biol Chem*, 387: 1469-78.

Sirl, M., T. Snajdrova, D. Gutierrez-Alanis, J. G. Dubrovsky, J. P. Vielle-Calzada, I. Kulich, and A. Soukup. 2020. 'At-Hook Motif Nuclear Localised Protein 18 as a Novel Modulator of Root System Architecture', *Int J Mol Sci*, 21.

Spartz, A. K., S. H. Lee, J. P. Wenger, N. Gonzalez, H. Itoh, D. Inze, W. A. Peer, A. S. Murphy, P. J. Overvoorde, and W. M. Gray. 2012. 'The SAUR19 subfamily of SMALL AUXIN UP RNA genes promote cell expansion', *Plant J*, 70: 978-90.

Spartz, A. K., H. Ren, M. Y. Park, K. N. Grandt, S. H. Lee, A. S. Murphy, M. R. Sussman, P. J. Overvoorde, and W. M. Gray. 2014. 'SAUR Inhibition of PP2C-D Phosphatases Activates Plasma Membrane H+-ATPases to Promote Cell Expansion in Arabidopsis', *Plant Cell*, 26: 2129-42.

Street, I. H., P. K. Shah, A. M. Smith, N. Avery, and M. M. Neff. 2008. 'The AT-hook-containing proteins SOB3/AHL29 and ESC/AHL27 are negative modulators of hypocotyl growth in Arabidopsis', *Plant J*, 54: 1-14.

Stroud, H., T. Do, J. Du, X. Zhong, S. Feng, L. Johnson, D. J. Patel, and S. E. Jacobsen. 2014. 'Non-CG methylation patterns shape the epigenetic landscape in Arabidopsis', *Nat Struct Mol Biol*, 21: 64-72.

Stroud, H., S. Otero, B. Desvoyes, E. Ramirez-Parra, S. E. Jacobsen, and C. Gutierrez. 2012. 'Genome-wide analysis of histone H3.1 and H3.3 variants in Arabidopsis thaliana', *Proc Natl Acad Sci U S A*, 109: 5370-5.

Su, Y., C. S. Kwon, S. Bezhani, B. Huvermann, C. Chen, A. Peragine, J. F. Kennedy, and D. Wagner. 2006. 'The N-terminal ATPase AT-hook-containing region of the Arabidopsis chromatin-remodeling protein SPLAYED is sufficient for biological activity', *Plant J*, 46: 685-99.

Sura, W., M. Kabza, W. M. Karlowski, T. Bieluszewski, M. Kus-Slowinska, L. Paweloszek, J. Sadowski, and P. A. Ziolkowski. 2017. 'Dual Role of the Histone Variant H2A.Z in Transcriptional Regulation of Stress-Response Genes', *Plant Cell*, 29: 791-807.

Suzuki, M., N. Shinozuka, T. Hirakata, M. T. Nakata, T. Demura, H. Tsukaya, and G. Horiguchi. 2018. 'OLIGOCELLULA1/HIGH EXPRESSION OF OSMOTICALLY RESPONSIVE GENES15 Promotes Cell Proliferation With HISTONE DEACETYLASE9 and POWERDRESS During Leaf Development in Arabidopsis thaliana', *Front Plant Sci*, 9: 580.

Szemenyei, H., M. Hannon, and J. A. Long. 2008. 'TOPLESS mediates auxin-dependent transcriptional repression during Arabidopsis embryogenesis', *Science*, 319: 1384-6.

Tamada, Y., J. Y. Yun, S. C. Woo, and R. M. Amasino. 2009. 'ARABIDOPSIS TRITHORAX-RELATED7 is required for methylation of lysine 4 of histone H3 and for transcriptional activation of FLOWERING LOCUS C', *Plant Cell*, 21: 3257-69.

Tang, Y., X. Liu, X. Liu, Y. Li, K. Wu, and X. Hou. 2017. 'Arabidopsis NF-YCs Mediate the Light-Controlled Hypocotyl Elongation via Modulating Histone Acetylation', *Mol Plant*, 10: 260-73.

Tasset, C., A. Singh Yadav, S. Sureshkumar, R. Singh, L. van der Woude, M. Nekrasov, D. Tremethick, M. van Zanten, and S. Balasubramanian. 2018. 'POWERDRESS-mediated histone deacetylation is essential for thermomorphogenesis in Arabidopsis thaliana', *PLoS Genet*, 14: e1007280.

Taverna, S. D., H. Li, A. J. Ruthenburg, C. D. Allis, and D. J. Patel. 2007. 'How chromatin-binding modules interpret histone modifications: lessons from professional pocket pickers', *Nat Struct Mol Biol*, 14: 1025-40.

Tayengwa, R., P. Sharma Koirala, C. F. Pierce, B. E. Werner, and M. M. Neff. 2020. 'Overexpression of AtAHL20 causes delayed flowering in Arabidopsis via repression of FT expression', *BMC Plant Biol*, 20: 559.

Tetko, I. V., G. Haberer, S. Rudd, B. Meyers, H. W. Mewes, and K. F. Mayer. 2006. 'Spatiotemporal expression control correlates with intragenic scaffold matrix attachment regions (S/MARs) in Arabidopsis thaliana', *PLoS Comput Biol*, 2: e21.

Thorstensen, T., A. Fischer, S. V. Sandvik, S. S. Johnsen, P. E. Grini, G. Reuter, and R. B. Aalen. 2006. 'The Arabidopsis SUVR4 protein is a nucleolar histone methyltransferase with preference for monomethylated H3K9', *Nucleic Acids Res*, 34: 5461-70.

Tsukada, Y., J. Fang, H. Erdjument-Bromage, M. E. Warren, C. H. Borchers, P. Tempst, and Y. Zhang. 2006. 'Histone demethylation by a family of JmjC domain-containing proteins', *Nature*, 439: 811-6.

Tsutsui, K. M., K. Sano, and K. Tsutsui. 2005. 'Dynamic view of the nuclear matrix', *Acta Med Okayama*, 59: 113-20.

Turck, F., F. Roudier, S. Farrona, M. L. Martin-Magniette, E. Guillaume, N. Buisine, S. Gagnot, R. A. Martienssen, G. Coupland, and V. Colot. 2007. 'Arabidopsis TFL2/LHP1 specifically associates with genes marked by trimethylation of histone H3 lysine 27', *PLoS Genet*, 3: e86.

Ueda, M., and M. Seki. 2020. 'Histone Modifications Form Epigenetic Regulatory Networks to Regulate Abiotic Stress Response', *Plant Physiol*, 182: 15-26.

Van Bortle, K., and V. G. Corces. 2012. 'Nuclear organization and genome function', *Annu Rev Cell Dev Biol*, 28: 163-87.

Van Leene, J., D. Eeckhout, B. Cannoot, N. De Winne, G. Persiau, E. Van De Slijke, L. Vercruysse, M. Dedecker, A. Verkest, K. Vandepoele, L. Martens, E. Witters, K. Gevaert, and G. De Jaeger. 2015. 'An improved toolbox to unravel the plant cellular machinery by tandem affinity purification of Arabidopsis protein complexes', *Nat Protoc*, 10: 169-87.

Vandenbussche, F., J. P. Verbelen, and D. Van Der Straeten. 2005. 'Of light and length: regulation of

hypocotyl growth in Arabidopsis', *Bioessays*, 27: 275-84.

Wang, T. Y., Z. M. Han, Y. R. Chai, and J. H. Zhang. 2010. 'A mini review of MAR-binding proteins', *Mol Biol Rep*, 37: 3553-60.

Wasag, P., and R. Lenartowski. 2016. 'Nuclear matrix - structure, function and pathogenesis', *Postepy Hig Med Dosw (Online)*, 70: 1206-19.

Weiste, C., and W. Droge-Laser. 2014. 'The Arabidopsis transcription factor bZIP11 activates auxin-mediated transcription by recruiting the histone acetylation machinery', *Nat Commun*, 5: 3883.

Wong, M. M., G. B. Bhaskara, T. N. Wen, W. D. Lin, T. T. Nguyen, G. L. Chong, and P. E. Verslues. 2019. 'Phosphoproteomics of Arabidopsis Highly ABA-Induced1 identifies AT-Hook-Like10 phosphorylation required for stress growth regulation', *Proc Natl Acad Sci U S A*, 116: 2354-63.

Xi, Y., S. R. Park, D. H. Kim, E. D. Kim, and S. Sung. 2020. 'Transcriptome and epigenome analyses of vernalization in Arabidopsis thaliana', *Plant J*, 103: 1490-502.

Xiao, C., F. Chen, X. Yu, C. Lin, and Y. F. Fu. 2009. 'Over-expression of an AT-hook gene, AHL22, delays flowering and inhibits the elongation of the hypocotyl in Arabidopsis thaliana', *Plant Mol Biol*, 71: 39-50.

Xiao, J., U. S. Lee, and D. Wagner. 2016. 'Tug of war: adding and removing histone lysine methylation in Arabidopsis', *Curr Opin Plant Biol*, 34: 41-53.

Xiao, J., and D. Wagner. 2015. 'Polycomb repression in the regulation of growth and development in Arabidopsis', *Curr Opin Plant Biol*, 23: 15-24.

Xiong, S. X., Q. Y. Zeng, J. Q. Hou, L. L. Hou, J. Zhu, M. Yang, Z. N. Yang, and Y. Lou. 2020. 'The temporal regulation of TEK contributes to pollen wall exine patterning', *PLoS Genet*, 16: e1008807.

Xu, L., Z. Zhao, A. Dong, L. Soubigou-Taconnat, J. P. Renou, A. Steinmetz, and W. H. Shen. 2008. 'Di- and tri- but not monomethylation on histone H3 lysine 36 marks active transcription of genes involved in flowering time regulation and other processes in Arabidopsis thaliana', *Mol Cell Biol*, 28: 1348-60.

Xu, Y., E. S. Gan, and T. Ito. 2013. 'The AT-hook/PPC domain protein TEK negatively regulates floral repressors including MAF4 and MAF5', *Plant Signal Behav*, 8.

Xu, Y., E. S. Gan, J. Zhou, W. Y. Wee, X. Zhang, and T. Ito. 2014. 'Arabidopsis MRG domain proteins bridge two histone modifications to elevate expression of flowering genes', *Nucleic Acids Res*, 42: 10960-74.

Xu, Y., Y. Wang, H. Stroud, X. Gu, B. Sun, E. S. Gan, K. H. Ng, S. E. Jacobsen, Y. He, and T. Ito. 2013. 'A matrix protein silences transposons and repeats through interaction with retinoblastoma-associated proteins', *Curr Biol*, 23: 345-50.

Yadeta, K. A., M. Hanemian, P. Smit, J. A. Hiemstra, A. Pereira, Y. Marco, and B. P. Thomma. 2011. 'The Arabidopsis thaliana DNA-binding protein AHL19 mediates verticillium wilt resistance', *Mol Plant Microbe Interact*, 24: 1582-91.

Yan, W., D. Chen, C. Smaczniak, J. Engelhorn, H. Liu, W. Yang, A. Graf, C. C. Carles, D. X. Zhou, and K. Kaufmann. 2018. 'Dynamic and spatial restriction of Polycomb activity by plant histone demethylases', *Nat Plants*, 4: 681-89.

Yan, Y., L. Shen, Y. Chen, S. Bao, Z. Thong, and H. Yu. 2014. 'A MYB-domain protein EFM mediates flowering responses to environmental cues in Arabidopsis', *Dev Cell*, 30: 437-48.

Yang, C., W. Shen, L. Yang, Y. Sun, X. Li, M. Lai, J. Wei, C. Wang, Y. Xu, F. Li, S. Liang, C. Yang, S. Zhong,

M. Luo, and C. Gao. 2020. 'HY5-HDA9 Module Transcriptionally Regulates Plant Autophagy in Response to Light-to-Dark Conversion and Nitrogen Starvation', *Mol Plant*, 13: 515-31.

Yang, H., Z. Han, Y. Cao, D. Fan, H. Li, H. Mo, Y. Feng, L. Liu, Z. Wang, Y. Yue, S. Cui, S. Chen, J. Chai, and L. Ma. 2012. 'A companion cell-dominant and developmentally regulated H3K4 demethylase controls flowering time in Arabidopsis via the repression of FLC expression', *PLoS Genet*, 8: e1002664.

Yang, H., H. Mo, D. Fan, Y. Cao, S. Cui, and L. Ma. 2012. 'Overexpression of a histone H3K4 demethylase, JMJ15, accelerates flowering time in Arabidopsis', *Plant Cell Rep*, 31: 1297-308.

Yang, L., X. Chen, Z. Wang, Q. Sun, A. Hong, A. Zhang, X. Zhong, and J. Hua. 2020. 'HOS15 and HDA9 negatively regulate immunity through histone deacetylation of intracellular immune receptor NLR genes in Arabidopsis', *New Phytol*, 226: 507-22.

Yang, Z., S. Qian, R. N. Scheid, L. Lu, X. Chen, R. Liu, X. Du, X. Lv, M. D. Boersma, M. Scalf, L. M. Smith, J. M. Denu, J. Du, and X. Zhong. 2018. 'EBS is a bivalent histone reader that regulates floral phase transition in Arabidopsis', *Nat Genet*, 50: 1247-53.

Yasui, D., M. Miyano, S. Cai, P. Varga-Weisz, and T. Kohwi-Shigematsu. 2002. 'SATB1 targets chromatin remodelling to regulate genes over long distances', *Nature*, 419: 641-5.

Yu, C. W., X. Liu, M. Luo, C. Chen, X. Lin, G. Tian, Q. Lu, Y. Cui, and K. Wu. 2011. 'HISTONE DEACETYLASE6 interacts with FLOWERING LOCUS D and regulates flowering in Arabidopsis', *Plant Physiol*, 156: 173-84.

Yu, C. W., R. Tai, S. C. Wang, P. Yang, M. Luo, S. Yang, K. Cheng, W. C. Wang, Y. S. Cheng, and K. Wu. 2017. 'HISTONE DEACETYLASE6 Acts in Concert with Histone Methyltransferases SUVH4, SUVH5, and SUVH6 to Regulate Transposon Silencing', *Plant Cell*, 29: 1970-83.

Yu, X., L. Li, L. Li, M. Guo, J. Chory, and Y. Yin. 2008. 'Modulation of brassinosteroid-regulated gene expression by Jumonji domain-containing proteins ELF6 and REF6 in Arabidopsis', *Proc Natl Acad Sci U S A*, 105: 7618-23.

Yun, J., Y. S. Kim, J. H. Jung, P. J. Seo, and C. M. Park. 2012. 'The AT-hook motif-containing protein AHL22 regulates flowering initiation by modifying FLOWERING LOCUS T chromatin in Arabidopsis', *J Biol Chem*, 287: 15307-16.

Yun, M., J. Wu, J. L. Workman, and B. Li. 2011. 'Readers of histone modifications', *Cell Res*, 21: 564-78.

Zang, C., D. E. Schones, C. Zeng, K. Cui, K. Zhao, and W. Peng. 2009. 'A clustering approach for identification of enriched domains from histone modification ChIP-Seq data', *Bioinformatics*, 25: 1952-8.

Zeitz, M. J., K. S. Malyavantham, B. Seifert, and R. Berezney. 2009. 'Matrin 3: chromosomal distribution and protein interactions', *J Cell Biochem*, 108: 125-33.

Zhang, C., X. Du, K. Tang, Z. Yang, L. Pan, P. Zhu, J. Luo, Y. Jiang, H. Zhang, H. Wan, X. Wang, F. Wu, W. A. Tao, X. J. He, H. Zhang, R. A. Bressan, J. Du, and J. K. Zhu. 2018. 'Arabidopsis AGDP1 links H3K9me2 to DNA methylation in heterochromatin', *Nat Commun*, 9: 4547.

Zhang, X., Y. V. Bernatavichute, S. Cokus, M. Pellegrini, and S. E. Jacobsen. 2009. 'Genome-wide analysis of mono-, di- and trimethylation of histone H3 lysine 4 in Arabidopsis thaliana', *Genome Biol*, 10: R62.

Zhang, X., O. Clarenz, S. Cokus, Y. V. Bernatavichute, M. Pellegrini, J. Goodrich, and S. E. Jacobsen. 2007. 'Whole-genome analysis of histone H3 lysine 27 trimethylation in Arabidopsis', *PLoS Biol*, 5: e129.

Zhao, J., D. S. Favero, H. Peng, and M. M. Neff. 2013. 'Arabidopsis thaliana AHL family modulates

hypocotyl growth redundantly by interacting with each other via the PPC/DUF296 domain', *Proc Natl Acad Sci U S A*, 110: E4688-97.

Zhao, J., D. S. Favero, J. Qiu, E. H. Roalson, and M. M. Neff. 2014. 'Insights into the evolution and diversification of the AT-hook Motif Nuclear Localized gene family in land plants', *BMC Plant Biol*, 14: 266.

Zhao, L., T. Peng, C. Y. Chen, R. Ji, D. Gu, T. Li, D. Zhang, Y. T. Tu, K. Wu, and X. Liu. 2019. 'HY5 Interacts with the Histone Deacetylase HDA15 to Repress Hypocotyl Cell Elongation in Photomorphogenesis', *Plant Physiol*, 180: 1450-66.

Zhao, S., L. Cheng, Y. Gao, B. Zhang, X. Zheng, L. Wang, P. Li, Q. Sun, and H. Li. 2019. 'Plant HP1 protein ADCP1 links multivalent H3K9 methylation readout to heterochromatin formation', *Cell Res*, 29: 54-66.

Zhao, Y. 2018. 'Essential Roles of Local Auxin Biosynthesis in Plant Development and in Adaptation to Environmental Changes', *Annu Rev Plant Biol*, 69: 417-35.

Zhao, Y., S. K. Christensen, C. Fankhauser, J. R. Cashman, J. D. Cohen, D. Weigel, and J. Chory. 2001. 'A role for flavin monooxygenase-like enzymes in auxin biosynthesis', *Science*, 291: 306-9.

Zheng, M., X. Liu, J. Lin, X. Liu, Z. Wang, M. Xin, Y. Yao, H. Peng, D. X. Zhou, Z. Ni, Q. Sun, and Z. Hu. 2019. 'Histone acetyltransferase GCN5 contributes to cell wall integrity and salt stress tolerance by altering the expression of cellulose synthesis genes', *Plant J*, 97: 587-602.

Zheng, Z., Y. Guo, O. Novak, X. Dai, Y. Zhao, K. Ljung, J. P. Noel, and J. Chory. 2013. 'Coordination of auxin and ethylene biosynthesis by the aminotransferase VAS1', *Nat Chem Biol*, 9: 244-6.

Zhou, J., X. Wang, J. Y. Lee, and J. Y. Lee. 2013. 'Cell-to-cell movement of two interacting AT-hook factors in Arabidopsis root vascular tissue patterning', *Plant Cell*, 25: 187-201.

Zlotorynski, E. 2017. 'Transcription: Paused means poised', *Nat Rev Mol Cell Biol*, 18: 404-05.

7 Abbreviation

me	methylation
ac	acetylation
ub	ubiquitination
ph	phosphorylation
K	lysine
R	arginine
HKMTs	histone lysine methyltransferases
SDG	set domain group
ATX1	ARABIDOPSIS TRITHORAX1
ASHR3	ASH1-related protein 3
KYP/SUVH4	KRYPTONITE/SU(VAR)3-9-HOMOLOG 4
SUVR5	SU(VAR)3-9-RELATED protein 5
PRC2	Polycomb Repressive Complex 2
CLF	CURLY LEAF
SWN	SWINGER
MEA	MEDEA
LSD1	Lysine-specific demethylase1
FLD	FLOWERING LOCUS D
LDL1/2/3	LSD1-LIKE 1/2/3
JmjC	Jumonji C
ELF6	Early Flowering 6
REF6	Relative of Early Flowering 6
IBM1	Increase in Bonsai Methylation 1
CMT3	CHROMOMETHYLASE 3
MBT	malignant brain tumor
PWWP	Pro-Trp-Trp-Pro
PHD	plant homeodomain
ALs	Alphin1-like proteins
SHL	SHORT LIFE
EBS	EARLY BOLTING IN SHORT DAYS
MRG1	MORF4-related gene 1

NAP1	NUCLEOSOME ASSEMBLY PROTEIN 1
NRP1	NAP1-RELATED PROTEIN 1
LHP1	LIKE HETEROCHROMOTIN PROTEIN 1
HP1	HETEROCHROMOTIN PROTEIN 1
EMF1	EMBRYONIC FLOWER 1
ADCP1	AGENET DOMAIN CONTAINING PROTEIN 1
HATs	Histone Acetyltransferases
HDACs	Histone Deacetylases
GNAT	GCN5-related N-terminal acetyltransferases
MYST	MOZ, Ybf2/Sas3, Sas2, and Tip60-related
CBP	CREB-binding protein
TAF1	TATA-binding protein-associated factor
ADA2a	ALTERATION/DEFICIENCY IN ACTIVATION 2a
CTL1	CHITINASE-LIKE PROTEIN 1
PGX3	POLYGALACTURONASE INVOLVED IN EXPANSION3
WOX5/14	WUSCHEL RELATED HOMEOBOX 5/14
SCR	SCARECROW
PLT1/2	PLETHORA ½
RPD3/HDA1	Reduced Potassium Dependence3/Histone Deacetylase-1
SIR2	Sirtuin-like
TEs	transposable elements
CCA1	CIRCADIAN CLOCK-ASSOCIATED1
LHY	LATE ELONGATED HYPOCOTYL
TOC1	TIMING OF CAB EXPRESSION1
HY5	ELONGATED HYPOCOTYL 5
ATGs	autophagy-related genes
NLR	Nod-Like Receptor
HOS15	HIGH EXPRESSION OF OSMOTICALLY RESPONSIVE GENES 15
TPL/TPR	TOPLESS/TOPLESSRELATED
Aux/IAA	AUXIN/INDOLE-3-ACETIC ACID
ARF	AUXIN RESPONSE FACTOR
BR	brassinosteroid
BES1	BRI1-EMS-SUPPRESSOR1
PIF3	PHYTOCHROME INTERACTING FACTOR3

NF-YCs	Nuclear Factor-YC homologs
ROP	RHO GTPASE OF PLANTS
MARs	matrix attachment regions
SARs	scaffold attachment regions
NMPdb	nuclear matrix protein database
RNP	ribonucleoproteins
SATB1	special AT-rich sequence-binding protein 1
SAF-A	scaffold attachment factor A
MFP1	MAR binding filament-like protein 1
AHLs	AT-hook motif nuclear localized proteins
HMG	High mobility group
PPC	Plant and Prokaryotic Conserved
DUF296	Domain of Unknown Function #296
TEK	TRANSPOSABLEELEMENT SILENCING VIA AT-HOOK
ESC	ESCAROLA
SOB3	SUPPRESSOR OF PHYTOCHROME B4-#3
YUC	YUCCA
AGF1	AT-hook protein of GA feedback regulation 1
AGPs	Arabinogalactan proteins
CalS5	CALLOSE SYNTHASE5
AMs	axillary meristems
SE	embryogenesis
BBM	BABY BOOM
ADM	ADMETOS
HAI1	Highly ABA-Induced 1
TAA	TRYPTOPHAN AMINOTRANSFERASE OF ARABIDOPSIS
IPyA	indole-3-pyruvate
IAA	Indole-3-acetic acid
TIR1	TRANSPORT INHIBITOR RESPONSE 1
AFB	AUXIN SIGNALING F-BOX
ARFs	auxin response factors
SAUR	SMALL AUXIN UP-REGULATED RNA
TAP	tandem affinity purification
FRS	FAR1 RELATED SEQUENCE

GI	GIGANTEA
BiFC	bimolecular fluorescence complementation
Co-IP	Co-immunoprecipitation
DEGs	differentially expressed genes
DGs	down-regulated genes
UGs	up-regulated genes
GO	Gene Ontology
ChIP-seq	Chromatin immunoprecipitation followed by sequencing
LCMS	LIQUID CHROMATOGRAPHY MASS SPECTROMETRY
TSSs	transcription start sites
TESs	transcription end sites
FRAP	Fluorescence Recovery After Photobleaching

8 Appendix

Supplementary Table 1: List of primers used in this study

Name	Sequence	Description
pDonar-AHL22-CDS-F	AAAAAGCAGGCTCCACCATGGATCAGGTCT	CDS cloning for AHL22 (AT2G45430)
pDonar-AHL22-CDS-R1	AGAAAGCTGGGTCTTAGAAAGATGGTCTCG	
pDonar-AHL22-CDS-R2	AGAAAGCTGGGTCGAAAGATGGTCTCGGAGTTCC	
pDonar-AHL29-CDS-F	aaaaagcaggctccaccATGGACGGTGGTTACGATCAAT	CDS cloning for AHL29 (AT1G76500)
pDonar-AHL29-CDS-R	AGAAAGCTGGGTCAAAGGCTGGTCTTGGTGGTG	
pDonar-FRS12-CDS-F	AAAAAGCAGGCTCCACCATGGAGAGTGTAGATACTGAG	CDS cloning for FRS12 (AT5G18960)
pDonar-FRS12-CDS-R	AGAAAGCTGGGTCTCATCTCTGCCAACAAAGTTTC	
pENTR-FRS12-CDS-F	CACCATGGAGAGTGTAGATACTGAG	
pENTR-FRS12-CDS-R	TCTCTGCCAACAAAGTTTCTTCCCAC	
TSK108-FRS7-CDS-F1	gcgGGATCCATGGTTGTCAAAACTTATCCATTAG	CDS cloning for FRS7 (AT3G06250)
TSK108-FRS7-CDS-R1	gcgGAGCTCTCTGCCAACACAGTTTCTTC	
TSK108-FRS7-CDS-F2	gcgGGATCCgATGGTTGTCAAAACTTATCCATTAG	
TSK108-FRS7-CDS-R2	gcgGAGCTCTCATCTCTGCCAACACAGTTTCTTC	
TSK108-HDA15-CDS-F1	gcgGTCGACATGGTTGTAGAAACTATCGAGAGG	CDS cloning for HDA15 (AT3G18520)
TSK108-HDA15-CDS-R1	gcgCTGCAGCTTTGATCTTGAAATCATACGAGC	
TSK108-HDA15-CDS-F2	gcgGTCGACgATGGTTGTAGAAACTATCGAGAGG	
TSK108-HDA15-CDS-R2	gcgCTGCAGCTACGACGGATTAGGAAGAATGC	
Δ AHL22-F	TCATCTGTCGTTAACTTACACTCTCTCTCGGG	The deletion of the G-R-F-E-I-L region in AHL22 (Δ AHL22)
Δ AHL22-R	AAGGAATGATCCCGAGAGAGAGTGTAAGTTAAC	
SAUR6-RT-qPCR-F	GAAGAGGAGATTCGTGGTT	RT-qPCR for AT2G21210
SAUR6-RT-qPCR-R	GAAGTGCTAAGGCGAGAG	
SAUR14-RT-qPCR-F	CTAGCTCTCTTGATGTTCCC	RT-qPCR for AT4G38840
SAUR14-RT-qPCR-R	GATTGTGAGGCCACCCATTG	
SAUR15-RT-qPCR-F	CAAGAGGATTCATGGCGGTC	RT-qPCR for AT4G38850
SAUR15-RT-qPCR-R	TTAAGCCGCCCATTGGATG	
SAUR16-RT-qPCR-F	GGCAAGAAACAATGCTACGAC	RT-qPCR for AT4G38860
SAUR16-RT-qPCR-R	CCTCTGCTTGTTGAAGAAGG	
SAUR20-RT-qPCR-F	GAGATATCTGGTGCCAATC	RT-qPCR for AT5G18020
SAUR20-RT-qPCR-R	CATCGTTGGAACCGAGAAG	
SAUR21-RT-qPCR-F	AGATATTTGGTGCCGCTCTC	RT-qPCR for AT5G18030
SAUR21-RT-qPCR-R	TGATCATTGGAGCCGAGAAG	
SAUR50-RT-qPCR-F	ATCTCCTTCTCCATAACTCTC	RT-qPCR for AT4G34760
SAUR50-RT-qPCR-R	TGTATCTGCTTCTGTTCTCT	

SAUR51-RT-qPCR-F	GTGCTCGAGCTTGGGAAAG	RT-qPCR for
SAUR51-RT-qPCR-R	GCTGAAACTCAGGTCGGGTC	AT1G75580
SAUR78-RT-qPCR-F	ACCACCACTCAACCTCCTC	RT-qPCR for
SAUR78-RT-qPCR-R	GAAGAAGACCGATCCACGAG	AT1G72430
SAUR14-MAR-qPCR-F	CTGACTCCTTTCTGCTCTGC	MAR-qPCR for
SAUR14-MAR-qPCR-R	GAATCTGCTTCGATGATTGC	AT4G38840
SAUR15-MAR-qPCR-F	CTCAAAGCTTTCTCCAAGAC	MAR-qPCR for
SAUR15-MAR-qPCR-R	GTCGACGATGATTCCCTTCG	AT4G38850
SAUR16-MAR-qPCR-F	CTCCTCACTAGCTCTCTCAC	MAR-qPCR for
SAUR16-MAR-qPCR-R	GCTCGAGCATCTCTTGAGG	AT4G38860
SAUR20-MAR-qPCR-F	CTTTTCATACATCTTCAGAAG	MAR-qPCR for
SAUR20-MAR-qPCR-R	TGGTGGAGCGGCTTAGAATC	AT5G18020
SAUR21-MAR-qPCR-F	CATCCATCTTAATAAGCTTC	MAR-qPCR for
SAUR21-MAR-qPCR-R	ATGCGGTGGAGCGGCTTAG	AT5G18030
SAUR78-MAR-qPCR-F	CAACAACTCTCTTGTTCCAAC	MAR-qPCR for
SAUR78-MAR-qPCR-R	CGAAAGAAGGCCATTTCTTC	AT1G72430
SAUR14/15-ChIP-qPCR-F	gaacattacttgtagataacc	ChIP-qPCR for
SAUR14/15-ChIP-qPCR-R	ggcaaagccatgtgcttgc	AT4G38840 and AT4G38850
SAUR16-ChIP-qPCR-F	ggcactaaccaaaattttag	ChIP-qPCR for
SAUR16-ChIP-qPCR-R	aggaagatgaggataggatgc	AT4G38860
SAUR20-ChIP-qPCR-F	agatcaactactaatgagttg	ChIP-qPCR for
SAUR20-ChIP-qPCR-R	ggtagagacagaaccatgttc	AT5G18020
SAUR21-ChIP-qPCR-F	ggcccaaactcaattaattatg	ChIP-qPCR for
SAUR21-ChIP-qPCR-R	gtggtcttgaagcgtgggac	AT5G18030
SAUR78-ChIP-qPCR-F	gatagatggatgagggaatg	ChIP-qPCR for
SAUR78-ChIP-qPCR-R	aatggtgtaatgatcacttg	AT1G72430
ahl22-1 LP	GAAAAGACTCGTGACTGTTTGC	*ahl22-1*
ahl22-1 RP	AAGACGGTGACACTTTCCATG	(SALK_018866) genotyping
ahl18-1 LP	ATCAATCCGAGATCAGACCG	*ahl18-1*
ahl18-1 RP	TTTTCATCAACCTCACGTTCC	(SAIL_779_H11) genotyping
frs7-1 LP	TGAAACAACCATGAGAAAGCC	*frs7-1*
frs7-1 RP	CAACTCTTATGCTACGCGGAC	(FLAG_196C09) genotyping
frs12-1 LP	ATTGACATCCAATTCGACAGC	*frs12-1*
frs12-1 RP	GTTCTTGTGTTCGTTGGCTTC	(SALK_030182) genotyping
hda15-1 LP	CTTCTCTGTTCATCGTTTCGC	*hda15-1*
hda15-1 RP	AGCAACATTCTCTCGTCGAAC	(SALK_004027) genotyping

9 Acknowledgement

10 Curriculum Vitae

First name, Last name: Linhao, Xu
Date of Birth: 12th June 1992
Nationality: Chinese

EDUCATION

2018.10-Present.	PhD candidate, enrolled at Martin Luther University, Halle, Germany and thesis was prepared at Leibniz Institute of Plant Genetics and Crop Plant Research (IPK), Germany Thesis: Insights into the role of an Arabidopsis nuclear matrix binding protein AHL22 in chromatin regulation and hypocotyl growth Supervisor: Jun. Prof. Dr. Hua Jiang
2015.09-2018.06.	Master of Agronomy, Fujian Agriculture and Forestry University, China Thesis: Purification and Characterization of Arabidopsis SWR1 complex Supervisor: Prof. Dr. Israel Ausin
2013.12-2014.09.	Visiting student, University of British Columbia (UBC), Canada
2011.09-2015.06.	Bachelor of Agronomy, Fujian Agriculture and Forestry University, China

WORK EXPERIENCE

2018.07-2018.09.	Lab technician in Jun Xiao's Lab, Institute of Genetics and Developmental Biology, CAS, Beijing, China

CONFERENCES

Linhao Xu, Jinping Cheng, Hua Jiang. Mutation of histone H3 serine 28 to alanine influences H3K27me3-mediated gene silencing in *Arabidopsis thaliana*. 7th European Workshop on Plant Chromatin, Průhonice, Prague, 18-20 May 2022 (Poster).

Linhao Xu, Hua Jiang. Elucidating the mechanism of AHL22-mediated H3K9me2 deposition in Arabidopsis. Plant Science Student Conference, Halle, Germany, 2019 (Poster).

SCIENTIFIC TRAINING

6 May 2022	IPB Doctoral Training Course (DoCou): An overview on the available tools for RNA-seq data analysis by Khabat Vahabi.
16-17 February 2021	Diagenode virtual ChIP workshop.
27 Jan 2021	INDEPTH-Academy technical webinar on smFISH.

PUBLICATION

1. **Linhao Xu**, Jinping Cheng, Hua Jiang (2022). Insights into an Arabidopsis nuclear matrix binding protein AHL22 in transcriptional control. (in preparation)

2. **Linhao Xu**, Jinping Cheng, Hua Jiang (2022). Mutation of histone H3 serine 28 to alanine influences H3K27me3-mediated gene silencing in *Arabidopsis thaliana*. (In revision)

3. **Xu L**, Jiang H. Writing and Reading Histone H3 Lysine 9 Methylation in Arabidopsis. **Frontiers in Plant Science**. 2020. https://doi.org/10.3389/fpls.2020.00452

4. Jinping Cheng, **Linhao Xu**, Valentin Bergér, Astrid Bruckmann, Chao Yang, Veit Schubert, Klaus D Grasser, Arp Schnittger, Binglian Zheng, Hua Jiang. H3K9 demethylases IBM1 and JMJ27 are required for male meiosis in *Arabidopsis thaliana*. **New Phytologist**. May 2022. https://doi.org/10.1111/nph.18286

5. Cheng J, Zhang G, **Xu L**, Liu C, Jiang H. Altered H3K27 trimethylation contributes to flowering time variations in polyploid Arabidopsis thaliana ecotypes. **J Exp Bot**. 2021 Oct 26: erab470. doi: 10.1093/jxb/erab47

6. Yafei Wang, Zhenhui Zhong, Yaxin Zhang, **Linhao Xu**, Suhua Feng, Shima Rayatpisheh, James A. Wohlschlegel, Zonghua Wang, Steven E. Jacobsen & Israel Ausin. NAP1-RELATED PROTEIN1 and 2 negatively regulate H2A.Z abundance in chromatin in Arabidopsis. **Nat Commun** 11, 2887 (2020). https://doi.org/10.1038/s41467-020-16691-x

7. Magdalena E. Potok, Yafei Wang, **Linhao Xu**, Zhenhui Zhong, Wanlu Liu, Suhua Feng, Bilguudei Naranbaatar, Shima Rayatpisheh, Zonghua Wang, James A. Wohlschlegel, Israel Ausin and Steven E. Jacobsen. Arabidopsis SWR1-associated protein methyl-CpG-binding domain 9 is required for histone H2A.Z deposition. **Nat Commun** 10, 3352 (2019). https://doi.org/10.1038/s41467-019-11291-w

11 Eidesstattliche Erklärung/Declaration under Oath

Ich erkläre an Eides statt, dass ich die Arbeit selbstständig und ohne fremde Hilfe verfasst, keine anderen als die von mir angegebenen Quellen und Hilfsmittel benutzt und die den benutzten Werken wörtlich oder inhaltlich entnommenen Stellen als solche kenntlich gemacht habe.

I declare under penalty of perjury that this thesis is my own work entirely and has been written without any help from other people. I used only the sources mentioned and included all the citations correctly both in word or content.

_____   _____

Datum / Date   Unterschrift des Antragstellers /
                                                                                Signature of the applicant

12 Erklärung über bestehende Vorstrafen und anhängige Ermittlungsverfahren/Declaration concerning Criminal Record and Pending Investigations

Hiermit erkläre ich, dass ich weder vorbestraft bin noch dass gegen mich Ermittlungsverfahren anhängig sind. / *I hereby declare that I have no criminal record and that no preliminary investigations are pending against me.*

_____	_____
Datum / Date	Unterschrift des Antragstellers / *Signature of the applicant*